

**A novel method for the analysis of 5-aminoimidazole-4-carboxamide-1- $\beta$ -D-ribofuranoside (AICAR) in urine by isotope ratio mass spectrometry for anti-doping purposes**

Frédéric Séguin

A Thesis

in

The Department

of

Chemistry and Biochemistry

Presented in Partial Fulfillment of the Requirements

for the Degree of Master of Science (Chemistry) at

Concordia University

Montreal, Quebec, Canada

March 2021

© Frédéric Séguin, 2021

CONCORDIA UNIVERSITY  
School of Graduate Studies

This is to certify that the thesis prepared

By: Frédéric Séguin

Entitled: A novel method for the analysis of 5-aminoimidazole-4-carboxamide-1- $\beta$ -D-ribofuranoside (AICAR) in urine by isotope ratio mass spectrometry for anti-doping purposes

and submitted in partial fulfillment of the requirements for the degree of

Master of Science in Chemistry

---

complies with the regulations of the University and meets the accepted standards with respect to originality and quality.

Signed by the final examining committee:

\_\_\_\_\_  
Dr. Rafik Naccache Chair

\_\_\_\_\_  
Dr. Dajana Vuckovic Examiner

\_\_\_\_\_  
Dr. Christopher Wilds Examiner

\_\_\_\_\_  
Dr. Yves Gélinas Co-Supervisor

\_\_\_\_\_  
Dr. Karine Lalonde Co-Supervisor

Approved by \_\_\_\_\_  
Dr. Yves Gélinas  
Graduate Program Director

\_\_\_\_\_  
Dr. Pascale Sicotte  
Dean Faculty of Arts and Science

Date: March 9, 2021

## **Abstract**

A novel method for the analysis of 5-aminoimidazole-4-carboxamide-1- $\beta$ -D-ribofuranoside (AICAR) in urine by isotope ratio mass spectrometry for anti-doping purposes

Frédéric Séguin

In the last 20 years, isotopic ratio mass spectrometry coupled with gas chromatography (GC/C/IRMS) applied to carbon stable isotope ( $^{13}\text{C}/^{12}\text{C}$ ) ratios (CSIR) has been a fundamental tool in the field of anti-doping analysis. Some compounds, such as testosterone, can be found in human urine as the result of natural metabolism or exogenous intake, sometimes leaving its carbon isotopic signature as the only proof of an antidoping violation. More recently, the appearance of a new non-steroidal compound named 5-aminoimidazole-4-carboxamide-1- $\beta$ -D-ribofuranoside (AICAR) has been of major concern. Experiments made on mice, combined with rumors in the world of sport, has made the compound a suspect for anti-doping authorities. As an intermediate in the purine synthesis, AICAR is also present in urine. The development of a GC/C/IRMS method to distinguish between natural and synthetic AICAR therefore appears necessary, but is not done without issues as AICAR is a non-volatile and unstable molecule at high temperatures. Existing methods use trimethylsilyl (TMS) derivatization, which damages combustion furnaces and adds 9 carbon atoms to the AICAR molecule.

This work therefore proposes a new GC/C/IRMS method that uses acetylation as an alternative route to analyze the CSIR of AICAR for anti-doping purposes. The different issues encountered when developing such method are described as well as the data obtained from its validation and from the analysis of 46 urines samples. A comparison of the results from this work with the existing literature is also made. The results suggest that the use of CSIR to determine the origin of AICAR in urine is more complex than previously reported.

## Acknowledgements

My first and dearest thanks go to my wife, Carine Roy-Gu  rette and children, Vincent, Florence, Jade and Cassandre who somehow manage to still love the stubborn and eternal student that I am. I am also grateful to my parents, Anne Par   and Pierre S  guin and grand-parents, Paul and Suzanne S  guin for instilling in me that education is an influential value. I also wish to thank my supervisors, Dr Yves G  linas and Dr Karine Lalonde for their much appreciated technical and moral support, my supervisory committee members Dr Dajana Vuckovic and Dr Christopher Wilds, as well as Christiane Ayotte for approving this project. Finally, thank you to Anic Imfeld, Aleshia Kormendi, Nicolas LeBerre and Andrew Barber for their help and sense of humor.

This work was funded by the Partnership for Clean Competition (PCC), the Canadian Foundation for Innovation (CFI) and the Discovery program of the Natural Sciences and Engineering Research Council of Canada (NSERC). The NSERC, the *Fonds de Recherche du Qu  bec - Nature et Technologies (FRQNT)*, Hydro-Quebec and the Concordia University are also acknowledged for scholarships to Fr  d  ric S  guin.

### **Contribution by authors**

All analyses and tests were carried out by Frédéric Séguin under the supervision of Dr Karine Lalonde and Dr Yves Gélinas. GC/C/IRMS measurements as well as GC-MS and GC tests were done at Concordia University whereas sample preparation (PBA extraction, semi-preparative HPLC) was performed at the *Laboratoire de contrôle du dopage* from the *Institut National de la Recherche Scientifique (INRS) – Centre Armand-Frappier Santé biotechnologie*. Help for instrument setup was provided by Dr Karine Lalonde, Dr Yves Gélinas, Dr Andrew Barber and Nicolas LeBerre. All figures and tables were created by Frédéric Séguin, with the exception of Figure 3.1 which was adapted from previous work done by Dr Karine Lalonde. Data analysis was done by Frédéric Séguin with help from Dr Karine Lalonde.

## Table of contents

List of figures .....	xi
List of tables .....	xv
List of abbreviations .....	xvii
1 General introduction.....	1
1.1 Background.....	1
1.2 AICAR in the scientific literature and in the media .....	6
1.2.1 AICAR nomenclature.....	6
1.2.2 Early work.....	7
1.2.3 AICAR as an AMPK activator.....	7
1.2.4 ZMP as a bioactive molecule in cells.....	10
1.2.5 Effects of AICAR on the purine metabolism .....	15
1.2.6 Other effects .....	18
1.2.7 Effects of AICAR on pluricellular organisms.....	18
1.2.8 Narkar et al. (2008) .....	19
1.2.9 Possible therapeutic uses of AICAR.....	20
1.2.10 Toxicity and occurrence in metabolic diseases .....	21
1.2.11 AICAR as a doping agent: How mainstream media exaggerated research .....	22
1.3 Stable isotope ratios .....	23
1.3.1 General presentation.....	23
1.3.2 Carbon stable isotope ratios (CSIR).....	26
1.3.3 CSIR in anti-doping analyses.....	27

1.3.4 GC/C/IRMS for CSIR.....	30
1.3.4.1 The use of endogenous reference compounds .....	32
1.3.4.2 Adaptation of GC/C/IRMS to AICAR.....	33
1.4 General objectives of the thesis .....	34
1.5 Organization of the thesis .....	34
2 Materials and methods .....	36
2.1 Materials .....	36
2.1.1 Nucleic acid analogs .....	36
2.1.2 Other materials .....	36
2.2 Methods.....	37
2.2.1 Reference material stock solutions.....	37
2.2.2 External EA-IRMS analyses .....	37
2.2.3 Urine samples.....	37
2.2.4 Negative and positive reference urines .....	37
2.2.5 PBA gel.....	38
2.2.6 PBA extraction buffers.....	38
2.2.7 PBA extraction .....	38
2.2.8 First semi-preparative HPLC .....	39
2.2.9 Acetylation .....	40
2.2.10 Second semi-preparative HPLC .....	40
2.2.11 GC method development.....	41
2.2.12 GC/C/IRMS method for AICAR and uridine analysis .....	41
2.2.13 GC/C/IRMS method validation.....	42

2.2.14 GC/C/IRMS steroid analysis.....	43
2.2.15 GC-MS .....	45
2.2.16 LC-MS/MS.....	45
2.2.17 AICAR bought on online .....	47
2.2.18 Details of the acetylation experiment.....	48
3 Method design, optimization and validation .....	50
3.1 Uridine as a new endogenous reference compound.....	52
3.2 Solid-phase extraction.....	52
3.2.1 C18, HLB and MCX sorbents.....	53
3.2.2 Phenylboronic acid.....	56
3.2.3 PBA gel performance .....	58
3.2.3.1 Recovery .....	58
3.2.3.2 PBA specificity .....	59
3.2.3.3 Carry-over .....	59
3.3 Semi-preparative HPLC.....	60
3.3.1 Choice of solvents for the mobile phase .....	61
3.3.2 Choice of HPLC column.....	61
3.3.3 Performance of the ACME® PLUS column.....	62
3.3.4 Second HPLC: After acetylation.....	63
3.4 Acetylation.....	64
3.4.1 Choice of reagents.....	66
3.4.2 Reaction parameters .....	67
3.4.3 Yield and reproducibility .....	69

3.5 GC/C/IRMS .....	70
3.5.1 Gas chromatography .....	70
3.5.1.1 Choice of chromatographic column .....	70
3.5.1.2 GC temperature parameters.....	72
3.5.2 Combustion .....	74
3.5.3 Correction of $\delta^{13}\text{C}$ values with reference material .....	78
3.5.4 Correction for acetylation .....	81
3.6 Mandatory method characteristics .....	83
3.7 Method validation .....	85
3.7.1 AICAR and uridine stability in stored urine .....	85
3.7.2 Peak purity and identification .....	88
3.7.3 Validated parameters.....	90
4 Results and discussion.....	92
4.1 CSIR of synthetic AICAR .....	93
4.2 Sample results and comparison with existing literature .....	93
4.3 The influence of the origins of the C atoms in AICAR and uridine .....	97
4.4 Evaluation of steroids and uridine as ERCs.....	99
5 Conclusion.....	107
5.1 Future work.....	107
5.2 General conclusions .....	109
Bibliography.....	112
Appendix 1 Acetylation experiment .....	126
Appendix 2 Method validation supplemental data.....	128

Appendix 3 Individual  $\delta^{13}\text{C}$  measurements for all samples ..... 131

Appendix 4 AICAR and uridine concentration in urine samples..... 135

## List of figures

**Figure 1.1:** A) Molecular structure of 5-aminoimidazole-4-carboxamide-1- $\beta$ -D-ribofuranoside (AICAR in this work) and B) 5-aminoimidazole-4-carboxamide-1- $\beta$ -D-ribofuranoside 5'-monophosphate (ZMP in this work). Atom numbering is based on the official nomenclature of IUPAC.

**Figure 1.2:** Examples of purines 1) adenine; 2) guanine; 3) adenosine; 4) adenosine-5'-monophosphate (AMP); 5) 2'-deoxyadenosine; 6) 2'-deoxyadenosine-5'-monophosphate; 7) guanosine; 8) guanosine-5'-monophosphate (GMP); 9) 2'-deoxyguanosine and 10) 2'-deoxyguanosine-5'-monophosphate.

**Figure 1.3:** Schematic of the pyrimidine (left) and purine (right) pathways, adapted from the Kyoto Encyclopedia of Genes and Genomes (KEGG) [47-49] and [43, 50, 51]. Compound abbreviations are in black and enzyme abbreviations are in blue. The question mark indicates an unknown enzyme. 5'-NT: 5'-nucleotidase, ADSL: adenylosuccinate lyase, ADSS: adenylosuccinate synthase, AMP: adenosine monophosphate, AICAR: 5-aminoimidazole-4-carboxamide-1- $\beta$ -D-ribofuranoside, AK: adenosine kinase, AMP: adenosine monophosphate, ATIC: 5-aminoimidazole-4-carboxamide ribonucleotide formyl transferase/IMP cyclohydrolase, GMP: guanosine monophosphate, GPMS: guanosine monophosphate synthase, IMP: inosine monophosphate, IMPDH: inosine monophosphate dehydrogenase, orotidine 5'-P: orotidine 5'-phosphate, sZMP: 5'-phosphoribosyl-4-succinocarboxamide-5-aminoimidazole ribonucleotide, UCK: uridine-cytidine kinase, UMP: uridine monophosphate, UMPS: uridine monophosphate synthase, UPP: uridine phosphorylase, PRPP: phosphoribosyl pyrophosphate, XMP: xanthine monophosphate, ZMP: 5-aminoimidazole-4-carboxamide-1- $\beta$ -D-ribofuranoside 5'-monophosphate.

**Figure 1.4:** Schematic of the purine catabolic pathway excerpt from the KEGG [47-49]. Compound abbreviations are in black and enzyme abbreviations are in blue. 5'-NT: 5'-nucleotidase, ADA: adenosine deaminase, AMP: adenosine monophosphate, AMPD: adenosine monophosphate deaminase, GMP: guanosine monophosphate, GMPS: guanosine monophosphate synthase, GDA: guanine deaminase, IMP: inosine monophosphate, IMPDH: inosine monophosphate dehydrogenase, PNP: purine nucleoside phosphorylase, XDH: xanthine dehydrogenase, XMP: xanthine monophosphate.

**Figure 1.5:** Molecular structure similarities between 1. Left: Stigmasterol, a phytosterol, 2. Center: Cholesterol, a sterol found in small amounts in plants but mostly in animals and 3. Right: Testosterone, a sex hormone and AAS.

**Figure 1.6:** Simplified representation of a GC/C/IRMS. The sample is injected (1), then carried with a stream of helium in the GC where the analytes get separated in a chromatography column (2). They then one by one enter the combustion furnace (3) and get converted to CO<sub>2</sub> and H<sub>2</sub>O. When exiting the furnace, water is diffusively removed using a Nafion<sup>®</sup> membrane and the CO<sub>2</sub> enters the MS where it is ionized by electron impact in the ion source (4). Monitoring CO<sub>2</sub> gas (MG) can also be introduced in the MS for measurement calibration (5). Once formed, the ions are separated by their mass using a magnetic field from an electromagnet (6). A signal for  $m/z = 44, 45$  and  $46$  can then be acquired (7) and analyzed by computer software (8).

**Figure 2.1:** AICAR ordered from the Internet. The one on the left (Anexic) contained pure AICAR whereas the one on the right (Pharma Grade) contained a UV-invisible substance that could not be identified.

**Figure 3.1:** Comparison of this work method flowchart (Panel C) to those of Piper et al. 2014 (Panel A) and Buisson et al. 2017 (Panel B). The two main modifications are: 1) The derivatization step which uses acetylation instead of silylation (TMS) and 2) the choice of ERC. The use of a structurally similar ERC allows the identical treatment of AICAR and the ERC.

**Figure 3.2:** Similarities between the chemical structures of AICAR (left) and uridine (right).

**Figure 3.3:** Tautomeric forms of anionic uridine.

**Figure 3.4:** AICAR's UV signal (black arrow) after the extraction of 200 (blue), 500 (red) and 1000  $\mu$ L (green) of urine from a volunteer on HLB cartridge. Note how the signal decreases from 500 to 1000  $\mu$ L.

**Figure 3.5:** PBA's related chemistry. 1) PBA free molecule, 2) Chemical structure when bonded on PA gel and 3) Mechanism for 1,2-cis-diol fixation on PBA at alkaline pH.

**Figure 3.6:** UV chromatogram for a urine extracted by SPE with 1) a C18 cartridge, 2) a HLB cartridge, 3) a MCX cartridge and 4) the PBA gel. The arrows point the expected elution time of

uridine (left) and AICAR (right). Analyte concentrations were low in this sample, but peaks are visible in the PBA extract after zooming. Units are as in Figure 3.4.

**Figure 3.7:** Example of HPLC chromatograms obtained after PBA gel extraction with the ACME<sup>®</sup> column using the method's final version. Left: for a standard mix of AICAR and uridine, and right: for a urine sample. A: AICAR and U: Uridine. Note the very distinctive AICAR peak in the sample and the >1-minute gap between AICAR and uridine.

**Figure 3.8:** Example of HPLC chromatograms obtained on an ACME<sup>®</sup> column after acetylation. Left: for a standard mix of 3-Ac-uridine and 3-Ac-AICAR, and right: for a urine sample. Note the elution order swap between the free and acetylated forms of AICAR and uridine.

**Figure 3.9:** Trisilylated form of AICAR.

**Figure 3.10:** The acetylation reaction. 1) General acetylation of an alcohol yielding an ester and of an amine yielding an amide. 2) Chemical structures of Ac<sub>2</sub>O and Pyr. 3) Acetylation mechanism of the C5'-OH of AICAR with Ac<sub>2</sub>O and Pyr.

**Figure 3.11:** Total Ion Count GC-MS chromatogram of acetylated AICAR using Et<sub>3</sub>N. The arrow shows the peak with M<sup>+</sup> at  $m/z = 426$  corresponding to 4-Ac-AICAR.

**Figure 3.12:** Peak shape comparison between the Agilent's DB-5MS (top) and CP Sil (bottom) columns.

**Figure 3.13:** Symmetry factor comparison between the DB-5MS (left) and CP Sil (right) columns. Orange dots: 3-Ac-AICAR, and blue dots: 3-Ac-uridine.

**Figure 3.14:** Influence of the injector temperature on the GC-FID signal for 3-Ac-AICAR (orange squares) and 3-Ac-uridine (blue triangles). For each point  $n = 2$  and error bars are  $\pm 1$  SD. Results obtained with a DB-5MS column.

**Figure 3.15:** Increase in the  $\delta^{13}\text{C}$  values (orange) and decrease in the  $\delta^{18}\text{O}$  values (blue) as the O<sub>2</sub> level decreases in the GC/C/IRMS combustion chamber. CSIR values uncorrected for <sup>17</sup>O (<sup>45</sup> $\delta$ , yellow) were stable throughout the test.

**Figure 3.16:** Influence of the approximate O<sub>2</sub> levels on the  $\delta^{13}\text{C}$  (‰) values of a 3-Ac-AICAR standard.

**Figure 3.17:** Relation for various molecules between their external and internal  $\delta^{13}\text{C}$  values. Red: triacetylated AICAR and uridine, blue: steroid acetates and grey: triacetin and glycerol hexaacetate.

**Figure 3.18:** AICAR (left) and uridine (right) long-term stability in urine when stored at  $+4^\circ\text{C}$  (top) and  $-20^\circ\text{C}$  (bottom) for two urine samples spiked with  $5\ \mu\text{g/mL}$  of both substances. Blue triangles: Sample 1, and orange squares: Sample 2. Missing points were not determined.

**Figure 3.19:** Examples of the 45/44 ratio pattern for a pure peak (left) and a peak co-eluting with an interference (right) possibly altering the  $\delta^{13}\text{C}$  value.

**Figure 3.20:** Examples of mass spectra for 3-Ac-AICAR (left) and 3-Ac-uridine (right). Circled  $m/z$  values are the ones suggested by this work for analyte identification.

**Figure 3.21:** 3-Ac-AICAR total ion count (TIC) chromatogram from a sample (upper panel) and ion extract chromatography of the same peak (lower panel) using  $m/z = 384, 259, 137$  and  $97$ .

**Figure 4.1:** AICAR  $\delta^{13}\text{C}$  (orange circles) and  $\Delta\delta^{13}\text{C}_{\text{A-U}}$  (grey triangles) values versus AICAR concentration for all samples in which AICAR and uridine could be analyzed ( $n = 43$ ).

**Figure 4.2:**  $\Delta\delta^{13}\text{C}_{\text{A-U}}$  (blue) and  $\Delta\delta^{13}\text{C}_{\text{A-Pd}}$  (orange) value distribution ( $n = 43$  for  $\Delta\delta^{13}\text{C}_{\text{A-U}}$  and  $34$  for  $\Delta\delta^{13}\text{C}_{\text{A-Pd}}$ ). Values on the x axis represent  $\Delta\delta^{13}\text{C}$  values (in ‰) distributed in 1‰ half-open intervals with the first number included and the second one excluded.

**Figure 4.3:** Correlation between Andro and Pd  $\delta^{13}\text{C}$  values (blue circles,  $n = 34$ ) as well as AICAR and Pd  $\delta^{13}\text{C}$  values (orange circles,  $n = 44$ ).

**Figure 4.4:** Correlation between AICAR and uridine  $\delta^{13}\text{C}$  values measured for this work ( $n = 43$ ).

**Figure 4.5:** Correlation between uridine and Andro  $\delta^{13}\text{C}$  values measured for this work ( $n = 34$ ).

## List of tables

**Table 1.1:** Non exhaustive list of AMPK activation effects excerpt from [32-33].

**Table 1.2:** Effects of incubation with 700  $\mu$ M of AICAR on key players participating in the purine (and pyrimidine) metabolism for CHO cells, excerpt from Sabina et al.'s publication [31].

**Table 1.3:** Examples of applications for SIR.

**Table 2.1:** Analyte masses calculated with [172] and used for LC-MS/MS analyses.

**Table 3.1:** Approximate ( $\pm 10\%$ ) SPE recoveries obtained with the MCX, HLB and C18 sorbents.

**Table 3.2:** PBA gel recovery for AICAR and uridine in water and urine. Results are given as  $\% \pm$  SD.

**Table 3.3:** Tested parameters and reagents for acetylation.  $< 1$  minute corresponds to a 5-10 second stir on vortex before adding water to stop the reaction. RT: room temperature.

**Table 3.4:** Acetylation yields (%) for AICAR and uridine for three different masses.

**Table 3.5:** Optimal GC parameter values.

**Table 3.6:** Precision achieved by the GC/C/IRMS instrument under suitable  $O_2$  levels. The measured  $\delta^{13}C$  values were corrected with the MG only.

**Table 3.7:** Table 3.7: Precision results over a 50-hour long sequence for RMs bought already acetylated (no in-house acetylation) and acetylated during the course of this work.

**Table 3.8:** Long-term precision for 3-Ac-AICAR and 3-Ac-uridine in the Mix-AU, QCN and QCP. The SDs obtained are all  $< 0.50\%$  and demonstrate the good performance of the two-point calibration method.

**Table 3.9:** Characteristics to be included in the method as stated in the TD2019IRMS [158].

**Table 3.10:** Table 3.10: Effect of long-term (87 days) storage on  $\delta^{13}C$  values corrected for acetylation of urinary AICAR and uridine when stored at  $-20$  and  $+4^\circ C$ . Values in parenthesis express the  $\delta^{13}C$  (‰) difference when compared to the same urine stored only at  $-80^\circ C$ .

**Table 3.11:** Proposed  $m/z$  values for 3-Ac-AICAR and 3-Ac-uridine GC-MS identification.

**Table 3.12:** WADA requirements [158] for parameters assessed during method validation that could be adapted to AICAR CSIR analysis.

**Table 4.1:** All published  $\delta^{13}\text{C}$  values for AICAR bought from commercial sources, either certified or not. The mean value is  $-4.1\text{‰}$  and the SD  $0.8\text{‰}$ .

**Table 4.2:** Summary of all  $\delta^{13}\text{C}$  measurements for this work and that of Piper et al. (2014).

**Table 4.3:** Origins of the different C atoms for AICAR and uridine molecules. This information was obtained using the KEGG [47-49]. Atom numbering can be better understood using Figures 1.1 and 3.2.

**Table 4.4:** Table 4.4:  $\Delta\delta^{13}\text{C}_{\text{A-ERC}}$  values presented as mean  $\pm$  SD from this work and from Piper et al. (2014).

**Table 4.5:** Reference limit values reported by Piper et al. (2014) for three different ERCs: Pd, Et and Andro with five samples for which  $\Delta\delta^{13}\text{C}_{\text{A-ERC}}$  results were high in this work.

## List of abbreviations

%RSD	Relative Standard Deviation
3-Ac-AICAR	5-Amino-1-(2',3',5'-tri-O-acetyl- $\beta$ -D-ribofuranosyl)-imidazole-4-carboxamide
3-Ac-uridine	2',3',5'-Tri-O-acetyluridine
3-PGA	3-Phosphoglyceric acid
4-Ac-AICAR	5-Acetamido-1-(2',3',5'-tri-O-acetyl- $\beta$ -D-ribofuranosyl)-imidazole-4-carboxamide
AAS	Androgenous Anabolic Steroids
Ac <sub>2</sub> O	Acetic Anhydride
AcCl	Acetyl Chloride
Acetyl-CoA	Acetyl Coenzyme A
AcOEt	Ethyl Acetate
ACN	Acetonitrile
ADP	Adenosine Diphosphate
ADSL	Adenylosuccinate Lyase
ADSS	Adenylosuccinate Synthase
AICAR	5-Aminoimidazole-4-carboxamide-1- $\beta$ -D-ribofuranoside
AMP	Adenosine Monophosphate
AMPK	Adenosine Monophosphate-Activated Protein Kinase
amu	Atomic Mass Unit
Andro	Androsterone
ATIC	5-Aminoimidazole-4-carboxamide ribonucleotide formyl transferase/IMP cyclohydrolase
ATP	Adenosine Triphosphate
a.u.	Arbitrary Units
C	Carbon
<sup>12</sup> C	Carbon 12
<sup>13</sup> C	Carbon 13

$^{14}\text{C}$	Carbon 14
CA	California
CAM	Crassulacean Acid Metabolism
CAN	Canada
CIRM	Certified Isotopic Reference Material
CHO	Chinese Hamster Ovary
$\text{CO}_2$	Carbon dioxide
CSIA	Compound-Specific Isotope Analysis
CSIR	Carbon Stable Isotope Ratios
CTP	Cytidine Triphosphate
$\text{CuO}$	Copper (II) oxide
D	Deuterium
DHEA	Dehydroepiandrosterone
EA	Elemental Analyzer
EA-IRMS	Isotope Ratio Mass Spectrometry coupled with an Elemental Analyzer
ERC	Endogenous Reference Compound
ES	External Standard
Et	Etiocolanolone
$\text{Et}_3\text{N}$	Triethylamine
FID	Flame Ionization Detector
GC	Gas Chromatograph
GC/C/IRMS	Isotope Ratio Mass Spectrometry coupled to Gas Chromatography via a Combustion interface
GC-MS	Mass Spectrometry coupled with Gas Chromatography
GDP	Guanosine Diphosphate
GEOTOP	<i>Centre de recherche sur la dynamique du système Terre</i>
GLUT-4	Glucose Transporter Type-4
GMP	Guanosine Monophosphate
GMPS	Guanosine Monophosphate Synthase

GTP	Guanosine Triphosphate
H	Hydrogen
HCOOH	Formic Acid
He	Helium
HGPRT	Hypoxanthine-Guanine Phosphoribosyltransferase
HMG-CoA	3-Hydroxy-3-methylglutaryl-coenzyme A
HPLC	High-Performance Liquid Chromatography
Hsp90	Heat Shock Protein 90
IEAE	International Atomic Energy Agency
IMP	Inosine Monophosphate
IMPDH	Inosine Monophosphate Dehydrogenase
INRS-AFSB	<i>Institut National de la Recherche Scientifique - Centre Armand-Frappier Santé et Biotechnologie</i>
IOC	International Olympic Committee
IS	Internal Standard
ISL	International Standard for Laboratories
ISO/IEC	International Organization for Standardization/International Electrotechnical Commission
IUPAC	International Union of Pure and Applied Chemistry
iv	Intravenous
KEGG	Kyoto Encyclopedia of Genes and Genomes
KIE	Kinetic Isotope Effects
MeOH	Methanol
Mix-Ac	Standard mix containing 3-Ac-AICAR and 3-Ac-uridine of known $\delta^{13}\text{C}$ values
Mix-AU	Standard mix containing AICAR and uridine of known $\delta^{13}\text{C}$ values
MP	Mobile Phase
MS	Mass Spectrometer
<i>m/z</i>	Mass-to-Charge Ratio

$^{14}\text{N}$	Nitrogen 14
$^{15}\text{N}$	Nitrogen 15
$\text{N}_2$	Dinitrogen
$\text{N}_2\text{O}$	Nitrous Oxide
nA	Nanoampere
NY	New York
$\text{NH}_4\text{Ac}$	Ammonium Acetate
$\text{NH}_4\text{OH}$	Ammonium Hydroxide
NO	Nitric Oxide
$\text{NO}_2$	Nitrogen Dioxide
$\text{NO}_x$	Nitrogen Oxides
$\text{O}_2$	Dioxygen
$^{16}\text{O}$	Oxygen 16
$^{17}\text{O}$	Oxygen 17
$^{18}\text{O}$	Oxygen 18
OAA	Oxaloacetic acid
ON	Ontario
PA	Polyacrylamide
PBA	Phenyboronic Acid
PCIRM	Primary Certified Isotopic Reference Material
Pd	$5\beta$ -Pregnanediol
PDB	<i>Pee Dee Belemnite</i>
PED	Performance Enhancing Drug
PEP	Phosphoenol Pyruvate
PFK	Phosphofructokinase
PPAR $\delta$	Peroxisome Proliferator-Activated Receptor $\delta$
PGC-1 $\alpha$	Peroxisome Proliferator-Activated Receptor Gamma Coactivator 1-alpha
PK	Pharmacokinetic

Pyr	Pyridine
qPCR	Quantitative Polymerase Chain Reaction
QC	Quebec
QCs	Quality-Control Samples
QCN	Reference urine containing only endogenous AICAR
QCP	Reference urine containing exogenous AICAR
RBC	Red Blood Cells
RI	Rhode Island
RM	Reference Material
RT	Room Temperature
RuBisCO	Ribulose-1,5-bisphosphate Carboxylase/Oxygenase
RuBP	Ribulose 1,5-biphosphate
<sup>32</sup> S	Sulfur 32
<sup>34</sup> S	Sulfur 34
SD	Standard Deviation
SIM	Single Ion Monitoring
SIM/dd MS <sup>2</sup>	Single Ion Monitoring followed by the equivalent of a data-dependant tandem mass spectrometry
SIR	Stable Isotope Ratios
SPE	Solid-Phase Extraction
SP	Stationary Phase
sZMP	5'-phosphoribosyl-4-succinocarboxamide-5-aminoimidazole ribonucleotide
T	Testosterone
TC	Target Compound
TD2015IDCR	WADA Technical Document on the Minimum criteria for chromatographic-mass spectrometric confirmation of the identity of analytes for doping control purposes
TD2019DL	WADA Technical Document for the decision limits for the confirmatory quantification of threshold substances

TD2019IRMS	WADA Technical Document for the detection of synthetic forms of endogenous anabolic androgenic steroids by GC-C-IRMS
USA	United States of America
UTP	Uridine Triphosphate
UV	Ultra-Violet
UV-HPLC	High-Performance Liquid Chromatography with Ultra-Violet detection
VEGF	Vascular Endothelial growth Factor
VPDB	<i>Vienna Pee Dee Belemnite</i>
WADA	World Anti-doping Agency
XMP	Xanthine Monophosphate
ZDP	5-Aminoimidazole-4-carboxamide-1- $\beta$ -D-ribofuranoside 5'-Dinophosphate
ZMP	5-Aminoimidazole-4-carboxamide-1- $\beta$ -D-ribofuranoside 5'-Monophosphate
ZTP	5-Aminoimidazole-4-carboxamide-1- $\beta$ -D-ribofuranoside 5'-Triphosphate
$^{45}\delta$	Raw $\delta^{13}\text{C}$ value uncorrected for the presence of $^{17}\text{O}$
$\delta^{13}\text{C}$	Carbon stable isotope signature
$\delta^{13}\text{C}_D$	$\delta^{13}\text{C}$ value of the derivatization reagent in the mass balance formula
$\delta^{13}\text{C}_T$	$\delta^{13}\text{C}$ value of the underivatized compound in the mass balance formula
$\delta^{13}\text{C}_{TC}$	$\delta^{13}\text{C}$ value of the target compound in the determination of $\Delta\delta^{13}\text{C}_{TC-ERC}$ values
$\delta^{13}\text{C}_{TD}$	$\delta^{13}\text{C}$ value of the derivatized compound in the mass balance formula
$\delta^{13}\text{C}_{ERC}$	$\delta^{13}\text{C}$ value of the ERC in the determination of $\Delta\delta^{13}\text{C}_{TC-ERC}$ values
$\delta^{15}\text{N}$	Nitrogen stable isotope signature
$\Delta\delta^{13}\text{C}_{TC-ERC}$	$\delta^{13}\text{C}$ difference (‰) between the target compound and the ERC as determined by $\delta^{13}\text{C}_{TC}$ (‰) - $\delta^{13}\text{C}_{ERC}$ (‰)
$\Delta\delta^{13}\text{C}_{A-U}$	$\delta^{13}\text{C}$ difference (‰) between AICAR and uridine as determined by $\delta^{13}\text{C}_{AICAR}$ (‰) - $\delta^{13}\text{C}_{Uridine}$ (‰)
$\Delta\delta^{13}\text{C}_{A-steroids}$	$\delta^{13}\text{C}$ difference (‰) between AICAR and the steroids analyzed in general (Pd, Andro and Et) as determined by $\delta^{13}\text{C}_{AICAR}$ (‰) - $\delta^{13}\text{C}_{Steroids}$ (‰)

$\Delta\delta^{13}\text{C}_{\text{A-Andro}}$	$\delta^{13}\text{C}$ difference (‰) between AICAR androsterone as determined by $\delta^{13}\text{C}_{\text{AICAR}} (\text{‰}) - \delta^{13}\text{C}_{\text{Andro}} (\text{‰})$
$\Delta\delta^{13}\text{C}_{\text{A-Et}}$	$\delta^{13}\text{C}$ difference (‰) between AICAR and etiocholanolone as determined by $\delta^{13}\text{C}_{\text{AICAR}} (\text{‰}) - \delta^{13}\text{C}_{\text{Et}} (\text{‰})$
$\Delta\delta^{13}\text{C}_{\text{A-Pd}}$	$\delta^{13}\text{C}$ difference (‰) between AICAR and 5 $\beta$ -pregnanediol as determined by $\delta^{13}\text{C}_{\text{AICAR}} (\text{‰}) - \delta^{13}\text{C}_{\text{Pd}} (\text{‰})$
$\delta^{18}\text{O}$	Oxygen stable isotope signature

## 1. General introduction

### 1.1 Background

On a global scale, the fight against doping in sports is led by the World Anti-Doping Agency (WADA), a non-profit organization founded in 1999 under the International Olympic Committee's (IOC) initiative [1]. To ensure prohibited substances and methods are clearly identified, WADA is responsible for the annual publication of the official Prohibited List (the List), an International Standard readily accessible to athletes and anti-doping laboratories all around the world [2]. The fact that this document has to be republished – and therefore updated – at least once a year, underlines the non-static nature of anti-doping rules and regulations. In fact, since the publication of the first version of the List by the IOC at the end of the 1960s, the document has evolved from a handful of specific compounds (mostly narcotics and stimulants) to a staggering 9-page long list comprising over 300 forbidden specific substances, classes of substances, as well as physical, chemical and biomolecular prohibited methods, all divided into 11 different categories [3]. Although necessary to ensure new products and scientific discoveries are taken into account, these annual updates put a strain on WADA-accredited laboratories. Since it is their responsibility to follow new regulations in order to maintain their accreditation, they are forced to adjust continuously, updating their detection methods whenever changes are made to the List.

When the 2009 List of Prohibited Substances was published, the five-letter acronym “AICAR” appeared for the first time in Section *M3. Gene Doping*<sup>1</sup>, referring to a molecule whose full name is 5-aminoimidazole-4-carboxamide-1-β-D-ribofuranoside (also AICAr, AICAR-riboside or acadesine, see Figure 1.1) [4]. AICAR was given as a specific example for a newly prohibited class of doping agents known as peroxisome proliferator-activated receptor  $\delta$  (PPAR $\delta$ ) and adenosine monophosphate-activated protein kinase (AMPK) agonists (referred to as PPAR $\delta$ -AMPK agonists in WADA's original document).

What prompted WADA to add AICAR to the 2009 Prohibited List was scientific and anecdotal evidence that AICAR had already been used, or could be used as a performance enhancing drug (PED). Indirect evidence of AICAR being used in high-level competitions had been discovered in

---

<sup>1</sup> AICAR has since been moved to Section *S4. Hormone and Metabolic Modulators*. Section *M3* has since been renamed *Gene and cell doping* and redefined in a more precise manner.

2009 when police investigated bins used by cyclists during the Tour de France [5]. Traces of AICAR, among other substances, were identified by means of laboratory analysis. AICAR's addition to the List was also further justified by subsequent events, like the arrest in Madrid, Spain, in March 2012 of Alberto Beltrán Niño, a Colombian doctor known to have worked for many cycling teams [6]. This was not Dr Niño's first time getting in trouble with the law however, as he had already been arrested back in 2001 in Italy with a car loaded with doping products. But this time, he was found carrying only two: a compound named TB-500 (thymosin beta-4, a protein) and AICAR.

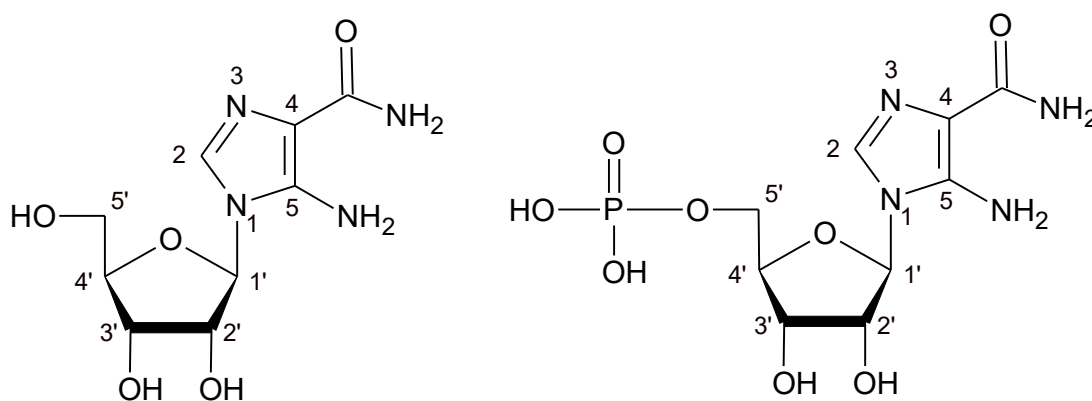


Figure 1.1: A) Molecular structure of 5-aminoimidazole-4-carboxamide-1- $\beta$ -D-ribofuranoside (AICAR in this work) and B) 5-aminoimidazole-4-carboxamide-1- $\beta$ -D-ribofuranoside 5'-monophosphate (ZMP in this work). Atom numbering is based on the official nomenclature of IUPAC.

AICAR was not the only compound added to the List in 2009, for instance Section *M3* also included another newly listed class of compounds named PPAR $\delta$  agonists, with a molecule identified as GW 1516 (2-[2-methyl-4-[[4-methyl-2-[4-(trifluoromethyl)phenyl]-1,3-thiazol-5-yl]methylsulfanyl]phenoxy]acetic acid, also GW 501516 or Endurobol) as a specific example. As discussed below, these two substances – AICAR and GW 1516 – are often administered simultaneously and therefore have shared a common history over the years. While analytical methods could be readily implemented for the detection of GW 1516 in athletes' urine [7, 8], the case of AICAR proved to be much more difficult. This can be easily understood by the fact that urinary AICAR has two possible origins:

1. *Exogenous* - AICAR is a drug that was initially developed by PeriCor Therapeutics under the name Acadesine. The compound has reached phase III of clinical studies, under the licence of what was then Schering-Plough, for its possible beneficial effects on reperfusion injuries during coronary artery bypass grafts when administered preventively [9]. The trial was eventually terminated in 2010 after an interim futility analysis yielded unsatisfactory probability for the drug to achieve acceptable efficacy [9, 10]. To this day, AICAR is not approved by health authorities, but it can be easily bought online;
2. *Endogenous* – As a nucleic acid analog, AICAR is also a naturally occurring molecule, present in every living cell’s intracellular environment and excreted in human urine at relatively high concentrations (i.e., in the low µg/mL range) [11-14].

Since there is no structural difference between the endogenous and exogenous forms of AICAR, the sole detection of the compound in urine samples by conventional analytical methods does not provide any information on its origin. As a consequence, no laboratory method was available to establish without a doubt the origin of the compound as a urinary component during its first few years on the List and building an AICAR doping case based on available techniques was altogether impossible. One could question the relevance of adding a new product on the List when there is no working method to determine if it has been used illicitly, but laboratory results are not the only proof available to build a doping case. An athlete’s testimony or confession, for instance, could be used against him/herself or another athlete in front of a sport court [2]. Adding a substance to the List also has a deterring effect towards doping as laboratories are usually discreet about their analytical capacities and most athletes are not aware of the analytical limitations of WADA accredited laboratories. To further increase deterrence with regard to doping involving “difficult” doping agents, WADA encourages long-term storage of samples – especially samples collected during internationally important sporting events – since retesting old samples can uncover new doping cases and increases the chances that laboratory analyses expose such cases years later.

Since laboratory evidence is exact and not arbitrary, it is by far the best asset for anti-doping authorities to identify cheaters and so the development of a method that specifically establishes the origin of AICAR in urine is essential. The first attempts at establishing AICAR’s origin in urine samples focused on evaluating normal levels of the urinary molecule. Thomas et al. (2010)

[12], from the German Sport University in Köln (Germany) WADA accredited laboratory, measured AICAR concentrations in nearly 500 athlete samples in the hope of determining a threshold above which suspicion could be raised. This approach was replicated by two subsequent studies [11, 13]. Although it was possible to establish that normal levels of the compound in urine (means of roughly 0.5 to 1  $\mu\text{g/mL}$ ) were lower than the ones measured right after oral ingestion (a maximum around 10  $\mu\text{g/mL}$  after a 10-gram oral ingestion [11]) or after iv injection (concentrations  $> 100 \mu\text{g/mL}$  are expected [12]), this methodology had very limited application potential. This is mainly because of (i) the wide distribution of concentration in undoped individuals with population outliers that overlap with positive cases, and (ii) the very high clearance rate of AICAR resulting in a very narrow detection window [15, 16]. A reasonable doubt can therefore be raised by every athlete for whom a suspicious amount of AICAR has been found in a urine sample. Since these concentration studies could not establish any definitive threshold for a positive test, WADA could not provide laboratories with any instructions on how to report an adverse analytical finding and WADA's AICAR-related documentation was left unchanged.

In 2013, another attempt was made by Thomas et al. [17], this time by measuring normal concentrations of the phosphorylated form of AICAR, 5-aminoimidazole-4-carboxamide-1- $\beta$ -D-ribofuranoside 5'-monophosphate (ZMP, also in Figure 1.1) in red blood cells (RBC). The team evaluated the range of normal ZMP concentrations in erythrocytes from blood samples of 99 athletes. They also showed that intracellular ZMP levels remain stable over time for a given individual, which makes possible the determination of a "baseline" concentration. Increasing the amount of available external AICAR, for instance by blood perfusion or oral intake of high enough dosage, disrupts this baseline concentration as AICAR is known to be quickly internalized and converted to ZMP by erythrocytes [15, 16]. Moreover, this sudden rise in ZMP concentration is expected to last for the lifetime of the RBC, extending AICAR's detection window to a few days [17]. Despite the fact that blood collection is more invasive and less common than urine, this technique proved to be promising. However, its application relied on ZMP's baseline concentrations in RBC being monitored over time for every athlete in order to detect any abnormal variation. This type of data acquisition is said to be longitudinal and is already performed by WADA for inclusion in the Athlete Biological Passport (ABP) in which every tested athlete has a record of monitored hematological and steroidal parameters [18].

Unfortunately, no follow-up was ever made on Thomas et al.'s work and the ZMP level in RBC was never implemented as a parameter of the ABP.

The best analytical tool anti-doping laboratories have in hand to distinguish between compounds that can have both endogenous and exogenous origins is the measurement of carbon stable isotope ratios (CSIR). CSIR analysis has been commonplace in the field of anti-doping research and biomonitoring for the last 30 years or so [19]. It is mostly used to detect the exogenous administration of androgenic anabolic steroids (AAS), for which the most well-known example is testosterone (T) whose presence in urine can either stem from exogenous administration or simply from the metabolism of androgens naturally produced by the human body. CSIR analysis relies on small but detectable differences in the ratio of carbon 13 ( $^{13}\text{C}$ ) to carbon 12 ( $^{12}\text{C}$ ) for target compounds such as T metabolites within a given sample [20]. The measurement is said to be compound-specific, meaning that it allows the determination of a mean  $^{13}\text{C}/^{12}\text{C}$  value for the carbon (C) atoms of single molecules that are selectively isolated from a sample's matrix. For reasons detailed below, the  $^{13}\text{C}/^{12}\text{C}$  ratio of T having a synthetic source is lower than the one of T that is naturally excreted in human urine. Abnormally low T-specific  $^{13}\text{C}/^{12}\text{C}$  values can then ultimately allow for the detection of the synthetic product's administration.

In 2009, when AICAR was classified as a prohibited substance by WADA, it was not known whether a CSIR method could be developed as there was no existing information on the isotopic composition of commercially available AICAR. Indeed, a CSIR method would not be feasible if synthetic AICAR was too similar in its  $^{13}\text{C}/^{12}\text{C}$  ratio relative to the range of possible endogenous values. A CSIR protocol was eventually published in 2014 demonstrating the feasibility of using C isotopes for detecting AICAR doping by Piper et al. also from the German Sport University [11]<sup>2</sup>. Properly implementing this method was however not an easy task, as described by a follow-up paper by Buisson et al. (2017) from the Paris, France, anti-doping laboratory [22]. Conventionally-used solid phase extraction (SPE) techniques could not recover AICAR from urine in a quantitative way, so Piper had to rely on the unpleasant task of freeze-drying urine to pre-concentrate it before purification by high-performance liquid chromatography (HPLC). Since the AICAR molecule needs to be stabilized in order to resist the high temperatures required

---

<sup>2</sup> Another unsuccessful attempt by the same laboratory to use nitrogen stable isotopes ( $\delta^{15}\text{N}$ ) is also worth mentioning [21].

during CSIR analyses, a chemical derivatization step was also critical to doing CSIR work. But the choice of derivatization agent chosen for the two publications caused method artefacts and forced the laboratory to change instrument consumables each time AICAR was injected. This lack of reliability has no place in a quality-controlled setting like an anti-doping laboratory that routinely has to defend results in a court.

To date, AICAR is still a prohibited substance under WADA's Prohibited List. However, because the analytical difficulties associated with its measurement are not trivial, WADA has not yet obliged all laboratories to implement their own version of a CSIR method for AICAR and only two out of the 30 WADA-accredited laboratories that have developed functional methods so far. The principal goal of this work is the development and the implementation of a new CSIR method with improved reliability, robustness and ease of use that can be uniformly adapted and put into practice by other WADA laboratories.

## **1.2 AICAR in the scientific literature and in the media**

Over the years, AICAR has not only been the subject of many scientific studies but has also been featured multiple times in mainstream media. The goal of the next sections is not only to make a thorough description of all AICAR-related literature, but also to allow the reader to understand how studies on AICAR, especially those conducted on mice, eventually had the unintended consequence of promoting AICAR doping in individuals attempting to increase endurance during sporting activities – a use for AICAR that has not deliberately been tested by the scientific community.

### **1.2.1 AICAR nomenclature**

When reviewing the literature about AICAR, one of the first observations made is the ambiguity in the appropriate use of the acronym itself. Depending on the publication, it can either refer to the ribonucleo"s"ide or the ribonucleo"t"ide form of the molecule (Figure 1.1). Other forms of the acronym (e.g. rAICA) can also be found in early works [23]. For the sake of simplicity, this work will refer to the nucleoside as AICAR, whereas the nucleotide will be designated by ZMP (where the "Z" refers to imida"Z"ole), a commonly used abbreviation. The term "acadesine" is mostly employed to designate the pharmaceutical product.

### 1.2.2 Early work

The history of AICAR in the scientific literature is as old as the science of nucleic acids, even though very few publications mentioning the molecule were issued in the 1950s and 1960s. At the time, cell culture research (made on e.g., *E. coli* [24, 25], *B. Subtilis* [26], *S. Typhimurium* [27], human [28] and rabbit [29] erythrocytes) were focused on elucidating the histidine and purine *de novo*<sup>3</sup> pathways in which the ribonucleotide form of AICAR, ZMP (Figure 1.1), takes part as an active intermediate. The low intracellular concentration of ZMP made difficult its detection and therefore, the study of its properties. Further HPLC development and the synthesis of larger amounts of AICAR and ZMP eventually helped overcome these issues. At the end of the 1970s and beginning of the 1980s, it was realized that AICAR, as an adenosine analog, could be picked up by adenosine transporters and carried through cell membranes where phosphorylation by adenosine kinase to ZMP was then possible and allowed AICAR to enter the cell's metabolism [30, 31]. This led to the exploration of possible therapeutic properties for the compound. Although results were inconclusive and never led to practical applications, those studies helped shed light on ZMP being an active molecule in the intracellular environment rather than just an intermediate metabolite. For the rest of the 1980s and the first half of the 1990s, the amount of published work involving AICAR remained scarce, but interest was on the rise.

### 1.2.3 AICAR as an AMPK activator

It has been known since the 1960s that living cells regulate their energy through the purine-related adenosine mono-, di- and triphosphate (AMP-ADP-ATP) system. Chemical energy is stored in the form of ATP which is used as a source of energy for the vast majority of intracellular processes. In order to keep enough spare energy supplies, the ATP:ADP ratio is constantly kept around 10:1, which is about 8 orders of magnitude higher than the system's equilibrium ratio ( $\approx 10^{-7}$ ). However, the mechanism by which the relative concentrations of the nucleotides are monitored took a couple more decades to be elucidated. Even though it had been suspected for a long time that the three nucleotides themselves were somehow involved in the signaling pathways of their own concentration fluctuation, it is only in the 1980s that AMPK was identified as the enzyme acting as a metabolic "switch" following the rupture of cellular

---

<sup>3</sup> The term "*de novo*" refers here to a bottom-up synthesis, i.e. adding up together smaller molecules to build a new compound of larger dimension. Pathways in which molecules are recycled are termed "salvage pathways".

homeostasis in mammalian cells. More precisely, AMPK is very sensitive to an increase of the AMP:ATP ratio. AMP is an allosteric activator of AMPK, meaning it does not bind to the AMPK's active site, but rather to an allosteric site to allow a conformational change that increases the enzyme reactivity. Consistently, high concentrations of ATP inhibit AMPK by preventing new binding to its allosteric site. Any cellular stress demanding energy and therefore interfering with the AMP to ATP ratio (e.g., hypoxia, hypoglycemia, physical exercise) activates AMPK. Despite this central role played by the enzyme in cellular energy management, authors writing about AMPK often stress that this initial activation by AMP is only a very small part of the whole cascade of reactions that subsequently takes place. AMPK has many downstream targets and therefore, many effects on other enzymes and gene expressions (Table 1.1) [32, 33].

Table 1.1: Non exhaustive list of AMPK activation effects excerpt from [32, 33].

Effect	Pathway affected	Fast or acute (F) Chronic via gene expression (G)
Stimulation/Increase	Fatty acid oxidation	F,G
	Glucose uptake	F,G
	Glycolysis	F,G
	NO production	F
Inhibition/Decrease	Fatty acid synthesis	F,G
	Sterol/Isoprenoid synthesis	F
	Triacylglycerol synthesis	F
	Lipolysis	F
	Apoptosis	F
	Autophagy	F
	Protein synthesis	F

Researchers who first tried to study AMPK's targets and mechanisms of action soon realized that isolating the protein's specific effects was difficult since any action activating the enzyme, i.e., any stress depleting the levels of ATP, could result in non-specific side-effects on the cell. They then looked for ways to activate AMPK without disturbing the intracellular pool of nucleotides.

In 1994, two studies by Sullivan et al. on human hepatocytes [34] and on rat adipocytes [35] reported that this was possible by incubating cell cultures with low concentrations of AICAR. Even though not as potent as AMP by a roughly 20-fold factor, ZMP obtained by AICAR phosphorylation can activate AMPK by binding to the same allosteric site while leaving unchanged levels of ATP, ADP and AMP within cells. This was a turning point for AICAR, arousing scientific interest and giving rise to a very distinctive spike in the number of publications from the mid-1990s to the early 2000s pertaining to the mechanisms linked to AMPK [36], the isolation of many of its properties and the study of the cascade of enzymatic reactions and metabolisms triggered by the enzyme. A large proportion of the work on AICAR was then related to AMPK and its effects, as opposed to the purine and histidine pathways.

Amusingly, the effects of AMPK's activation had been discovered before the enzyme was even properly identified. These include terpenoid and sterol synthesis inhibition through the inactivation of the 3-hydroxy-3-methylglutaryl-coenzyme A reductase (HMG-CoA reductase) as well as fatty acid and triglycerides synthesis inhibition after inactivation of acetyl coenzyme A (Acetyl-CoA) [37 and references therein], two ATP-consuming processes. In parallel, catabolic mechanisms producing ATP, like glycolysis accompanied by an increase in glucose uptake as well as fatty acid oxidation, are promoted by AMPK [33 and references therein]. In their 2003 minireview on the topic, Hardie et al. summarized AMPK activation in the simplest way:

“AMPK activation switches off anabolic pathways and other processes that consume ATP, while switching on catabolic pathways that generate ATP.”[33] This straightforward explanation highlights how an AMPK activator like AICAR can mimic the effect of exercise, however it hides the complexity associated to AMPK when it comes to regulating cellular homeostasis.

AMPK has multiple direct and indirect targets, including mostly other enzymes that can in turn be activated (or inactivated) by phosphorylation, but also transcription factors for specific sets of genes (see [38] for a detailed recent review). Notably, AMPK has been linked to skeletal muscle gene expression in men [39]. Another important element associated with AMPK's activation is PPAR $\delta$ , a nuclear receptor associated to lipid metabolism and studied as a possible target for chronic diseases, like type-II diabetes, obesity and atherogenic inflammation [40]. In humans, one of its targets is the peroxisome proliferator-activated receptor gamma coactivator 1-alpha (PGC-1 $\alpha$ ). PGC-1 $\alpha$  is a transcriptional coactivator playing a major role in mitochondrial biogenesis and therefore, intracellular energy management [41]. As discussed in the section

describing the effects of AICAR on pluricellular organisms, AICAR's ability to mimic exercise upon AMPK's activation is PPAR $\delta$ -dependant.

To fully describe AMPK downstream targets and effects is beyond the scope of this work, not only because of the very large amount of information, but also because a lot of research is still ongoing in the field and paints but a fragmented picture of what is actually occurring. Table 1.1 describes AMPK's confirmed and most often described effects that can be found in the literature.

#### **1.2.4 ZMP as a bioactive molecule in cells**

It is interesting to note that AICAR alone does not play any known active role in the intracellular environment. However, its presence is detectable, not only in cells (in small concentration because of its rapid conversion into ZMP [42]), but also in body fluids [11-13, 43, 44]. The enzyme converting ZMP to AICAR by dephosphorylation is not known either [43]. To become part of a cell's metabolism, AICAR has to be "activated" by phosphorylation of its hydroxyl group at the C5' position. Its phosphorylated form, ZMP, is generally described as an intermediate in the purine *de novo* synthesis. Purines (i.e., adenine, guanine and related molecules, see Figure 1.2) are primordial in all life forms. Their intracellular synthesis and breakdown are described by the purine metabolic pathway (Figures 1.3 and 1.4), a complex mapping of all molecules and enzymes involved in the biosynthesis and catabolism of purines and purine-related compounds. Even though variations in metabolic routes are expected among life forms, it is striking that the pathways involved are conserved in all eukaryote organisms [45]. In addition to their role in the ATP-ADP-AMP system, the importance of the purine metabolism is also highlighted by the proximity of the genetic coding language across organisms with purines used as building blocks of DNA and RNA [46]. The purine *de novo* pathway is usually depicted as starting with 5-phospho-alpha-D-ribose 1-diphosphate (PRPP) at the top end, then going downstream through the intermediates and the purines themselves. A simplified version is presented in Figure 1.3.

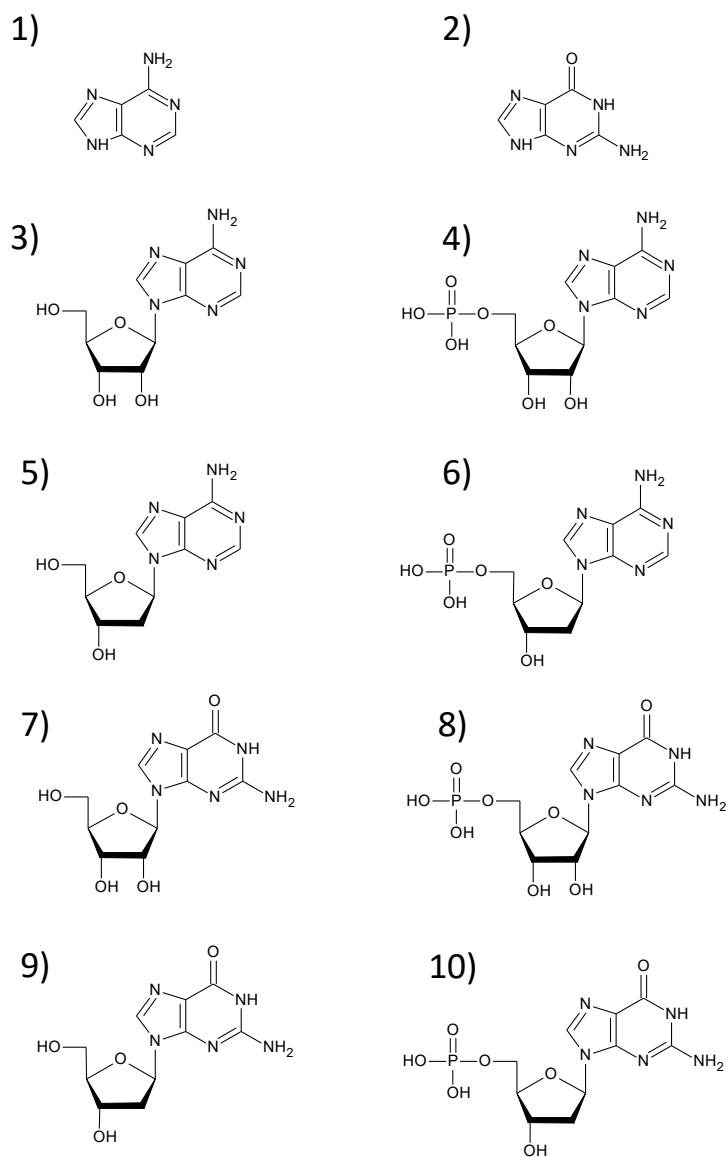


Figure 1.2: Examples of purine nucleobases, nucleosides and nucleotides 1) adenine; 2) guanine; 3) adenosine; 4) adenosine-5'-monophosphate (AMP); 5) 2'-deoxyadenosine; 6) 2'-deoxyadenosine-5'-monophosphate; 7) guanosine; 8) guanosine-5'-monophosphate (GMP); 9) 2'-deoxyguanosine and 10) 2'-deoxyguanosine-5'-monophosphate.

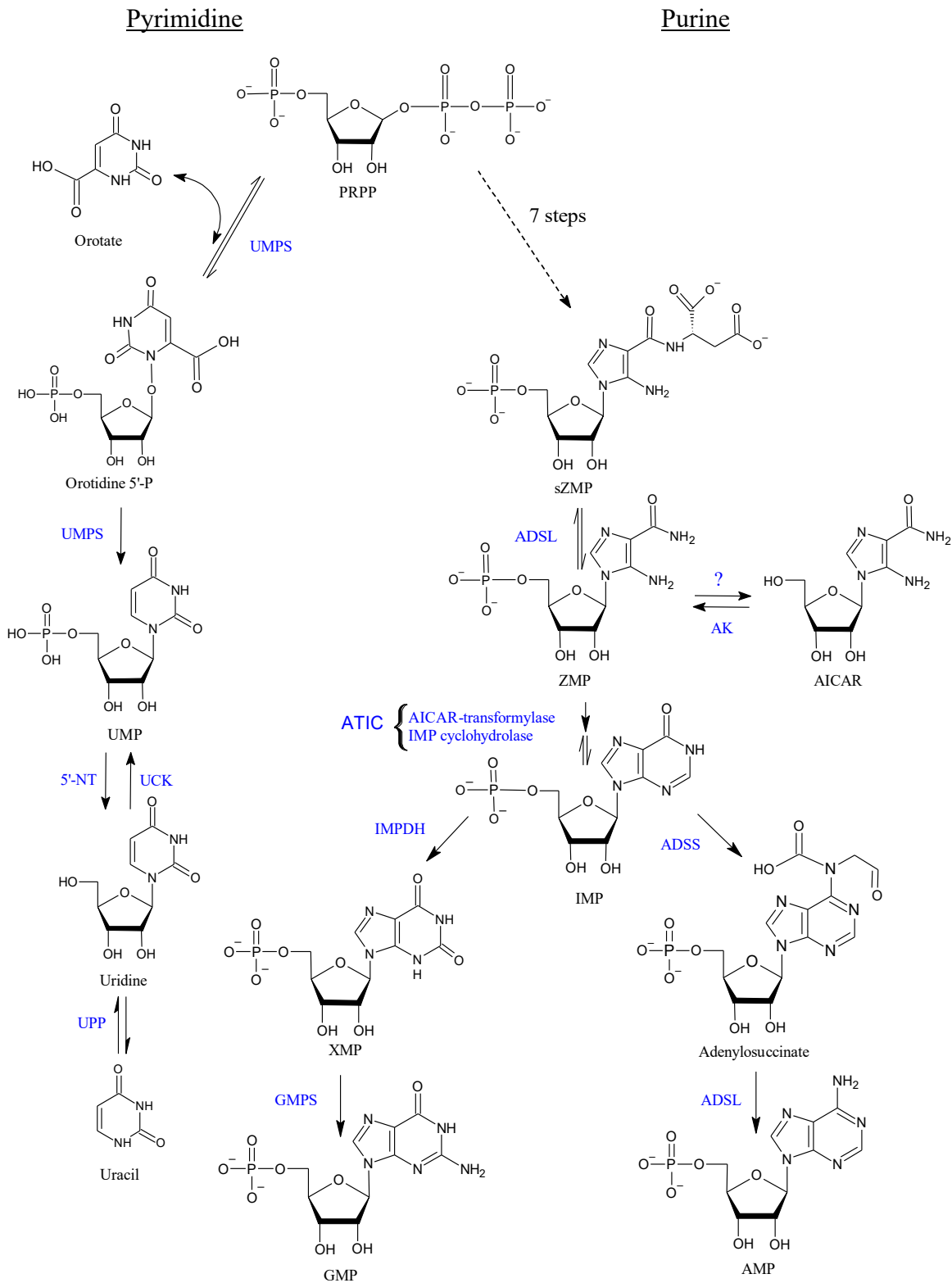


Figure 1.3: Schematic of the pyrimidine (left) and purine (right) pathways, adapted from the Kyoto Encyclopedia of Genes and Genomes (KEGG) [47-49] and [43, 50, 51]. Compounds

abbreviations are in black and enzyme abbreviations are in blue. The question mark indicates an unknown enzyme. 5'-NT: 5'-nucleotidase, ADSL: adenylosuccinate lyase, ADSS: adenylosuccinate synthase, AMP: adenosine monophosphate, AICAR: 5-aminoimidazole-4-carboxamide-1- $\beta$ -D-ribofuranoside, AK: adenosine kinase, AMP: adenosine monophosphate, ATIC: 5-aminoimidazole-4-carboxamide ribonucleotide formyl transferase/IMP cyclohydrolase, GMP: guanosine monophosphate, GMPS: guanosine monophosphate synthase, IMP: inosine monophosphate, IMPDH: inosine monophosphate dehydrogenase, orotidine 5'-P: orotidine 5'-phosphate, sZMP: 5'-phosphoribosyl-4-succinocarboxamide-5-aminoimidazole ribonucleotide, UCK: uridine-cytidine kinase, UMP: uridine monophosphate, UMPS: uridine monophosphate synthase, UPP: uridine phosphorylase, PRPP: phosphoribosyl pyrophosphate, XMP: xanthine monophosphate, ZMP: 5-aminoimidazole-4-carboxamide-1- $\beta$ -D-ribofuranoside 5'-monophosphate.

When it is assembled endogenously, ZMP is synthesized from 5'-phosphoribosyl-4-succinocarboxamide-5-aminoimidazole ribonucleotide (succinyl-ZMP or sZMP) by adenylosuccinate lyase (ADSL) and then further metabolized to inosine monophosphate (IMP) by a protein named ATIC (5-aminoimidazole-4-carboxamide ribonucleotide formyl transferase/IMP cyclohydrolase). As its full name suggests, ATIC displays two enzymatic activities: AICAR-transformylase and IMP cyclohydrolase. Following its formation, IMP can be (i) converted to adenylosuccinate by adenylosuccinate synthase (ADSS) and then form AMP with the help of ADSL; or (ii) transformed into xanthine monophosphate (XMP) by IMP dehydrogenase (IMPDH) which can in turn produce guanosine monophosphate (GMP) by GMP synthase (GMPS) activity. Intracellular levels of ZMP are usually low and tightly regulated by a feedback mechanism in which ZMP inhibits ADSL, the enzyme responsible for its own synthesis. Since an accumulation of ZMP can lead to cytotoxicity, the feedback regulation of the ADSL enzymatic activity is crucial [43, 45, 47-50].

Purines are usually catabolized by dephosphorylation followed by a cleavage of the bond between the sugar and the nitrogenous base, respectively producing adenosine and adenine in the case of AMP as well as guanosine and guanine in the case of GMP. Guanine follows the path of conversion to xanthine which in turn is oxidised to uric acid. The same fate awaits adenine that

must however be converted to hypoxanthine prior to its oxidation to xanthine [47-49, 52]. This process is summarized in Figure 1.4. Pharmacokinetic (PK) studies have shown that in humans, almost half of AICAR administered by intravenous (iv) injection is ultimately converted to uric acid [15, 16].

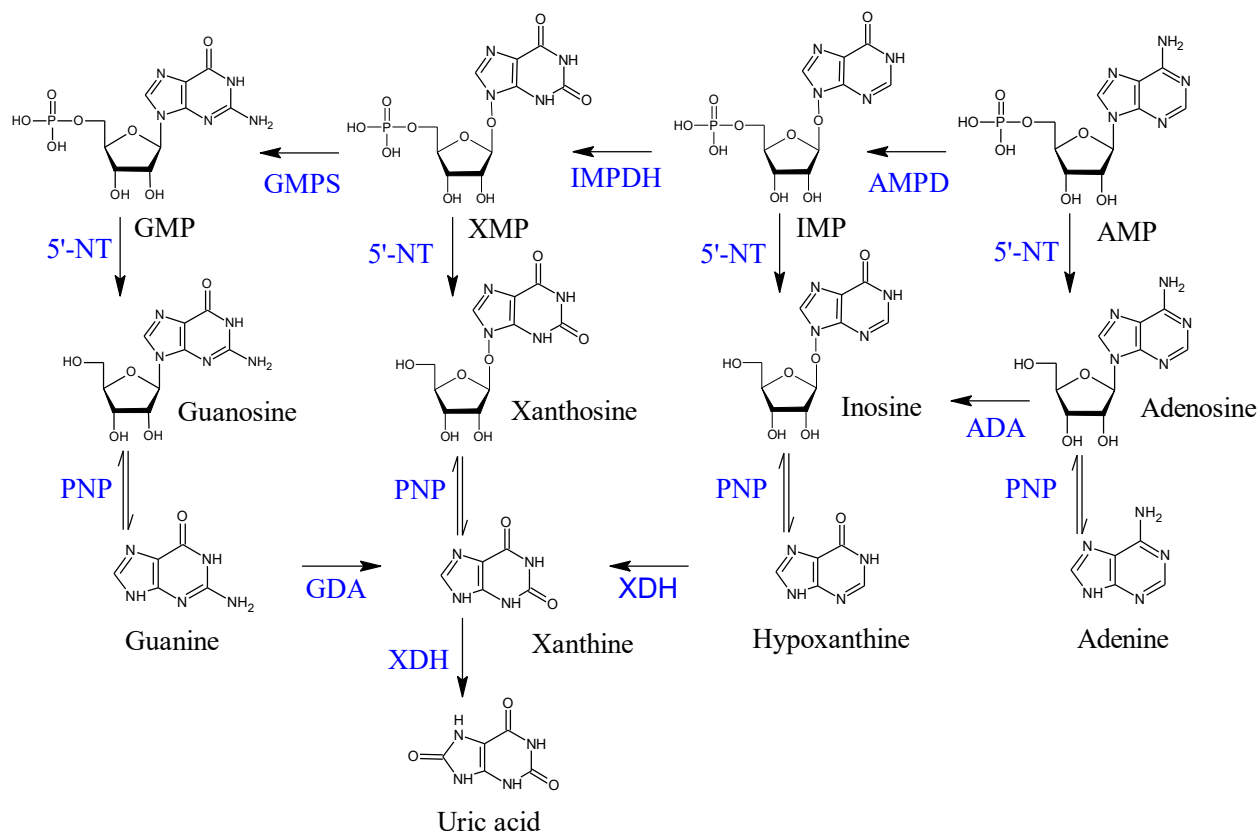


Figure 1.4: Schematic of the purine catabolic pathway excerpt from the KEGG [47-49]. Compounds abbreviations are in black and enzyme abbreviations are in blue. 5'-NT: 5'-nucleotidase, ADA: adenosine deaminase, AMP: adenosine monophosphate, AMPD: adenosine monophosphate deaminase, GMP: guanosine monophosphate, GMPS: guanosine monophosphate synthase, GDA: guanine deaminase, IMP: inosine monophosphate, IMPDH: inosine monophosphate dehydrogenase, PNP: purine nucleoside phosphorylase, XDH: xanthine dehydrogenase, XMP: xanthine monophosphate.

Aside from the purine metabolism, ZMP has also been associated with other metabolic pathways. For example, in some micro-organisms (e.g., budding yeast [*S. cerevisiae*] and some strains of *E.*

*coli*), it has been demonstrated that a non-negligible proportion of ZMP was produced as a by-product of the histidine pathway [50, 53]. ZMP is also indirectly linked to the pentose phosphate pathway, which supplies PRPP to the purine, pyrimidine and histidine pathways in some microorganisms and to the purine and pyrimidine pathways in mammalian cells [54]. Finally, intracellular ZMP accumulation has been shown to interfere with the folate and methionine metabolisms [50].

### **1.2.5 Effects of AICAR on the purine metabolism**

Early studies on the purine metabolism proved to be difficult since intracellular levels of the intermediates involved, like ZMP and sZMP, are typically low (i.e., <0.05 nmol per mg of cell protein [31]). This likely explains the relatively small amount of work published on the topic before the 1970s. However, the knowledge gathered using isotopic tracers before 1960 was already impressive, as reported by Hartman and Buchanan in 1959 [55]. The purine pathway had also been studied extensively in many types of cells [56]. It was soon discovered that animal and human erythrocytes were unable to achieve total *de novo* synthesis of purines [28, 29].

Researchers then started to incubate erythrocytes from different origins with different purines and purine precursors, in attempts to identify which steps of the pathway required an external source of purine. This is how AICAR was found to have the ability to be internalized by cells and converted into ZMP [23]. At the end of the 1970s and during the 1980s, the development of radioimmunoassay and HPLC allowed for detection of smaller quantities of analytes and progressively enhanced the analytical capacities of metabolism studies (e.g., [31]). AICAR has been used in incubation experiments with a plethora of different cells, including but not limited to budding yeast (*S. cerevisiae*) [50], *E. coli* [53], rabbit [29, 57] and human [58] erythrocytes, human adipocytes [59], mouse [60] and human [61] fibroblasts, skeletal [62] and vascular [63] muscle cells of mammalian origin and ovary cells of animal origin [31].

Sabina et al. (1985) carried out experiments using Chinese Hamster Ovary (CHO) cells to document extensively AICAR's effects on the purine and pyrimidine metabolism [31]. Their results are summarized in Table 1.2 and can be more easily understood using Figure 1.3. Upon incubation in a medium containing AICAR in the micromolar range (50 to 700  $\mu\text{M}$ ), they observed that ZMP – usually present at levels that are not quantifiable - could accumulate in CHO cells. They also noted that the concentration of intracellular ZMP was dependant on

AICAR's concentration in the incubation medium as well as on incubation time. This result suggested that AICAR's phosphorylation was not controlled or inhibited by any mechanism, since no intracellular concentration plateau was ever observed even after a 10-hour incubation. The metabolic fate of ZMP was dependant on its intracellular levels. At low levels, the expected pathway (i.e., conversion to IMP) occurred leading to the expansion of the IMP pool. Inosine and hypoxanthine, purine catabolites originating respectively from the hydrolysis of IMP and the phosphorolysis of inosine, were then excreted in the culture medium. A continuous increase of the adenylosuccinate concentration was also measured after up to 10 hours of incubation. Upon IMP accumulation, the adenylate and guanylate pools (that Sabina et al. [1985] measured as mono, di and triphosphate nucleotides) also increased. However, adenosine and guanosine nucleotides displayed different profiles. Adenylates concentrations quickly reached a maximum before returning to basal value after 8 hours of incubation. A similar behavior was observed for guanylates, but the concentration decrease was more pronounced and occurred after 5 hours of incubation until roughly 50% of the basal value was reached. At high ZMP concentrations, sZMP (the direct precursor of ZMP) and ZTP, the triphosphate form of AICAR, also accumulated. Finally, the pyrimidine pool, evaluated by measuring the concentrations of uridine triphosphate (UTP) and cytidine triphosphate (CTP), showed about 70% depletion after 10 hours. An increase in orotate, a pyrimidine precursor, was also noted.

Those results brought into light the complexity of the purine metabolism which can hardly be described as a system with enzymatic reactions proceeding unilaterally or in a way that is disconnected from other processes. In fact, to explain Sabina et al.'s (1985) results, many factors must be taken in consideration. These include, but are not limited to, enzyme feedback inhibition, reversed enzymatic activity, enzyme-substrate affinity constants and different reaction rates between enzymatic reactions. Another noteworthy aspect is how useful AICAR was to experiment on the purine metabolism by enabling to pinpoint a specific section of the pathway otherwise difficult to study. This could be interpreted as stating the obvious, but the consequences it had on the future of AICAR in scientific researches are important. This is evidenced by the increasing number of publications mentioning AICAR following Sabina et al.'s 1985 work [36].

Table 1.2: Effects of incubation with 700  $\mu$ M of AICAR on key players participating in the purine (and pyrimidine) metabolism for CHO cells, excerpt from Sabina et al.'s publication [31].

Compound/Group of compounds	Intracellular/Medium	Effect
ZMP	Intracellular	Detected after 5 min, steady increase to the end.
IMP	Intracellular	Fast increase within ca. 15 min, then stabilization.
Adenylosuccinate	Intracellular	Accumulation after ca. 30 min, steady increase to the end.
Adenylate pool (measured as AMP, ADP and ATP)	Intracellular	Fast increase to ca. 150% of basal value in the first hour, leveling off and return to basal value between 8 and 10 hours of incubation.
Guanylate pool (measured as GMP, GDP, GTP)	Intracellular	Fast increase to ca. 150% of basal value in the first hour, leveling off and decrease to <i>ca</i> 50% of basal value between 5 to 10 hours of incubation.
ZTP	Intracellular	Detected after 3 hours and steady increase to the end.
sZMP	Intracellular	Detected after 2 hours, base and nucleoside forms detected after 4 hours.
Pyrimidines (measured as UTP and CTP)	Intracellular	Steady decrease after 2 hours to reach ca. 30% of basal values.
Purine catabolites	Medium	Inosine and hypoxanthine detected after ca. 15 min and steady increase to the end.
Pyrimidine precursors	Medium	Orotate detected after 2 hours and steady increase to the end.

### 1.2.6 Other effects

AICAR and/or ZMP are present in a wide array of studies covering many different specialized topics. While the above sections describe the most encountered topics about the two compounds, it must be remembered that there is a growing number of target examples for intracellular ZMP, many of which are other nucleotide-binding enzymes and proteins, not necessarily related to AMPK nor the purine metabolism. Interesting examples include the inhibition of phosphofructokinase (PFK) and interaction with Heat Shock Protein 90 (Hsp90), both linked to tumor growth in specific cell lines [43].

### 1.2.7 Effects of AICAR on pluricellular organisms

Studies involving commonly used laboratory subjects are mostly linked to AMPK activation. Interesting findings include reduced fat storage in *Caenorhabditis elegans* (a microscopic worm) subjects and an increased resistance to anoxia in AICAR-administered *Drosophila melanogaster* (fruit fly) subjects. In vivo experiments done on larger animals are usually about potential therapeutic properties. Examples with mammals such as baboons [64], rabbits [65], rats [66-69] and dogs [70-73] and can be found as well as hundreds of studies performed with mice (see [60, 74-76] as examples).

As for humans, PK studies have been published in the 1990s after oral and iv administration of AICAR using a  $^{14}\text{C}$ -labelled tracer [15, 16]. Overall, the drug was tolerated well by all patients with only mild side-effects reported up to a dosage of 100 mg/kg. AICAR was found to be quickly internalized and converted to ZMP by RBC, with  $^{14}\text{C}$  from the nucleotide already accounting for 30% of all blood  $^{14}\text{C}$  at the end of perfusion. AICAR showed low oral bioavailability (< 5%) and the percentage of intact AICAR excreted in urine was small (< 10%). Uric acid, AICAR's major metabolite, represented almost half of the ingested  $^{14}\text{C}$ , with 44% recovered in urine and 4% in feces. Perhaps more relevant to this work, AICAR has been found to have high renal and total plasma clearance, meaning the drug's detection window is restricted to only a short period after its administration (roughly 10 hrs).

Aside from PK studies and the clinical trial already mentioned in Section 1.1, very little work with AICAR involving human subjects has been documented. Perhaps one exception worth mentioning is the effect of AICAR on type-II diabetes, for which a few studies have been conducted in the last 15 years [77-80].

The goal of most of the studies carried out on animals and humans is not to describe AICAR's effects on whole organisms in a general manner, but rather to monitor a small set of targeted and well-defined parameters. This considerably limits the information available on the consequences of AICAR administration on living organisms. An exception is the case of Narkar et al. (2008) [74] who undoubtedly published the most spectacular and widely disseminated results involving AICAR. These results will be discussed in greater detail as they not only sparked new interest for AICAR in the scientific community, but they also reached mainstream media where AICAR was depicted as a miracle product.

### **1.2.8 Narkar et al. (2008)**

The discussion so far on the molecular level impact of AICAR and AMPK activation has been leading up to a more complete understanding of the work of Narkar et al. (2008), who coined AICAR as “the exercise pill” and “promoted” its use as a doping agent in endurance sports. Professor Ron Evans at the Salk Institute for Biological Studies, California, USA, and his team studied the endurance-enhancing properties of GW 1516 and AICAR on mice (Narkar et al., 2008). Both compounds are depicted as pathway-specific drugs, since they display high affinities for PPAR $\delta$  and AMPK, respectively.

Despite showing an increase in muscle gene expression, mice treated with GW 1516 did not gain any endurance when evaluated on a treadmill. However, impressive results were obtained when physical training was used in combination with PPAR $\delta$ 's activation using GW1516. After a 4-week treatment, mice ran 68% longer and 70% further than the control group who had only been vehicle-trained. The authors then asked themselves the question: "What might be the molecular interface between mechanical exercise and PPAR $\delta$  transcription?" In other words, what process is triggered by physical exercise to activate PPAR $\delta$  and allow this “boost” by GW 1516? AMPK quickly came up as a possibility. To test their hypothesis, the team then used AICAR to specifically activate AMPK. Results were striking, as sedentary mice treated 4 weeks with AICAR ran 23% longer and 44% further than physically trained mice. A notable reduction of the mice fat-to-body weight ratio was also measured, results that corroborate some of the upregulated pathways in Table 1.2. This endurance-enhancing effect was not observed with mice deprived of the PPAR $\delta$  gene, meaning that the new “athletic” abilities of the mice were dependant on both AMPK and PPAR $\delta$ .

Pr Evans's team also used quantitative polymerase chain reaction (qPCR) to monitor genes known to be biomarkers that track the effects of the oxidative metabolism linked to physical exercise. More than a hundred different genes were investigated. This allowed the observation of unique gene signatures in the muscle cells of the rodent's quadriceps depending on whether AICAR and GW 1516 were administered alone, together or in combination with physical exercise. However, it is important to point out that AICAR alone does not act directly on genes, but rather activates different targets – including gene transcription factors – after its phosphorylation to ZMP. Since AMPK is an important target for ZMP, a lot of this gene activation is dependent on the protein.

Even though Narkar et al.'s results are impressive, titillating the public with a quick-fix for the physical discomfort of exercise with a pill, subsequent work has stressed the importance of being cautious when interpreting them. AMPK's activation by AICAR is no miracle, as the effects are mostly measured on a short-term period [81]. Its performance-enhancing effects measured on mice have never been replicated nor even tested on humans [38]. Moreover, GW 1516 has been found to be carcinogenic in many tissues and organs in animal models during the phase II clinical studies of the drug [9].

### **1.2.9 Possible therapeutic uses of AICAR**

AICAR has been used by Lowy and Williams in 1977 to investigate its effects on erythrocytes from a patient with the Lesch-Nyhan syndrome [23]. This condition is characterized by an enzymatic deficiency of hypoxanthine-guanine phosphoribosyltransferase (HGPRT). HGPRT takes part in the purine salvage pathway and catalyses the conversion of hypoxanthine into IMP, therefore a consequence of its deficiency is the accumulation of uric acid, a catabolic product of the purine breakdown, in blood and urine (Figure 1.3). Male patients with the Lesch-Nyhan syndrome are usually more affected, often showing severe physiological and neurological impairments with an odd tendency for self-mutilation. Lowy and Williams were interested in knowing if they could improve purine synthesis in HGPRT-deficient erythrocytes by by-passing the normal pathway by incubation with AICAR. Even though mammalian erythrocytes cannot achieve total purine synthesis by the *de novo* process, they display the ATIC activity necessary to complete the AICAR-to-ZMP conversion. AICAR could therefore be used to compensate for the

missing IMP from the purine salvage pathway. Of course, these experiments did not address the uric acid accumulation issue, but did help in our understanding of the purine biosynthesis.

AICAR was also tested for its potential beneficial actions on cardiac muscles after ischemia. It has been demonstrated that heart tissues going through a shortage in blood supply quickly become depleted of their purine and pyrimidine pool and that repletion requires a certain amount of time during which damages can occur. Since AICAR was known to have an effect on the level of purines in cell incubation experiments, attempts were made to see if the compound could be helpful to expedite the restoration of purine levels. Conflicting results were obtained on canine subjects [70, 71, 73], underlining the complexity of the biochemical pathways involved. Most of therapeutic possibilities associated to AICAR are related to its AMPK-activation properties. For example, the increase in glucose intake mediated by glucose transporter type-4 (GLUT-4) drew attention for possible insulin resistance treatment. AICAR has also been shown to improve angiogenesis and vascularization in mice post-ischemic hind limbs, by prompting the expression of the protein VEGF (vascular endothelial growth factor) in a process dependant on AMPK activation. Fat reduction by inhibition of lipogenesis as well as blood pressure control were also investigated [38, 81]. AMPK activation by AICAR also had anti-inflammatory effects by reducing cytokine levels, both *in vitro* on human aortic smooth muscle cells and *in vivo* in laboratory mice. Short-term effects of AICAR on brain functions, such as improved spatial memory, has been documented in mice. It is thought that these effects on the brain are indirect and also AMPK-dependant [81]. Anti-proliferative effects of ZMP were also studied on tumor growth for a few cell lines. This is thought to be due to ZMP's inhibition of PFK and interactions with Hsp90, two proteins believed to play an important role in cancer propagation [43].

### **1.2.10 Toxicity and occurrence in metabolic diseases**

Incubation of cells with AICAR leading to large ZMP accumulation is known to be cytotoxic. In yeast cells, millimolar concentrations of ZMP can cause histidine auxotrophy (incapacity to biosynthesize histidine) and eventually growth arrest [82]. ZMP accumulation is associated with accumulation of sZMP as well as the di- and triphosphate forms of ZMP (ZDP and ZTP, respectively) [43]. In yeast, recent work has demonstrated that ZMP itself, not its metabolites, is likely the cause of this toxicity. No negative effect has been established with the accumulation of intracellular AICAR (as a ribonucleoside) [82].

As for humans, erythrocytes of a subject displaying poor activity of the enzymeATIC (metabolizing ZMP to IMP) were also found to contain high levels of ZMP, ZDP, ZTP and sZMP. Such genetic condition is deleterious and causes severe neurological and physical impairments [83]. Following the same logic, ZMP is also thought to be the culprit in regards of the detrimental condition associated with the Lesch-Nyhan disease, mentioned earlier [84].

Very few negative effects are documented about treatment with moderate dosage of AICAR. As already mentioned, patients participating in PK and clinical studies with acadesine overall tolerated the drug well [15, 16]. A consequence of AICAR administration has been described by Aschenbach et al., who demonstrated that AICAR administration unavoidably leads to lactic acid accumulation in rat skeletal muscles [85]. It must be pointed out that only limited data is available for long-term use of AICAR.

### **1.2.11 AICAR as a doping agent: How mainstream media exaggerated research**

The scientific literature often referred to AICAR (and GW 1516) as an “exercise mimetic”, an expression perhaps not “flashy” enough for some media in which the product was given provocative labels such as “the exercise pill” [86] or “exercise in a pill” [87, 88]. Such a sensationalized description has to be taken *cum grano salis*, obviously, as the effects of the compounds are known to be limited in time and not fully understood, especially on the long-term scale. Nonetheless, this does not mean that AICAR is not to be taken seriously either. The arrest of Dr. Beltrán Niño, the traces of AICAR found in bins during the 2009 Tour de France, and rumors reported recently in the world of cycling [89] are reminders for anti-doping authorities to never lower their guard.

Concerns have also been raised outside the professional sport scene. Suppliers claiming to sell AICAR “for research purposes only” in order to evade regulatory agencies such as Health Canada and the Food and Drug Administration are numerous, therefore AICAR can be bought online by anyone, often without any guarantee on the product’s legitimacy and/or purity. Websites can be found to specify what they consider to be appropriate AICAR doses, even though such posology has never been determined for humans ([90-94] is only a small set of examples of what has been found during the making of this work). Because purchasing gram-amounts of AICAR is very expensive, recommended doses are usually much lower than the ones administered to rodents. For example, doses ranging from a daily 150 to 500 mg have been found

on the internet during the making of this work, whereas studies involving rodents typically used daily doses in the 150-500 mg/kg range (the equivalent of 12 to 40 g per day for an 80-kg individual). Errors in the animal-to-human dosage conversion were also uncovered, shining light on the incompetence of the advising persons. More alarmingly, AICAR is sometimes offered in combination with GW 1516, a product known to be carcinogenic for rats. Finally, it must be repeated that the efficacy of the compound as a PED has never been proven and that the medicinal properties reported for animal models have never been subjected to adequate testing in humans to validate claims often made by online AICAR suppliers.

Despite all the elements exposed in the paragraph above, the use of AICAR as a PED in amateur and professional sports is still dreaded, with some disciplines more susceptible than others. Endurance sports, for which a diminution of the fat-to-body weight ratio is an advantage (e.g., cycling, cross-country skiing), are particularly at risk. It is possible that AICAR consumption is a very rare occurrence in reality, but it is also plausible that the absence of appropriate detection methods for many years has allowed many cases to be missed out on. This kind of uncertainty places anti-doping authorities in a situation where *status quo* is unsustainable. For this reason, laboratories quickly turned to the best tool they have when prohibited substances can have both endogenous and exogenous origins: CSIR measurements.

### **1.3 Stable isotope ratios**

Anti-doping analyses are far from being the only concrete applications for which natural abundance stable isotope ratios are useful. Before explaining how they can be used to distinguish between endogenous and exogenous compounds in urine samples, a presentation of the general theoretical and practical concepts related to the topic will be made. The focus will then be turned to CSIR and how they are put to contribution in anti-doping sciences.

#### **1.3.1 General presentation**

In analytical chemistry, precise measurements of non-radioactive (stable) isotope ratios (SIR) have been used since the 1950s for a plethora of applications among a wide variety of fields. Even though this type of work is often related to earth sciences [95], more recent applications also include metabolomics [96, 97], forensic sciences [98], as well as more “exotic” fields like planetology [99, 100] for example. The ratio between two stable isotopes is usually reported with the heaviest (and less abundant) isotope as the numerator and the lightest (and more abundant)

isotope as the denominator. The number of different isotope ratios that can be found in the literature after an extensive review is very large and beyond the scope of this work. The most studied elements are typically hydrogen (D/H), carbon ( $^{13}\text{C}/^{12}\text{C}$ ), nitrogen ( $^{15}\text{N}/^{14}\text{N}$ ), oxygen ( $^{18}\text{O}/^{16}\text{O}$ ) and sulfur ( $^{34}\text{S}/^{32}\text{S}$ ), since they are in high abundance on Earth and closely related to life. Other specialized examples of work can be found on alkali (e.g., lithium [101]), earth alkaline metal (e.g., calcium [102] and strontium [103]), transition metals (e.g., iron [104]), halogens (e.g., chlorine [105]) and noble gases (e.g., krypton and xenon [106]). SIR can either be used as tracers (e.g., to follow the path of a given compound through an organism or process) or to give information about the source of a material. Interesting examples of applications for widely used elements can be found in Table 1.3.

Table 1.3: Examples of applications for SIR.

Isotopes	Application	References
D/H and $^{18}\text{O}/^{16}\text{O}$	Past climate reconstruction Resolving of hydrologic processes Origin of precipitations Geographical origin of human material	[107-110]
$^{13}\text{C}/^{12}\text{C}$	Source indicator of organic matter Detection of food adulterant Monitoring of climate changes Anti-doping analysis Forensic sciences	[111-117]
$^{15}\text{N}/^{14}\text{N}$	Trophic level determination Assessing the N cycle in aquatic environments	[118-120]
$^{34}\text{S}/^{32}\text{S}$	Origin of sulfide ore deposits	[121]

It should however be stressed that SIR measurements are not without challenge, both from an instrumental and an analytical point of view. Since the abundance of both isotopes can be very different from one another (for example  $^{15}\text{N}$  represents about 0.35% of naturally occurring nitrogen atoms while  $^{14}\text{N}$  makes up the remaining 99.65%), SIR are often very small. A problem

often encountered is the proper detection and quantification of heavier isotopes, often present in trace amounts. Moreover, significant variations observed between samples are often located on the fourth or even fifth decimal of the ratio. Accurately quantifying these differences therefore requires very specialized and delicately tuned equipment. Furthermore, to normalize inter-laboratory results to the same isotopic scale, the need for primary certified isotopic reference material (PCIRM) against which samples are measured was eventually brought forward [122]. For an element of interest, the measurement of an isotopic ratio can be given relatively to the one measured for a PCIRM. The result thus obtained is given as a per mil (‰) value on a delta ( $\delta$ ) scale specific to each element and having a general notation in the form of  $\delta^A X$  (‰). This is done using Equation 1a or 1b:

$$\delta^A X(\text{‰}) = \frac{R_S - R_{Std}}{R_{Std}} \times 1000 \quad (\text{Equation 1a})$$

$$\delta^A X(\text{‰}) = \frac{R_S}{R_{Std}} - 1 \times 1000 \quad (\text{Equation 1b})$$

where X is the chemical symbol of the element for which the SIR is measured, A is the mass number of the heavier isotope analyzed,  $R_S$  is the measured SIR of the analyzed sample and  $R_{Std}$  is the measured SIR of the PCIRM. In other words, introducing PCIRMs has established new relative measurement scales on which the PCIRM itself sets an arbitrary 0‰ value on the delta ( $\delta$ ) scale. The  $\delta$  value of any given sample can then be determined using Equation 1a or 1b. A value greater than 0‰ means that the sample contains a higher proportion of the heavy isotope relative to the PCIRM whereas negative  $\delta$  values are reserved for samples that are depleted in the heavy isotope relative to the PCIRM. Scales used for different elements are given names related to their PCIRM. For example, the scale employed for C stable isotope ratios is referred to as the VPDB scale, the four letters standing for PCIRM *Vienna Pee Dee Belemnite* [123]. In the 1950s and 60s, the first PCIRMs originated from natural materials. Nowadays, there is no need for supplying this “original” material to every laboratory measuring SIR; other materials that were calibrated against the original PCIRM by certifying bodies such as the International Atomic Energy Agency (IAEA) can be used; these materials are called certified isotopic reference materials (CIRMs). Using those CIRMs, working standards are also often calibrated in-house by the laboratories themselves for their daily analyses to reduce costs. This approach to anchor

isotopic measurements to a variety of certified materials has undeniably improved reproducibility among different laboratories and measurement techniques [122, 123].

Isotope ratio mass spectrometry (IRMS) is the general name for the instrumental technique by which SIR are measured. IRMS instruments are among the oldest and most specialized types of mass spectrometers (MS) [124]. Their sole purpose is to evaluate ratios between two to three isotopes of the same element through the acquisition of electronic signals specific to the isotopes of interest. The relative amplitude of these signals is proportional to the sample's isotopic ratio. IRMS measurements therefore rely on the quantitative chemical conversion of samples into small gas molecules (e.g., CO<sub>2</sub>, N<sub>2</sub>, H<sub>2</sub>, CO and SO<sub>2</sub>) prior to introduction in the MS, contrary to more conventional MS systems for organic compounds for which target molecules are ionized directly in the MS source and then sorted out based on their mass-to-charge ( $m/z$ ) ratio. For instance, converting all the C atoms from a sample to CO<sub>2</sub> allows the measurement of  $m/z = 45$ , a C dioxide molecule linked to <sup>13</sup>C (i.e., <sup>16</sup>O<sup>13</sup>C<sup>16</sup>O) and  $m/z = 44$  (i.e., <sup>16</sup>O<sup>12</sup>C<sup>16</sup>O), linked to <sup>12</sup>C. A third signal,  $m/z = 46$  (<sup>16</sup>O<sup>12</sup>C<sup>18</sup>O), is also acquired to account for the small isobaric interference of <sup>16</sup>O<sup>12</sup>C<sup>17</sup>O (also of  $m/z = 45$ ). This is possible assuming the <sup>18</sup>O/<sup>17</sup>O ratio is constant. Barring this small correction, the  $m/z = 45$  over  $m/z = 44$  ratio can be considered as being proportional to the <sup>13</sup>C/<sup>12</sup>C ratio [125].

Another particularity of IRMS is that each measurement, whether for an unknown sample or for a reference material (RM), includes many injections of an isotopically-constant monitoring gas (MG, e.g., CO<sub>2</sub> for CSIR). It is essentially the comparison of the isotopic makeup of this monitoring gas to the sample peak that allows the instrument to generate raw  $\delta$  values that can later be anchored to certified materials analyzed in a fashion that is identical to the unknown samples [125].

### 1.3.2 CSIR

C has two naturally occurring stable isotopes: <sup>12</sup>C (6 protons and 6 neutrons) accounting for 98.9% of all stable C and <sup>13</sup>C (6 protons and 7 neutrons) making up the remaining 1.1%; as well as one radioactive isotope: <sup>14</sup>C (6 protons and 8 neutrons) detectable in trace amounts in nature. Small variations in the <sup>13</sup>C/<sup>12</sup>C ratio can give information on the biochemical and physical transformations that different C pools have undergone; for example, fixation of C dioxide to generate plant material [126, 127] or preferential degradation of labile organic matter as C-rich

particles sink from the surface of the water column to the sediment [128]. The idea that CSIR measurement could differentiate C from an organic, atmospheric or carbonaceous source was first explored at the end of the 1930s [129] with limited success due to the analytical capacity of the time. More and more precise reporting of CSIR took place through the 1940s and 50s. Craig (1953) [130] was able to demonstrate that inorganic carbonates and plant-based organic C were isotopically-distinct, separated by more than 20‰ on the PDB scale<sup>4</sup>. The scope of CSIR applications has since widened considerably and detailed mapping of CSIR distribution on Earth has allowed work to be done in many different fields. In addition to the examples already listed in Table 1.3, other interesting applications include the combination of CSIR with H, N and S stable isotopes as dietary tracers to obtain information about the food chain of an ecosystem and trophic levels of organisms, living or extinct [131]. Artificially <sup>13</sup>C-enriched materials have also been used as tracers in laboratory experiments [132] and metabolism studies [133].

### 1.3.3 CSIR in anti-doping analyses

In the field of anti-doping sciences, the first work mentioning CSIR dates back to the beginning of the 1990s [134]. In 1994, Becchi et al. [135] published the first method relying on compound-specific CSIR measurements to detect the presence of synthetic T in human urine. The isotopic signature of urinary components that are biosynthesized and excreted in urine are linked to building blocks which ultimately are derived from the individual's diet. This explains the expression: "You are what you eat" [136] often used in the CSIR field. Since C isotopic signatures are generally well conserved within the human body [137], compounds excreted in urine largely reflect the isotopic composition of the bulk diet. Photosynthetic processes that fix C dioxide into plants that we eat (either directly or indirectly from the consumption of animal products) have by far the greatest influence on the isotopic composition of our diet as they involve kinetic isotope effects (KIE), a phenomenon that can be described as the tendency in a chemical reaction to favor some isotopes (usually lighter ones) over others. Ribulose-1,5-bisphosphate carboxylase/oxygenase (RuBisCO), the CO<sub>2</sub> fixing enzyme in the majority of plant organisms on Earth - marine and terrestrial - is slightly more prone to favor <sup>12</sup>CO<sub>2</sub> over <sup>13</sup>CO<sub>2</sub> [138, 139]. Expressed in terms of the VPDB scale, this atmosphere-to-plant <sup>13</sup>C depletion ranges from negligible to roughly -27‰ relatively to the atmospheric C dioxide ( $\delta^{13}\text{C} \approx -8\text{‰}$ ). The

---

<sup>4</sup> The former CSIR scale for carbon before 1993.

different extent of isotopic depletion from one plant species to another depends on the biochemical pathway used to convert CO<sub>2</sub> to sugar. Those biochemical processes are divided into three categories, each one of which fractionates atmospheric CO<sub>2</sub> to a different extent due to the relative preference of the plant's C fixation pathway for <sup>12</sup>C versus <sup>13</sup>C [140].

C3 plants form about 85% of plants. They use what is called the Calvin cycle to convert CO<sub>2</sub> in chloroplasts by means of RuBisCO which catalyzes the reaction between ribulose 1,5-biphosphate (RuBP), CO<sub>2</sub> and water to form 3-phosphoglyceric acid (3-PGA), the 3-C intermediate that defines C3 plants and that is eventually converted to a carbohydrate. Examples of C3 plants include soybeans, sugar beets as well as most trees and lawn grasses. Their δ<sup>13</sup>C value distribution is wide – roughly from -20 to -35‰ – with extreme values that vary slightly depending on the publication [127, 140-143].

The C4 metabolism (also Hatch-Slack pathway) is only used by about 5% of known plant species, however agricultural practices inflate the prevalence of C4 plants such as sugarcane and corn in our diets due to their resilience in dryer climates. C4 plants also use the Calvin cycle, but not right after CO<sub>2</sub> uptake. The absorbed C dioxide is first stored in the form of bicarbonate ions (HCO<sub>3</sub><sup>-</sup>) after its transformation by carbonic anhydrase. Next, the stored HCO<sub>3</sub><sup>-</sup> and phosphoenol pyruvate (PEP) are converted to oxaloacetic acid (OAA) by a PEP-carboxylase. OAA is then used to produce malic acid, a 4-C molecule giving its name to the metabolism. These first biochemical reactions happen within the chloroplasts of mesophyll cells, but malic acid is then transferred to an adjacent bundle sheath cell where it can be transformed back into CO<sub>2</sub> by RuBisCo and subsequently enter the Calvin cycle. Because the CO<sub>2</sub> fixing mechanism in C4 plants involves more steps than in C3 plants, some of which are more favorable to <sup>13</sup>C than others, their net depletion in terms of δ<sup>13</sup>C value is less pronounced ranging from -7 to -15‰ [140-145].

The third and last type of metabolism known is named the Crassulacean Acid Metabolism (CAM). CAM plants are very present in hot and arid environments and include cacti, pineapples, Agave and some species of ferns as examples. This family of plants alternate between the C3 and C4 pathways depending on the time of day. CAM plants open their stomata only at night to absorb CO<sub>2</sub> and store it as malic acid. This storage is similar to the C4 metabolism. Here however, the gas molecules are not displaced to another cell for storage, but rather left in the

same photosynthetic cells they were absorbed into. During the day, stomata are closed and decarboxylation of malic acid to CO<sub>2</sub> and further introduction to the Calvin cycle can occur. The range of possible δ<sup>13</sup>C values for CAM plants extends from -10 to -28‰ and therefore overlaps the values for C<sub>3</sub> and C<sub>4</sub> plants [140-142, 146].

Synthetic steroids sold as therapeutic agents are synthesized from phytosterols (see Figure 1.5) extracted from C<sub>3</sub> plants such as soy and bear δ<sup>13</sup>C signatures ranging from -26 to -33‰ [147], within the expected range of C<sub>3</sub> plants. In contrast, endogenously produced T and T metabolites mirror the isotopic signature of the diet of the individual who produced it, with δ<sup>13</sup>C values ranging from -15 to -25‰, depending on lifestyle and country of origin. Higher δ<sup>13</sup>C values (-15 to -18‰) are observed in the southern part of North-America, where corn – a C<sub>4</sub> plant – is a dietary staple of the human diet but also extensively used as feedstock in the meat and dairy industries. More depleted values (-22 to -25‰) are observed in European countries, reflecting a diet and agricultural practices that revolve around an abundance in C<sub>3</sub> plants [148].

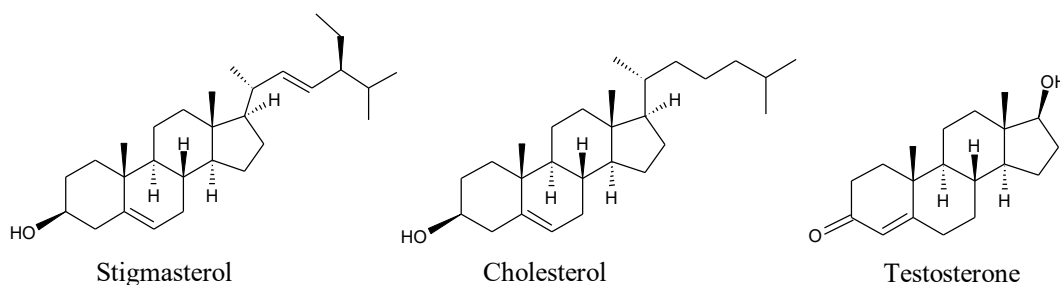


Figure 1.5: Molecular structure similarities between stigmasterol, a phytosterol (left), cholesterol, a sterol found in small amounts in plants but mostly in animals (center), and testosterone, a sex hormone and AAS (right).

Doping with endogenously-produced steroids like T can be detected because there are differences in the isotopic composition of steroids that are naturally produced by humans from dietary building blocks that are composed of a mixture of C<sub>3</sub> and C<sub>4</sub> plants (-15 to -25‰) and the exogenously administered steroids that are synthesized from materials extracted exclusively from a C<sub>3</sub> plant. When urinary T has an exogenous origin, its δ<sup>13</sup>C values – as well as the ones of its direct metabolites – are shifted when compared to other steroids that are not affected by T metabolism (e.g., cholesterol). This shift can be precisely measured by CSIR and constitutes a

direct proof of doping. Measuring these tiny differences in  $\delta^{13}\text{C}$  is the exclusive role of CSIR in the context of anti-doping sciences.

Since the 1990s, the scope of CSIR for anti-doping purposes has been extended to more molecules, including for example dehydroepiandrosterone (DHEA) [149, 150], boldenone [151] and 19-norandrosterone (19-NA), a metabolite of nandrolone [152]. Corticosteroids, whether endogenous (e.g. cortisol, cortisone and metabolites) [153, 154] or from the pharmaceutical industry (e.g. prednisone and prednisolone) [155] can also be found among more recent developments.

The extension of CSIR to AICAR has been shown to be possible by Piper et al. (2014) [11], not only by measuring CSIR values for AICAR extracted from urine samples, but also by making measurements on different synthetic samples bought from official and non-official suppliers. Interestingly, synthetic AICAR is enriched in  $^{13}\text{C}$  relative to its endogenous analog with  $\delta^{13}\text{C}$  values between -3 and -6‰. The reason for such high values is unknown. However, from a strict anti-doping point of view, this does not cause any issue since what matters is that the values of the exogenous product are located far enough from the endogenous one to make possible the distinction between the two.

#### **1.3.4 GC/C/IRMS for CSIR in anti-doping testing**

The type of isotopic analysis made in the field of anti-doping sciences is said to be compound-specific. This is because a  $\delta^{13}\text{C}$  value specific to each compound analyzed must be obtained for proper determination of its origin. Compound-specific isotope analysis (CSIA) requires the MS to be hyphenated with another instrument, most often a gas chromatograph (GC), in order to separate the target compounds prior to their isotopic evaluation. The type of instrument used for CSIA in this work is an isotope ratio mass spectrometer coupled to a GC and a combustion interface (abbreviated GC/C/IRMS). Sample extracts are first injected on a chromatography column in the gas phase, allowing separation of the different organic molecules. In an ideal situation, those compounds exit the GC as perfectly resolved components. They then enter a combustion interface made of a hollow quartz tube heated at high temperature (850 or 950°C depending on the catalyst used) in which one or many catalysts make possible the complete conversion of the analytes to  $\text{CO}_2$  and  $\text{H}_2\text{O}$ . Combustion water can be subsequently removed through a Nafion<sup>®</sup> drying membrane. Once in the MS, the  $\text{CO}_2$  originating from the analytes is

ionized by electron impact. The ions are then separated based on their mass and focused on different Faraday cups acting as detectors using an electro-magnet. Signals specific to three possible isotopic compositions of the CO<sub>2</sub> are acquired:  $m/z = 44$  for <sup>16</sup>O<sup>12</sup>C<sup>16</sup>O,  $m/z = 45$  for <sup>16</sup>O<sup>13</sup>C<sup>16</sup>O and  $m/z = 46$  for <sup>16</sup>O<sup>12</sup>C<sup>18</sup>O, as previously explained in Section 1.3.1 [20, 115, 156]. A simplified diagram of a GC/C/IRMS instrument can be seen in Figure 1.6.

The first GC/C/IRMS instrument intended to be used in a major sport event was installed for the 1996 Olympic Games in Atlanta, USA. However, because the technology was new at the time, no routine analyses were performed. The first official use of IRMS during the Games was in Nagano, Japan for the 1998 Winter Olympics, but the definitive implementation of the method was only done two years later in Sydney, Australia [19].

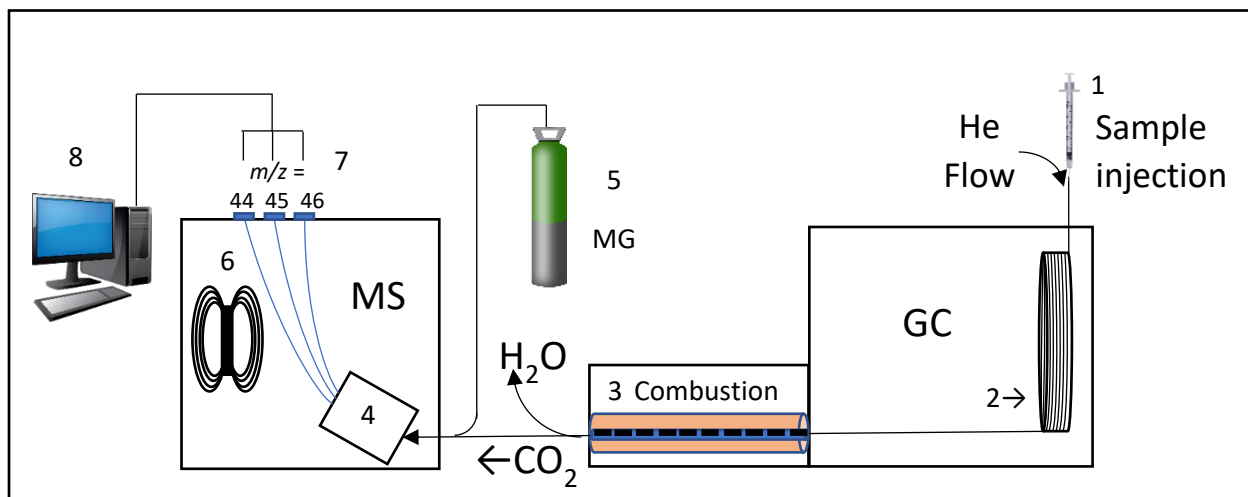


Figure 1.6: Simplified representation of a GC/C/IRMS. The sample is injected (1), then carried with a stream of helium in the GC where the analytes get separated in a chromatography column (2). They then one by one enter the combustion furnace (3) and get converted to CO<sub>2</sub> and H<sub>2</sub>O. When exiting the furnace, water is diffusively removed using a Nafion<sup>®</sup> membrane and the CO<sub>2</sub> enters the MS where it is ionized by electron impact in the ion source (4). Monitoring CO<sub>2</sub> gas (MG) can also be introduced in the MS for measurement calibration (5). Once formed, the ions are separated by their mass using a magnetic field from an electromagnet (6). A signal for  $m/z = 44, 45$  and  $46$  can then be acquired (7) and analyzed by computer software (8).

### 1.3.4.1 The use of endogenous reference compounds

An endogenous reference compound (ERC) is described as a molecule for which the  $\delta^{13}\text{C}$  value represents a normal or “benchmark” isotopic value for a given individual. Depending on the individual’s diet and country of origin, the measured values for the ERC will vary covering a range typically from -25 to -15‰. It is through the comparison to this normal endogenous value to the target compound (TC) that doping cases are built [157]. For most AAS, a difference between  $\delta^{13}\text{C}_{\text{TC}}$  and  $\delta^{13}\text{C}_{\text{ERC}}$  ( $\Delta\delta^{13}\text{C}_{\text{TC-ERC}}$ , Equation 2) exceeding 3‰ or 4‰ (depending on the TC analyzed) is considered to be abnormal [158].

$$\Delta\delta^{13}\text{C}_{\text{TC-ERC}} = \delta^{13}\text{C}_{\text{TC}} - \delta^{13}\text{C}_{\text{ERC}} \quad (\text{Equation 2})$$

ERCs are not randomly chosen as it is essential that their isotopic signature be independent from the TC. Indeed, synthetic T intake not only impacts the  $\delta^{13}\text{C}$  value of urinary T itself, but also affects other downstream metabolites, shifting their isotope values as well; therefore, these downstream metabolites are not appropriate ERCs [150]. Attention is also given to selecting a compound with a similar chemistry as the TC, in order to allow their analysis by a similar protocol. It is also important that the benchmark molecule be synthesized by a similar biochemical pathway and using similar building blocks so that the isotopic composition of the ERC and the TC are naturally similar in the absence of doping. In the case of AAS, a few examples of ERCs can be found in the literature, including but not limited to,  $5\beta$ -pregnanediol (Pd) [150, 159],  $3\alpha$ -androst-16-enediol [150], 11-ketoetiocholanolone [157, 160] and 11-hydroxyandrosterone [157].

In previous work [11, 22], some of those same ERCs used for AAS isotopic analysis were conserved to evaluate the origin of AICAR in urine samples. Proceeding this way has some advantages. AAS and AICAR are issued from different metabolic pathways, which ensure independent isotopic values for both molecules. Moreover, isotopic analysis of AAS is a method easily implementable by anti-doping laboratories, given the experience they possess with such protocols. However, the metabolic “distance” between AICAR and AAS-related ERCs introduces the possibility that natural isotopic variability in the distant pathways could cause large isotopic differences that make a negative sample look positive. This is theoretically possible, as examples of CSIA of different molecules from a single organism yielding different  $^{13}\text{C}/^{12}\text{C}$  ratios can be found in the literature [148, 161, 162]. Furthermore, the distribution of  $\Delta\delta^{13}\text{C}_{\text{A-ERC}}$  values

between AICAR and AAS ERCs measured by Piper et al. (2014) [11] was wider than the ones published for AAS versus their own traditional ERCs, meaning the CSIR of AICAR are on average more distanced from the AAS values than the steroids between themselves. Finally, steroids and nucleic acid analogs, like AICAR, have very different chemical properties. Isolating both with a single protocol is therefore nearly impossible. For these reasons, the use of a new ERC, specific to AICAR isotopic analysis, is necessary. However, choosing such a compound is not an easy task. An AICAR-specific ERC needs to respect the conditions specified above, but it also has to be suitable for GC/C/IRMS analysis. After many candidates were considered, uridine was selected for this work. Its use as a novel ERC for AICAR is further discussed in Chapters 3 and 4 of this thesis.

#### **1.3.4.2 Adaptation of GC/C/IRMS to AICAR**

The objective of this work is to make possible AICAR analysis by GC/C/IRMS. To reach that goal, many challenges have to be resolved. Inspiration can be obtained from existing AAS methods, but AICAR's case is much more complex for two reasons. First, AICAR and its ERC have to be extracted from the urine matrix and purified, something typically done using SPE and HPLC. Here, the relatively high polarity of AICAR and uridine is a disadvantage, especially when compared to steroids, which can be extracted by conventional reverse-phase SPE. A new approach, employing a polymer-based phenylboronic acid (PBA) gel and an HPLC column functional under 100%-water conditions had to be elaborated. Second, and perhaps the biggest obstacle to overcome in this work, AICAR is not volatile. This is of course an issue for gas chromatography. Gas-phase analyses of non-volatile compounds are often made possible with proper chemical derivatization [163, 164]. This is the case of some GC/C/IRMS methods in which AAS are acetylated to improve their chromatographic behavior [20, 165]. Acetylation was therefore tested on AICAR and uridine and both compounds could be analyzed by GC. A standardized acetylation protocol was subsequently developed.

Finally, statistical information must be gathered on both AICAR and uridine, but also on the  $\Delta\delta^{13}\text{C}_{\text{AICAR-uridine}}$  ( $\Delta\delta^{13}\text{C}_{\text{A-U}}$ ) values linking them (see Equation 2 and Section 1.3.4.1). This is important as these values are used to estimate the threshold that allows the identification of abnormal samples. In the case of AAS, these thresholds are based on statistical analyses of large sample sizes obtained during major international sport events like the Olympic Games [20] and in

long-term studies with samples of different geographical origins [148]. The thresholds used by WADA in its technical documentation [158] are based on such studies.

However, the amount of information available on the normal CSIR values of endogenous AICAR is very limited and no such “reference population” has ever been documented. This is even truer for uridine since to the author’s knowledge, no CSIA analysis has ever been published for this compound, at least in urine samples. Piper et al. (2014) [11] have published data for 63 samples - very far from the thousands of results available for AAS thus far - and ventured on the establishment of AICAR - specific threshold values using steroidal ERCs. Nevertheless, this small set of samples can by no means serve as a gold standard for normal  $\Delta\delta^{13}\text{C}_{\text{A-ERC}}$  values and any new available data is important and welcome. This work will therefore present data related to the analysis of 46 athletes’ urine samples gathered using a different methodology than Piper et al. and including CSIR measurements for AICAR, uridine, as well as three urinary steroids: 5 $\beta$ -pregnanediol (Pd), androsterone (Andro) and etiocholanolone (Et). The information gathered here could thus help WADA to eventually establish new guidelines for AICAR, even though results on the topic are still at a very preliminary stage.

#### **1.4 General objectives of the thesis**

In light of the information exposed in the above sections, the objectives of the present thesis can be enumerated as follows:

1. To develop and optimize an extraction protocol allowing the purification of AICAR and uridine from urine in order to make them GC/C/IRMS-analyzable.
2. To develop and optimize a GC/C/IRMS method, including a chemical derivatization step (acetylation), to allow compound-specific measurements of  $\delta^{13}\text{C}$  values of urinary AICAR and uridine.
3. To validate an analytical method as much as possible in agreement with WADA requirements for the determination of the origin of AICAR in human urine.
4. To verify if the GC/C/IRMS analysis of AICAR can be used to differentiate between its possible exogenous and endogenous origins, using either uridine, Pd, Andro or Et as an ERC.

## **1.5 Organization of the thesis**

As seen in the sections above, Chapter 1 of this thesis covers the general introduction on AICAR and stable isotopes, including a historical review of AICAR and related topics as presented in the literature. After a description in Chapter 2 of the materials and methods used for the present work, Chapter 3 describes how the whole GC/C/IRMS method developed for this thesis was designed, optimized and validated. In Chapter 4, the results for the  $\delta^{13}\text{C}$  measurements of AICAR, uridine and steroids in urine samples are presented and discussed. Finally, Chapter 5 suggests potential future work needed to further advance this topic as well as the general conclusions that can be drawn from this project.

## **2. Materials and methods**

### **2.1 Materials**

All solvents used were of HPLC grade or better. Acetonitrile (ACN), ethyl acetate (AcOEt), methanol (MeOH), n-hexane, ammonium acetate (NH<sub>4</sub>Ac) and ammonium hydroxide (NH<sub>4</sub>OH) were purchased from Caledon Laboratories Ltd (Georgetown, ON, CAN). Acetic anhydride (Ac<sub>2</sub>O), as well as an additional batch of AcOEt were from Fisher Scientific (Ottawa, ON, CAN). NH<sub>4</sub>Ac, formic acid (HCOOH) and pyridine (Pyr) were bought from Sigma-Aldrich (Oakville, ON, CAN). Deionized water was obtained through an Advantage 10 Milli-Q filtration system. Phenylboronic acid on polyacrylamide gel (Affi-Gel<sup>®</sup>) and glass Econo-Column<sup>®</sup> columns were purchased from Bio-Rad (Mississauga, ON, CAN). Helium (He), carbon dioxide (CO<sub>2</sub>) and oxygen (O<sub>2</sub>), used on the GC/C/IRMS system, were all of the highest possible purity and were bought from Praxair (Mississauga, ON, CAN).

#### **2.1.1 Nucleic acid analogs**

5-Aminoimidazole-4-carboxamide-1-β-D-ribofuranoside (AICAR), AICAR-<sup>13</sup>C<sub>2</sub>-<sup>15</sup>N, uridine, uridine-2-<sup>13</sup>C-1,3-<sup>15</sup>N<sub>2</sub>, 5-amino-1-(2',3',5'-tri-O-acetyl-β-D-ribofuranosyl)-imidazole-4-carboxamide (3-Ac-AICAR), 2',3',5'-tri-O-acetyluridine (3-Ac-uridine), thymidine and cytidine were all bought from Toronto Research Chemicals (North York, ON, CAN).

#### **2.1.2 Other materials**

Glycerol, D-sorbitol, Andro and Et were from Sigma-Aldrich (Oakville, ON, CAN) as well as one batch of triacetine (glycerol triacetate) and D-sorbitol hexaacetate. A supplemental batch for each of the two former products was also obtained from Fisher Scientific (Ottawa, ON, CAN). Estriol was obtained from Steraloids (Newport, RI, USA). The CU/USADA-33-1 standard of acetylated steroids originated from the Brenna Laboratory at Cornell University (Ithaca, NY, USA).

All RMs were stored either at RT, +4°C or -20°C, according to the manufacturer's recommendation.

## 2.2 Methods

### 2.2.1. Reference material stock solutions

Aqueous solutions of concentration roughly equal to 1 mg/mL were made for AICAR and uridine using standards with known C isotopic signature. The same was done for 3-Ac-AICAR and uridine, but these compounds displayed very poor solubility in water so AcOEt was used instead. RM solutions were kept at +4°C and analyzed regularly by HPLC using an ultra-violet detector (UV-HPLC) to detect any sign of degradation.

### 1.2.13 External EA-IRMS analyses

Compounds for which an external reference value was needed were analyzed by EA-IRMS in two different laboratories: The *Centre de recherche sur la dynamique du système Terre* (GEOTOP) at the *Université du Québec à Montréal* (UQÀM, Montreal, QC, Canada) and the UC Davis Stable Isotope Facility (University of California, Davis, CA, USA). All measurements made were traceable to an international PCIRM (e.g., IAEA-607). Results are available in Appendix 1.

### 2.2.3 Urine samples

Urines for method development were treated in accordance with the International Standard for Laboratories (ISL) [166]. Samples were first targeted using the AICAR concentration estimation as provided by the *Laboratoire de Contrôle du Dopage* of the *Centre Armand-Frappier Santé et Biotechnologie* of the *Institut National de la Recherche Scientifique (INRS-AFSB)*. Once urines had reached their minimum conservation time, they were anonymized and all the information linking them to their origin was destroyed. One exception to this was applied to samples for which a product potentially influencing the CSIR of AICAR had been declared (e.g., ribose, amino acid and folic acid supplements). In that case, the product in question was noted and all the other elements on the athlete's declaration were then also erased. Urines were always stored at -20°C until they had to be thawed for aliquoting and analysis.

### 2.2.4 Negative and positive reference urines

A negative reference urine (QCN) was made by pooling together aliquots of 10 urine samples with AICAR concentrations around 1 µg/mL.

A positive reference urine (QCP) was prepared by spiking a volunteer's urine with the equivalent of 10 µg/mL of synthetic AICAR with  $\delta^{13}\text{C}$  evaluated at  $-4.34 \pm 0.04\%$  in order to obtain a C isotopic signature as close as possible to the one of the synthetic material.

### **2.2.5 PBA gel**

PBA gels were prepared and used following Szymańska et al.'s (2007) [167] protocol with minor modifications. Gels were always prepared in batches (up to 10 at a time) and stored at +4°C in 0.25 M NH<sub>4</sub>Ac buffer (pH 8.2 – 8.6) when not used. Individual gels were made by weighing 200 mg of dry Affi-gel<sup>®</sup> and transferring in 6 or 12 cm<sup>3</sup> Econo-Columns<sup>®</sup>. They were then immersed in 3 mL of water for at least 5 minutes to allow them to swell. Prior to first use, gels were washed 10 times with 0.5 mL of MeOH and 0.5 mL of H<sub>2</sub>O in alternation (5 times each). Conditioning was then performed with 5 mL of 0.1 M HCOOH in a 50/50 (v/v) methanol-water mixture followed by 5 mL of 0.25 M NH<sub>4</sub>Ac buffer (pH 8.2 – 8.6). This last buffer was also used to rinse the gels after usage (5 to 10 mL) and as a storage solution. Gels were stored for a maximum of two months as per the manufacturer's recommendation. Szymańska et al. have reported using a single gel for 12 different urine samples without any loss of performance. Here, each individual gel was always used less than 10 times.

### **2.2.6 PBA extraction buffers**

NH<sub>4</sub>Ac 2.5 M buffer was prepared by dissolving 96.4 g of NH<sub>4</sub>Ac for 500 mL of H<sub>2</sub>O. The pH was then adjusted to 8.2-8.6 using 25% NH<sub>4</sub>OH. NH<sub>4</sub>Ac 0.25 M buffer was prepared by diluting the NH<sub>4</sub>Ac 2.5 M 10 times, typically 100 mL in 900 mL of H<sub>2</sub>O. The pH was once again adjusted to 8.2-8.6 with 25% NH<sub>4</sub>OH. The 0.1 M HCOOH solution was made by adding 4.4 mL of HCOOH to 1 000 mL of a 50/50 H<sub>2</sub>O/MeOH mixture. All solutions were stored at room temperature (RT) and showed good long-term pH stability. However, the NH<sub>4</sub>Ac 0.25 M buffer conservation period was limited to 3 months as a pH decrease, probably due to ammonia evaporation, was observed after 4-5 months of storage.

### **2.2.7 PBA extraction**

Extractions were performed for the most part by hooking up the glass columns containing the gels on a Qiagen (Toronto, ON, Canada) vacuum manifold to help speed up the process. Elution was let to proceed by gravity. The protocol was once again based on Szymańska et al.'s (2007)

[167]. Urines were extracted in batches, with every individual aliquot having its own PBA gel column. Before being loaded on gels, urine samples (3 mL for [AICAR]  $\geq$  2  $\mu\text{g/mL}$  and 6 mL for [AICAR]  $<$  2  $\mu\text{g/mL}$ ) were buffered with a 1-to-1 volume of 2.5 M  $\text{NH}_4\text{Ac}$  buffer (pH 8.2 – 8.6). Samples were then applied on the gel, immediately rinsed with 0.5 mL of 0.25 M  $\text{NH}_4\text{Ac}$  buffer and let to rest for 10 minutes. Cleaning of the gel was then done with 4 mL of 0.25 M  $\text{NH}_4\text{Ac}$  and 0.3 mL of 50/50 (v/v) methanol- $\text{H}_2\text{O}$  (in alternance and twice). Between each rinsing, a 3-minute delay was observed. Before elution, 0.5 mL of 0.1 M  $\text{HCOOH}$  in a 50:50 (v/v) methanol-water was introduced in the gel followed by another 3-minute waiting time. Elution was subsequently performed with 3 mL of 0.1 M  $\text{HCOOH}$  in a 50/50 (v/v) methanol-water.

Eluates were evaporated under a stream of nitrogen at 50°C. Residues were then transferred with 300  $\mu\text{L}$  of 50:50 (v/v) methanol- $\text{H}_2\text{O}$  in 2 mL glass vials containing a conical insert and centrifuged at 2500 rpm for 5 minutes. The supernatant was next transferred in a new set of 2-mL vials, but this time containing a bottom-spring conical insert. The liquid was once again evaporated under a stream of nitrogen at 50°C and the residue dissolved in 50  $\mu\text{L}$  of  $\text{H}_2\text{O}$  for semi-preparative HPLC.

### **2.2.8 First semi-preparative HPLC**

At this stage, an aqueous solution comprising unacetylated AICAR and uridine standards (hereafter named the “Mix-AU”) for which EA-IRMS analyses had been performed, was added within each HPLC sequence and were treated in the same way as the samples through the rest of the procedure. These standards later served to determine the contribution of the acetate moieties for each compound.

Two different 1100 Series HPCLs from Agilent (Mississauga, ON, Canada) were used for the analyses. AICAR and uridine were purified from the PBA extracts using an ACME<sup>®</sup> PLUS column (P/N ACMP-5-25046, 4.6 x 250, 5.0  $\mu\text{m}$ ) from Canadian Life Science (Montreal, QC, CAN). The totality (50  $\mu\text{L}$ ) of the samples was injected at a constant flow of 1 mL/min and the column compartment was kept at 40°C. The mobile phase was kept isocratic at 100%  $\text{H}_2\text{O}$  for 15 minutes and then brought to 50% acetonitrile/50 % methanol between 15 and 17 minutes. The organic solvents were maintained until 22 minutes and the return to 100%  $\text{H}_2\text{O}$  was done from 22 to 22.5 minutes. This aqueous-only composition was kept until completion at 25 minutes and for another 4.5 minutes of post-run, to make sure acceptable baseline was reached before the start of

the following analysis. Collection times for the AICAR and uridine fractions were determined prior to every sequence by injecting a standard mix containing RM of both substances. Elution, monitored by UV at  $\lambda = 192$  and  $265$  nm, occurred at roughly 11.1 minutes for uridine and 12.9 minutes for AICAR. Isotopic fractionation has been associated with partial peak recovery during semi-preparative HPLC [168], so a 0.2-minute leeway was given to the fraction collector at beginning and end of elution to make sure the entirety of each peak was recovered.

Fractions containing the analytes were recovered with either a Gilson (FC203B) or an Agilent (G1364F) fraction collector. Fractions were then evaporated under nitrogen at  $50^{\circ}\text{C}$  and transferred in reusable conical glass vials with  $300\ \mu\text{L}$  of methanol. For this step, the AICAR and uridine fractions were either transferred in their own separate vials or pooled together in the same vial for each sample in order to reduce the number of vials necessary. The transfer MeOH was then evaporated to dryness ( $\text{N}_2$  at  $50^{\circ}\text{C}$ ) before acetylation.

### **2.2.9 Acetylation**

The reusable vials in which acetylation was performed were cleaned thoroughly before use by washing with  $\text{H}_2\text{O}$  and MeOH. They were then heated at  $500^{\circ}\text{C}$  for at least 2 hours in order to remove any trace of organic material.

Acetylation was carried out by adding  $50\ \mu\text{L}$  of  $\text{Ac}_2\text{O}$  and  $50\ \mu\text{L}$  of Pyr in each dry fraction. Next, vials were capped and stirred on vortex for 5-10 seconds. They were then opened and  $15\ \mu\text{L}$  of water was added to quench the reaction before the whole mixture was evaporated under  $\text{N}_2$  at  $50^{\circ}\text{C}$ . To homogenize for each vial the time given for the reaction to occur, the procedure was done on a small number of vials (4 to 10) at a time. Before the second semi-preparative HPLC, the dry residues were re-dissolved in a  $\text{H}_2\text{O}$ -ACN-MeOH (70:15:15 v/v) mixture.

### **2.2.10 Second semi-preparative HPLC**

In a similar fashion as for the first semi-preparative HPLC, the second one was done with a standard mix of 3-Ac-AICAR and 3-Ac-uridine (with related EA-IRMS values) added to every injection sequence. This mix is referred to as the “Mix-Ac” standard hereafter. This RM then followed the sample extracts onto the GC/C/IRMS and were used to build a 2-point isotopic “calibration curve” to allow for a  $\delta^{13}\text{C}$ -specific correction of all other measurements made for AICAR and uridine.

Acetylated extracts were purified once again using the same HPLC instruments and column as described in the above section. From 0 to 9 minutes, an isocratic 70/15/15 (V/V/V) H<sub>2</sub>O/ACN/MeOH mobile phase was introduced in the column at 1 mL/min. From 9 to 11 minutes, this composition progressively switched to 50/50 (%) ACN/MeOH and the flow increased to 1.5 mL/min. These conditions were held for 3 minutes before the mobile phase was brought back to 70/15/15 (V/V/V) H<sub>2</sub>O/ACN/MeOH from 14 to 15 minutes. Then, the flow was restored to 1 mL/min and these conditions were kept constant until the end of analysis at 17 minutes as well as for a 2-minute post-run. Interestingly, the elution order of the two analytes was swapped, with 3-Ac-AICAR eluting around 7.3 minutes and 3-Ac-uridine at roughly 8.8 minutes (again monitored at  $\lambda = 192$  and 265 nm).

Fraction collection was done in a similar fashion as for the first HPLC purification. Collection times were determined this time with standards of triacetylated AICAR and uridine. The fractions were evaporated to dryness under N<sub>2</sub> at 50°C and transferred in 2-mL vials with conical inserts using 300  $\mu$ L of AcOEt which was then completely evaporated. The residues were reconstituted in volumes of AcOEt ranging from 10 to 50  $\mu$ L prior to GC/C/IRMS analysis, depending on analyte concentration.

### **2.2.11 GC method development**

Tests for the development of the GC method were performed on two different GCs: a 6890N and a 7890B, both from Agilent (Mississauga, ON, Canada) and equipped with a flame ionization detector (FID). Experiments were performed on a CP Sil 8 CB for amines (P/N CP7596; 30 m, 0.320 mm, 1.00  $\mu$ m; hereafter designated as the “CP Sil” column) and a DB-5MS (P/N 128-5522; 25 m, 0.200 mm, 0.33  $\mu$ m) column, the two from Agilent. Prior to first usage, columns were treated with a column protectant by the injection of 30 ng of n-sorbitol 3-5 times [169, 170]. This was necessary, especially for the DB-5MS column who showed signs of degradation after only a few injections of 3-Ac-AICAR. Data analysis was done on the ChemStation software (G2070BA) on the 6890N and the Qualitative Analysis Navigator on the 7890B (version B.08.00).

### **2.2.12 GC/C/IRMS method for AICAR and uridine analysis**

C isotopic analyses were done using an Agilent 6890N GC coupled to a combustion interface heated at 850°C and an Isoprime (Elementar Americas Inc.) IRMS. IonVantage (Build 1,7,3,0)

was the software by which the instrument was controlled and data analysis was done using the Continuous Flow Data Processing (CFDP) software. O<sub>2</sub> was added to the He carrier gas going in the combustion chamber. This chamber was made of a hollow quartz tube filled with roughly 5 cm of CuO pellets and then 1 cm of silver wool. An autosampler was installed on the GC to allow automatic multiple-injections sequences. Depending on the expected concentration of analyte, 1 to 3 µL of samples was injected by a 10-µL syringe, with the injector at 290°C and set to splitless mode. The chromatography was done at constant flow (2.4 mL/min) on a CP Sil column (see previous section). To avoid damaging the catalyst and the IRMS by solvent overflow, the solvent peak was diverted after passing through the GC column using a pressure differential and a Heart Split valve.

The GC oven initial temperature was 150°C. After one minute, the temperature increased with a ramp of 20°C/min until it reached 320°C. This last temperature was then kept constant for 6 minutes until the end of the analysis. During each injection, seven MG peaks (four at the beginning and three at the end) were analyzed. Each of them lasted 0.5 minute and a 0.5-minute delay was kept between consecutive peaks.

The instrument's stability was tested before each injection sequence by series of 10 CO<sub>2</sub> pulses lasting 30 seconds and spread 30 seconds apart. The δ<sup>13</sup>C value of the MG was measured for every pulse and the standard (SD) associated with each series was verified to always be < 0.1%. At least one blank injection was done before injecting any RM or sample.

### **2.2.13 GC/C/IRMS method validation**

The GC/C/IRMS was validated as much as possible with the TD2019IRMS [158]. However, since this document is related to AAS analysis, some aspects of validation had to be adapted. The combined uncertainty (U<sub>c</sub>) was calculated based on the formula given in the TD2015DL [158] and included the reproducibility of the QCN (as a SD) for AICAR and uridine and a factor to account for the “inter-laboratory error” associated with the measurement (estimated to 0.5‰ from data supplied by the *Laboratoire de contrôle du dopage* of the *INRS-AFSB*). Intra-day reproducibility was estimated by analyzing replicates of eight different urines and inter-day reproducibility was estimated using the data from the Mix-AU, QCN and QCP (Sections 2.2.4, 2.2.5 and 2.2.8). Accuracy was evaluated by spiking SigMatrix® urine diluent with AICAR and uridine standards of known CSIR values. The urine diluent was then taken through the whole

extraction protocol and the results were compared with the same standards but unextracted. Detailed results for method validation are all available in Appendix 2.

#### **2.2.14 GC/C/IRMS steroid analysis**

GC/C/IRMS analysis of steroids in urine samples was mostly done following a previously published protocol [150], including an update for the semi-preparative section [171]. Briefly, Sep-Pak<sup>®</sup> C18 SPE cartridges (Waters, P/N WAT036810) were successively conditioned with 5 mL of n-hexane, 5 mL of MeOH and 5 mL of H<sub>2</sub>O. A volume of 5 or 10 mL of each urine (depending on steroid concentrations) was then loaded on cartridge and rinsed with 5 mL of H<sub>2</sub>O as well as 5 mL of n-hexane. Elution was next done with 5 mL of MeOH and eluates were evaporated to dryness at 50°C under nitrogen. The dried residues were dissolved in 1 mL of 0.1 M phosphate buffer (pH 6.9) and roughly 1 200 units of  $\beta$ -glucuronidase was added to each one of them. Samples were then left to incubate at 50°C for 1 hour. After incubation, 0.4 mL of 1.0 M Cate buffer (pH 9) and 5 mL of n-hexane were added to each sample. A liquid-liquid extraction was then performed by stirring 30 seconds on vortex and centrifuging 5 min at 2500 rpm. Afterward, the supernatant n-hexane was recovered and evaporated to dryness 50°C under N<sub>2</sub>. The liquid-liquid extraction repeated a second time and once all the n-hexane had been evaporated, the dried residues were transferred with 200  $\mu$ L of MeOH in 2-mL glass vials containing a bottom-spring conical insert. The transfer MeOH was evaporated and the extracts reconstituted in 20  $\mu$ L of MeOH.

Steroids were purified by injecting the totality of the samples (20  $\mu$ L) on a 1260 Infinity II HPLC from Agilent (Mississauga, ON, Canada) using a “2-dimension” (2D) method as described by Lalonde et al. [171], with each dimension having its own quaternary pump and mobile phase composition. The first dimension was made of a single Eclipse XDB-Phenyl (Agilent, P/N 963967-912, 4.6 x 150, 3.5  $\mu$ m) column whereas the second dimension comprised two back-to-back C18 (Agilent, P/N 963967-902, 4.6 x 150 mm, 3.5  $\mu$ m) columns. The mobile phase of the first dimension was initially made up of 70/30 H<sub>2</sub>O/ACN mixture running at 1 mL/min. This H<sub>2</sub>O/ACN ratio was brought to 50/50 from 0 to 10 min, to 12/88 from 10 to 15 min and to 6/94 from 15 to 16.5 min, time at which the flow was increased to 2 mL/min. Between 16.5 and 18 min, the mobile phase composition was changed to 50/50 ACN/MeOH for 5 min. From 23 to 26.5 min, the initial 70/30 H<sub>2</sub>O/ACN was reinstated and kept constant until the rest of analysis at

30.5 min (plus a 2-min post-run). The flow was decreased to the initial 1 mL/min just before the end of the run between 30 and 30.5 min. As for the second dimension, a 60.8/34.2/5 H<sub>2</sub>O/ACN/MeOH isocratic ratio was set for the first 8.2 minutes of analysis. The solvent flow started at 1 mL/min but was immediately increased to 2 mL/min, then let constant from 1 to 8 minutes and quickly brought back to 1 mL/min in 0.2 min. From 8.2 to 19.9 min, the ratio of solvents was changed to 46.8/48.2/5 H<sub>2</sub>O/ACN/MeOH and immediately to 40/55/5 from 19.9 to 28 min. The switch from aqueous to organic-only solvents 50/50 ACN/MeOH) was then made between 28 to 30 minutes and kept isocratic for an additional 2 min, during which the flow was gradually augmented to 2 mL/min. The “loading” of the targeted steroids from the first to the second dimension happened from roughly 9 to 11 minutes (adjusted precisely for each analysis). UV signals were measured at  $\lambda = 192, 210$  and  $245$  nm.

Following the original protocol, a total of nine steroids were isolated by HPLC: testosterone (T), epitestosterone, dehydroandrosterone (DHEA), 5 $\alpha$ -androstane-3 $\alpha$ ,17 $\beta$ -diol (5 $\alpha$ -Adiol), 5 $\beta$ -pregnanediol (Pd), 5 $\beta$ androstane-3 $\alpha$ ,17 $\beta$ -diol (5 $\beta$ -Adiol), Et, Andro and 5 $\alpha$ -androst-16-en-3 $\alpha$ -ol (16-en). Et, Andro, Pd and 16-en were recovered after a single one-dimensional chromatography whereas T, E, DHEA, 5 $\alpha$ - and 5 $\beta$ -Adiol were loaded onto the second dimension for further purification before being collected. Even though all collected steroids were available for GC/C/IRMS analysis, it was decided in the end that only Et, A and Pd would be analyzed as they gave access to enough information regarding the C isotopic composition and could be compared to already published results [11, 22].

Following collection, fractions containing the steroids were evaporated to dryness at 50°C under N<sub>2</sub>, the residues were dissolved in MeOH and transferred in conical inserts placed inside of 2-mL glass vials. The MeOH was then evaporated and AcOEt was added as the GC/C/IRMS injection solvent. The final volumes of AcOEt used ranged from 12 to 250  $\mu$ L, depending on steroid concentration.

A volume of 1 to 3  $\mu$ L of each vial was injected on the GC/C/IRMS with the injector set at 270°C and using pulse pressure mode. The pulse pressure was 40 psi and lasted a minute after injection. The chromatography was made on a DB-5MS column at a constant flow of 1.2 mL/min. The GC oven initial temperature was 80°C. After a minute, the temperature was increased to 250°C at a rate of 15 °C/min, then increased to 275°C at 5°C/min and finally augmented to 320°C at

20°C/min. This final temperature was kept constant for 5 min. The Heart Split valve diverted the solvent peak to an FID until 10 minutes into analysis. At this time, it was closed to let the analytes reach the IRMS. A total of 7 MG peaks were analyzed for each injection, 4 before chromatography and 3 after. Steroid RMs, as described in [150], were used for measurement corrections. The instrument was controlled by the IonVantage software (Build 1,6,1,0) and data analysis was done using the CFDP software.

### **2.2.15 GC-MS**

Mass spectral analyses were made on a 7890B GC coupled to a 5977B MS, both from Agilent (Mississauga, ON, Canada) controlled by the Mass Hunter Workstation Software. When needed, AICAR and uridine fractions were re-dissolved in AcOEt prior to their injection. Analyses were performed in full scan mode (from  $m/z = 50$  to 600) and the same chromatographic conditions as with the GC/C/IRMS were used. Data analysis was done using Mass Hunter's Qualitative Analysis Navigator (version B.08.00).

### **2.2.16 LC-MS/MS**

Most of the urines analyzed by LC-MS/MS were first purified on PBA gel (see section above). Depending on availability, volumes of 50, 250 or 500  $\mu\text{L}$  were used for urine samples. A 1-to-1 volume of 2.5 M  $\text{NH}_4\text{Ac}$  buffer was then added and the volume was completed to 3 mL using 0.25 M  $\text{NH}_4\text{Ac}$  buffer. AICAR- $^{13}\text{C}_2$ - $^{15}\text{N}$ , uridine and uridine-2- $^{13}\text{C}$ -1,3- $^{15}\text{N}_2$  were added to urines as internal standards (ISs) before they were loaded on the gel, except in the case of the recovery estimation where they were added directly in the eluate. For 50- $\mu\text{L}$  samples, 20 ng of each IS was used, whereas for 250 and 500  $\mu\text{L}$  samples, the amount was 40 ng. After evaporation of the eluates, samples were transferred in conical plastic vials and dissolved in either 50  $\mu\text{L}$  (50  $\mu\text{L}$  of urine samples) or 200  $\mu\text{L}$  (250 and 500  $\mu\text{L}$  or urine samples) of water. For the stability tests (Chapter 3), 200  $\mu\text{L}$  of urine were used per aliquot along with 30 ng of each IS. The final volume of water was 200  $\mu\text{L}$ .

A 7-point calibration curve was made using 1.0 mg/mL and 0.1  $\mu\text{g/mL}$  aqueous stock solutions of AICAR and uridine. Those solutions were diluted in SigMatrix<sup>®</sup> (Sigma-Aldrich, Oakville, ON, Canada) urine diluent to concentrations of 0.25, 0.50, 1.0, 2.5, 5.0, 15 and 30  $\mu\text{g/mL}$ . A second set of 1.0 and 0.1 mg/mL stock solutions was also used to make three quality-control

samples (QCs) for which the concentrations were 0.75, 3.5, and 25  $\mu\text{g/mL}$ . Two different calibration curves were used to evaluate sample concentration for AICAR and uridine: the first for lower concentration samples comprised the standards from 0.25 to 2.5  $\mu\text{g/mL}$  and the second one for higher concentration samples was made with the standards from 2.5 to 30  $\mu\text{g/mL}$ . All calibration curves had  $r^2 > 0.997$  and all the results for QCs, except one, were within 20% of the expected value. These results are available in Appendix 4. A blank sample containing only the two ISs was also analyzed. Calibration standards, the QCs and the blank were treated like urine samples and 0.5 mL was extracted on PBA gel.

LC-MS/MS analyses were performed on a Q Exactive<sup>®</sup> Plus coupled with an Ultimate 3000 UHPLC, both made by Thermo Fisher scientific (Montreal, QC, Canada). The final HPLC separation method employed Eclipse XDB-Phenyl (P/N 963967-912; 4.6 x 150, 3.5  $\mu\text{m}$ ) column bought from Agilent (Mississauga, ON, Canada) heated at 40°C. A volume of 10  $\mu\text{L}$  of each vial was injected on the column with the mobile phase initially comprised of 95% H<sub>2</sub>O and 5% ACN at 0.5 mL/min. The mobile phase composition was then shifted to 50% ACN and 50% MeOH between 1 and 10 min and the flow increased to 0.8 mL/min from 10 to 10.5 min. This organic mobile phase and the new flow were then maintained for 4 min and the return to the initial conditions was done from 14.5 to 15 min. A 5-min equilibration was also observed from 15 to 20 min. Analyte detection was done using the Targeted SIM/dd MS<sup>2</sup> mode (targeted Single Ion Monitoring (SIM) followed by the equivalent of a data-dependant (dd) MS/MS (MS<sup>2</sup>) fragmentation. The SIM mode was programmed to include a range of  $\pm 3$  atomic mass units (amu) and the resolution of the instrument was set to 17,500. Precise masses of the ionic species to be detected were determined using an online calculator [172] and are available in Table 2.1. Both AICAR and uridine (and ISs) were first analyzed in positive ionization mode for the recovery estimation of the PBA gel. While this is possible for uridine based on examples in the literature [173], a lot of interference issues were encountered when testing many different matrices. Attempts with negative ionization were much more successful and therefore used for concentration determination of uridine in the samples. Data analysis was done using the Xcalibur<sup>®</sup> Qual Browser software (version 3.1.66.10).

Table 2.1: Analyte masses calculated with [172] and used for LC-MS/MS analyses.

Analyte/IS	Compound	Monoisotopic mass (amu)	Ionization mode	Ion $m/z$ (species)
Analytes	AICAR	258.0964	+	259.1042 (+H <sup>+</sup> )
	Uridine	244.0695	+	245.0773 (+H <sup>+</sup> )
			-	243.0617 (-H <sup>+</sup> )
IS	AICAR- <sup>13</sup> C <sub>2</sub> - <sup>15</sup> N	261.1002	+	262.1080 (+H <sup>+</sup> )
	Uridine-2- <sup>13</sup> C-1,3- <sup>15</sup> N <sub>2</sub>	247.0670	+	248.0748 (+H <sup>+</sup> )
			-	246.0592 (-H <sup>+</sup> )

### 2.2.17 AICAR bought on online

AICAR advertised online was bought from two different suppliers. The first was advertised on Ebay<sup>®</sup> and was sold by a company identified as Pharma Grade. The second one, supplied by Axenic was found on Amazon<sup>®</sup>. Both orders were delivered on time.

The Axenic sample arrived in a small reusable plastic bag placed inside a larger plastic envelope, on which were indicated analysis values for purity. The Pharma Grade sample was inside a glass vial and came with a small sealed plastic bottle identified as "Water for injection BP, solvent for parenteral use". Pictures of the samples can be seen in Figure 2.1. Both samples came in the form of a white powder that was soluble in water. They were weighed assuming 100% purity, dissolved as an aqueous solution to a concentration of 1 µg/mL and first analyzed by UV-HPLC. The Axenic sample was found to contain pure AICAR, at least from a UV point of view. The signal intensity of the product was also similar to a reference standard of the same concentration analyzed at the same time. Since the purity was good enough, this sample was directly acetylated, purified by HPLC and analyzed by GC/C/IRMS. As for the Pharma Grade sample, results were very different and much more concerning. Indeed, no UV signal was observed in relation with this sample, meaning it did not contain any AICAR nor any other UV-absorbant substance detectable with the HPLC method employed here. No GC/C/IRMS analysis was therefore performed on this material.



Figure 2.1: AICAR ordered from the Internet. The one on the left (Anexic) contained pure AICAR whereas the one on the right (Pharma Grade) contained a UV-invisible substance that could not be identified.

### 2.2.18 Details of the acetylation experiment

The masses used for each compound were as follows: AICAR and uridine 15  $\mu\text{g}$ , Andro, Et, estriol, sorbitol and glycerol 10  $\mu\text{g}$ . AICAR and uridine, Andro and Et, as well as glycerol and sorbitol, were acetylated and analyzed on GC/C/IRMS together. Estriol was acetylated and analyzed alone. Compounds were acetylated using the same protocol as for the sample method, with the exception of heat being applied to Andro, Et, glycerol and sorbitol (30 min at 50°C). Semi-preparative HPLC was unnecessary here, as the acetylated compounds were pure and reconstitution was made with a large volume enough (200  $\mu\text{L}$ ) to dilute the interferences originating from the reaction mixture.

Once acetylated, AICAR and uridine were analyzed using the same GC/C/IRMS method as described above. Glycerol triacetate and sorbitol hexaacetate were analyzed simultaneously, but with a different GC method to take into account the early elution of glycerol. The oven was set to 80°C for 1 minute before increasing the temperature to 320°C at 20°C/min. This final temperature was held for 10 minutes. Four pulses of reference gas were sent to the IRMS before the GC Heart Split valve was closed at 5.5 minutes into the analysis. The same method was used for Andro monoacetate, Et monoacetate and estriol triacetate, but to account for the late elution of triacetylated estriol two MG pulses had to be cut off of the end of the run. Only one more MG

pulse was therefore analyzed after analyte elution. For each tested compound, 5 acetylated replicates were analyzed.

Each of the aforementioned compound had a related RM, bought already acetylated and for which an EA-IRMS analysis had been performed. For AICAR and uridine, 1  $\mu\text{L}$  of a mix solution of 3-Ac-AICAR and 3-Ac-uridine, at respective concentrations of roughly 400 and 100  $\text{ng}/\mu\text{L}$ , was injected. For the steroids, 3  $\mu\text{L}$  of the "Brenna 33" mix with concentrations adjusted around 80  $\text{ng}/\mu\text{L}$  were analyzed. Finally, triacetine and sorbitol hexaacetate were dissolved at a concentration of 50  $\text{ng}/\mu\text{L}$  and 1  $\mu\text{L}$  of the solution was analyzed. RM analyses were done in triplicates.

### 3. Method design, optimization and validation

The three first objectives of this thesis, listed in Chapter 1, very practically aim at the development, the optimization and the validation of a method that is designed to diagnose AICAR doping using CSIR. The main goal of the following chapter is to explain how these objectives were met. As mentioned earlier, there are already two existing methods for that purpose: the first was published by Piper et al. in 2014 [11], and a more recent modification and adaptation of this same method was featured by Buisson et al. (2017) [22] who reported some issues with method robustness which affects the repeatability of GC/C/IRMS measurements. These analytical difficulties have precluded the widespread application of these procedures in other anti-doping laboratories and could undermine the credibility of AICAR positive cases presented in sport courts.

In an attempt to develop a reliable and easy-to-implement method, major modifications were made to improve robustness, selectivity during sample extraction and derivatization prior to GC/C/IRMS injection. Not so surprisingly, the best conditions were largely selected by trial and error, as many of the method's components had to be created or adjusted using a fit-for-purpose approach. Even though it is unconventional for most publications and theses to contain the detailed tribulations of method development, mainly out of concern for conciseness, it is the author's opinion that such information can be of great scientific value. Indeed, future scientists working on similar protocols could avoid repeating a mistake already made when developing the current method. This is why the following section details the range of parameters tested that eventually led to the final protocol of analysis as described in the "Material and methods" chapter.

Flow charts for the published CSIR methods for AICAR are shown in panel A and B of Figure 3.1. A proposed scheme for the novel method developed in this work is shown adjacent to the existing methods in panel C. The design and optimization of components of the method, depicted in this last panel, are described one by one in the following sections. Much like Buisson et al. (2017), SPE to quantitatively extract the AICAR/ERC duo from urine was used and like both methods, two orthogonal HPLC separations to isolate the compounds of interest from the urinary matrix were needed. However, differences can notably be found in the type of SPE sorbent and

chemical derivatization employed. This work also proposes a molecule that has never been used as an ERC in the past.

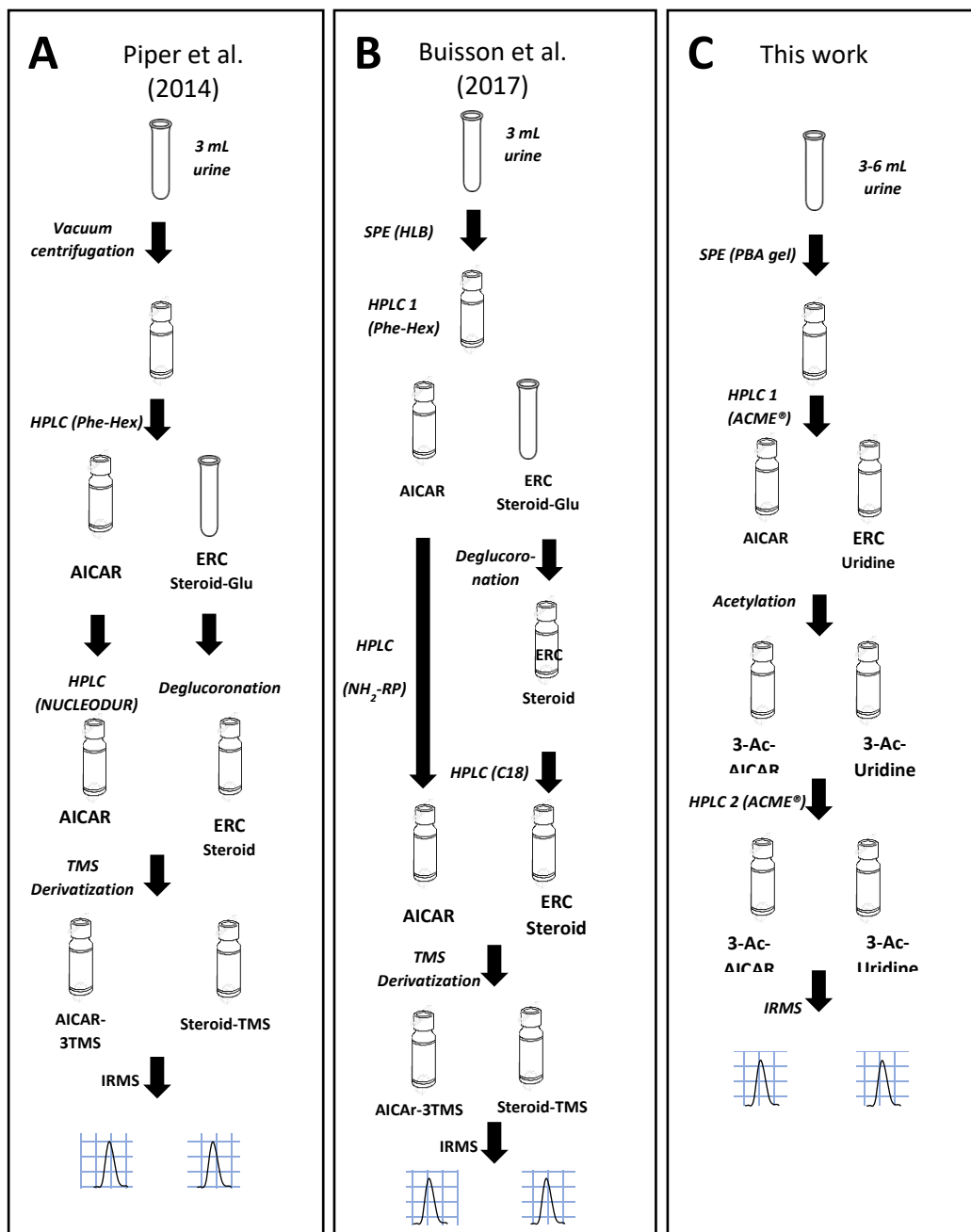


Figure 3.1: Comparison of this work method flowchart (Panel C) to those of Piper et al. 2014 (Panel A) and Buisson et al. 2017 (Panel B). The two main modifications are: 1) The derivatization step which uses acetylation instead of silylation (TMS) and 2) the choice of ERC. The use of a structurally similar ERC allows the identical treatment of AICAR and the ERC.

### 3.1. Uridine as a new endogenous reference compound

Uridine (Figure 3.2) is one of the four building blocks of RNA, along with cytidine, adenosine and guanosine. Within cells, it is first synthesized as uridine monophosphate (UMP) through the pyrimidine pathway [47-49, 51], a metabolic route independent from the purine pathway and therefore uridine's C isotopic signature is not expected to be affected by AICAR doping. The structural similarities between AICAR and uridine, both nucleosides, allows to treat both compounds identically during sample pre-treatment, which simplifies and streamlines the protocol (Figure 8) while ensuring that both the TC and the ERC can be directly compared on a like-for-like basis. Identical treatment is paramount to CSIR and has been outlined in several publications [174, 175]. Uridine is also a good candidate for acetylation, yielding 2',3',5'-tri-O-acetyluridine (3-Ac-uridine), a compound that can be analyzed by GC. For all these reasons, uridine meets all the requirements needed to be tested as an ERC for AICAR's isotopic analysis.

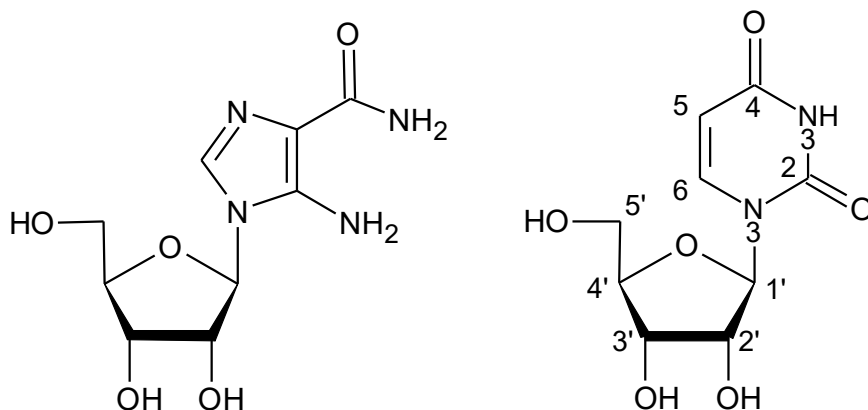


Figure 3.2: Similarities between the chemical structures of AICAR (left) and uridine (right).

### 3.2. Solid-phase extraction

In order to choose the best possible SPE option, various sorbents were tested. Piper et al. (2014) and Buisson et al. (2017) relied on rather universal extraction methods that could simultaneously extract both a polar compound such as AICAR as well as a relatively non-polar steroidal ERC. Piper et al. bypassed the solid phase extraction step altogether by directly purifying the analytes by HPLC after re-dissolving freeze-dried samples in a small volume of mobile phase. In contrast, Buisson et al. utilized “HLB” cartridges that rely on both hydrophilic and lipophilic interactions. Because uridine's chemical structure was close to AICAR's, it was attempted here to find a more

selective stationary phase that affords high analyte recovery. Low recoveries (< 50%) can be coupled to isotopic fractionation observed as a difference in the isotopic signature of the extracted AICAR/uridine compared to that found in the whole sample, not to mention an inadequately low signal measured on the GC/C/IRMS. Analysis of nucleotides, nucleosides and/or their analogs using SPE is rather common and many examples can be found in the literature for different bodily fluids (e.g., blood [176, 177], urine [167, 178] and cerebrospinal fluid [179]). Four different types of SPE sorbents were evaluated using fit-for-purpose protocols including reverse-phase (C18), hydrophilic-lipophilic balance (HLB), mixed-mode cation exchange (MCX) and phenylboronic acid (PBA) sorbents.

### **3.2.1. C18, HLB and MCX sorbents**

The best results that could be achieved with C18 (Waters, P/N WAT036810, 400 mg), HLB (Waters, P/N 186000132, 225 mg) and MCX (Waters, P/N 186000254, 60 mg) sorbents are presented in Table 3.1 alongside the protocol used for each cartridge type. Recoveries were all roughly estimated by UV-HPLC using peak areas of the analytes at  $\lambda = 265$  nm. Unfortunately, no satisfactory recovery was obtained for any of the above-mentioned sorbents.

C18 SPE is most efficient at extracting molecules of low polarity from polar matrices (e.g., steroids from urine), allowing more polar compounds to be washed off the cartridge. Recovered amounts of AICAR and uridine in the eluate were very low, always in the 0-10% range, regardless of the solvent used to elute the analytes (water or methanol). Surprisingly, further testing revealed that this loss was likely due to the irreversible adsorption of the analytes into the cartridge rather than poor retention of these polar compounds on the cartridge, presumably due to active sites within the sorbent bed. The option of C18 cartridges was thus abandoned.

MCX is a type of SPE that uses a polymer-based sorbent and allows for reverse-phase interactions between the analytes and the sorbent as well as cation exchange. It is often used for the extraction of protonated weak bases (e.g., amines) under acidic conditions. AICAR and uridine both possess amine or amide functionalities, making them plausible candidates for MCX SPE. A conventional protocol, where the sample is initially acidified using HCl, rinsed using a weaker solution of HCl and methanol and eluted in NH<sub>4</sub>OH, was followed ([180], Table 3.1). Whereas quantitative recoveries were achieved for AICAR in water, the protocol yielded no uridine at all. After further literature search, it was found that the N3 secondary amine of uridine

(Figure 3.2) behaves like a weak acid ( $pK_a \approx 9$ ) [181], meaning its protonation is very difficult even at  $pH \approx 1$ . This behavior can be explained by the three resonance structures presented on Figure 3.3 which allow the delocalization of a negative charge on uridine's nitrogenous ring, but also makes it very difficult for the molecule to bear a positive charge. Since extraction of both AICAR and uridine is necessary for the method to be efficient, MCX cartridges were discarded as a possible SPE candidate.

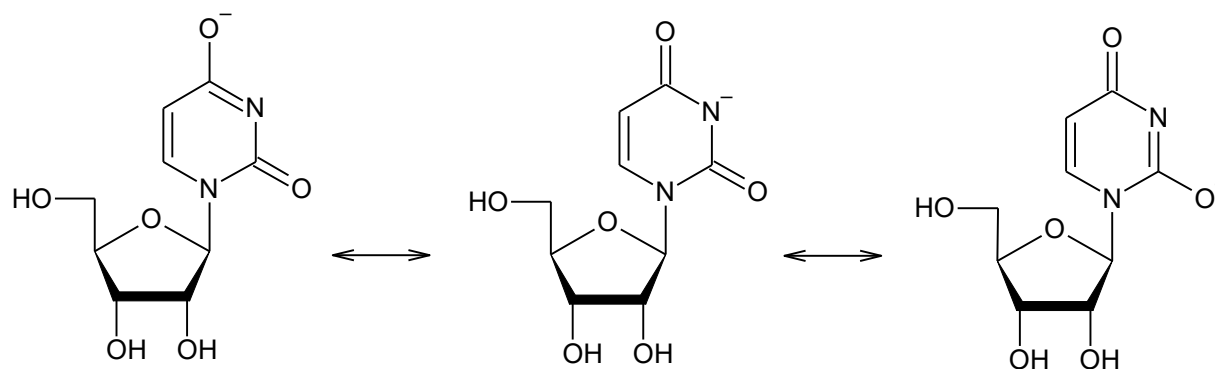


Figure 3.3: Resonance structure of anionic uridine.

HLB is a very versatile type of polymer-based SPE sorbent. It was used by Buisson et al. in their 2017 adaptation [22] of Piper and coworkers' method (2014). The fact that HLB is a very polyvalent type of SPE does have the advantage of simultaneously extracting both AICAR and steroidal ERCs from the urinary matrix, however this versatility come at the cost of specificity issues, leaving behind a great deal of potential matrix interferences alongside the target molecules in the resulting urine extract. Here, HLB cartridges were tested using an extraction protocol similar to the one of Buisson et al. (2017) and recovered amounts were promising when extracting AICAR and uridine from aqueous standard solutions (Table 3.1). Unfortunately, applying the same method to urine samples led to some complications. Attempts to carry-out the whole sample pre-treatment on real urine samples from HLB extraction through to GC injection (UV signals from HPLC chromatograms are not always discernible from matrix interferences when HLB cartridges are used and therefore can not be consistently used to evaluate recoveries from cartridges) resulted in little or no GC signals. After ruling out possible losses from other steps along the protocol (e.g., low acetylation yields), it was deduced that the major differences in recovery between aqueous standard solutions and urine samples likely originated from matrix

effects. A second experiment (Figure 3.4) confirmed this by showing that the volume of urine loaded on the cartridge had a major influence on AICAR and uridine recovery, with the best results achieved for the smallest sample volume (200  $\mu$ L compared to 500 and 1000  $\mu$ L).

Table 3.1: Approximate ( $\pm 10\%$ ) SPE recoveries obtained with the MCX, HLB and C18 sorbents.

MCX	Extraction procedure (based on Phenomenex protocol for equivalent product [180])	10 $\mu$ L of 5N HCl were added directly in urine before it was loaded on preconditioned (2 mL of methanol followed by 2 mL of water) MCX cartridges. Rinsing was then done with 2 mL of 0.1 N HCl and 2 mL of methanol and elution with 2 mL 1% NH <sub>4</sub> OH in methanol.	
	Recovery	AICAR in water: 100%	Uridine in water: 0%
HLB	Extraction procedure (based on Buisson et al. 2017 [22])	Cartridges were preconditioned with 5 mL of methanol and 5 mL of water. Urine was then loaded and rinsed with 5 mL of water and eluted with 5 mL of methanol.	
	Recovery	AICAR and uridine in water: 50-100%	AICAR and uridine in urine: 30-60% for volumes $\leq$ 1 mL
C18	Extraction procedure (from Ouellet and al. 2013 [150])	AICAR and uridine were spiked in water and passed on a preconditioned C18 cartridge (rinsed sequentially with 5 mL of hexane, methanol and water). The cartridge was then rinsed with 5mL water and hexane before elution in 5mL of methanol.	
	Recovery	AICAR and uridine in water: <10%	

These results have serious implications regarding the robustness of HLB cartridges for AICAR (and uridine) isolation in variable urinary matrices. Since no solution could be found to remedy this issue, HLB cartridges were left aside as volumes under 1 mL are not likely to generate sufficiently intense GC/C/IRMS signals for normal AICAR concentrations (i.e.,  $\approx 0.2\text{-}1\ \mu\text{g/mL}$ ).

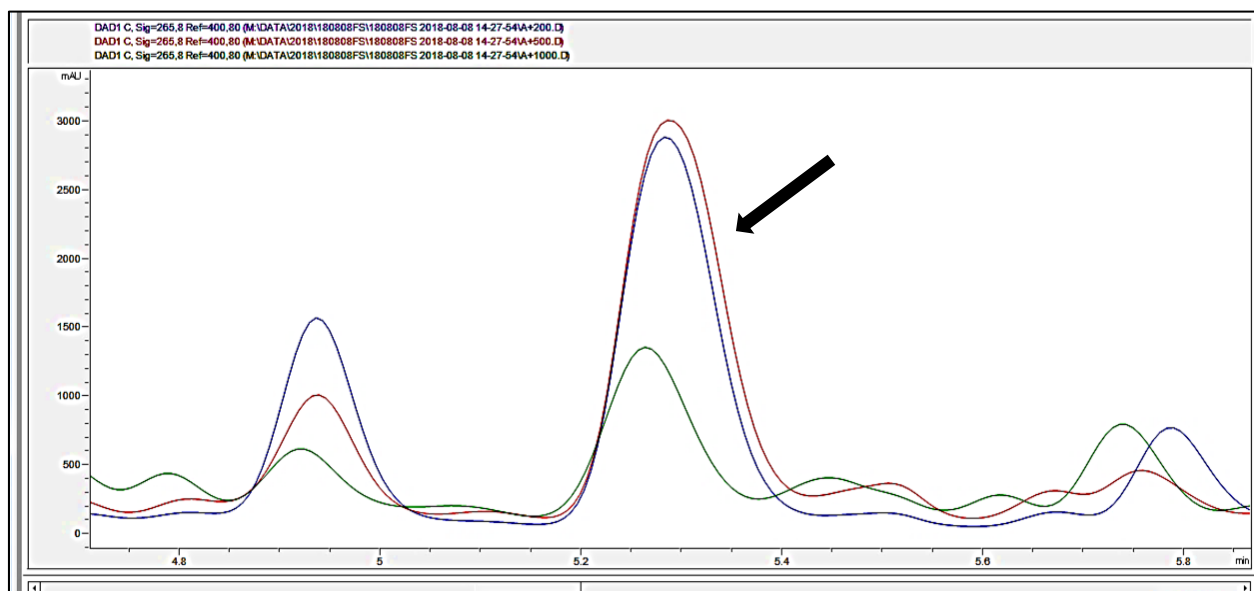


Figure 3.4: AICAR's UV signal (black arrow) after the extraction of 200 (blue), 500 (red) and 1000  $\mu\text{L}$  (green) of urine from a volunteer on HLB cartridge. Note how the signal decreases from 500 to 1000  $\mu\text{L}$ . Units are arbitrary units (AU, y-axis) and minutes (x-axis).

### 3.2.2. Phenylboronic acid

C18, MCX and HLB cartridges all rely on weak interactions (and ionic interactions in the case of MCX) to allow analyte retention on their sorbent. In light of the above results, the decision was taken to assay a different type of SPE, specifically targeting functional groups that are common to both AICAR and uridine. Phenylboronic acid (PBA) is known to form covalent bonds with coplanar cis-diol groups such as the ones found on non-deoxy nucleosides and nucleotides. Figure 3.5 shows PBA's structure as a free molecule (1) or bound to a polyacrylamide (PA) polymer (2), as well as the mechanism involving the covalent binding of AICAR to PBA (3). Under basic conditions, the boron atom captures a hydroxide ion and adopts a tetrahedral shape.

An exchange with a molecule containing a coplanar 1,2-cis-diol group is then possible [182, 183]. This chemistry requires the samples to be buffered at basic pH (i.e., 8.2 – 8.8) before being loaded on the gel. Once captured, the 1,2-cis-diols are rinsed with aqueous buffers or with an organic-aqueous mixture set at the desired pH. For elution of the analytes, the mechanism depicted in Figure 3.5 can then be reversed by lowering the pH (i.e., at ca. 3 in this work).

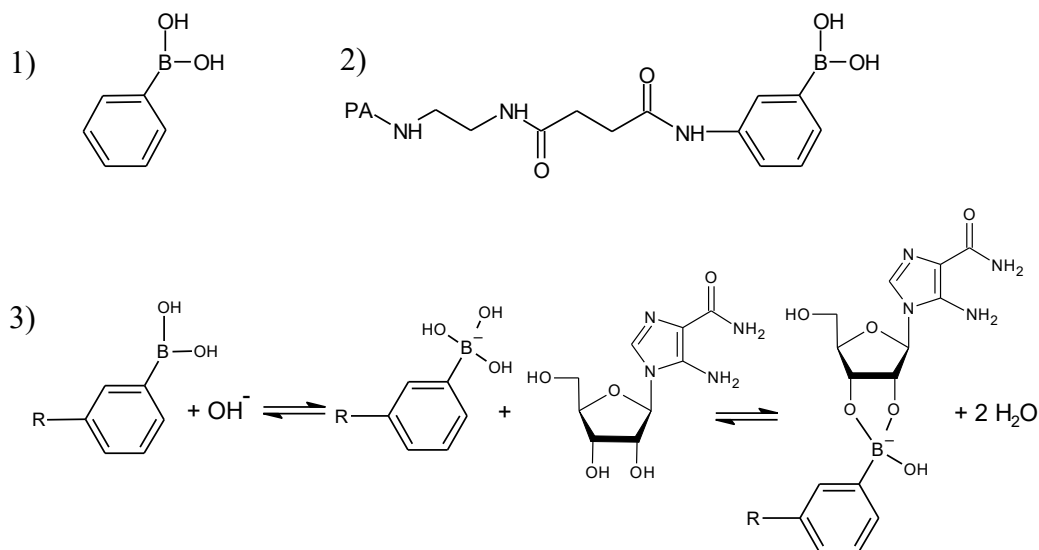


Figure 3.5: PBA's related chemistry. 1) PBA free molecule, 2) Chemical structure when bonded on PA gel and 3) Mechanism for 1,2-cis-diol fixation on PBA at alkaline pH.

Examples of PBA being used to isolate AICAR and other nucleosides from cell cultures can be found in the literature [184, 185]. Szymańska et al. (2007) [167] used this technique as sample pre-treatment to analyze 13 nucleosides in urine by capillary electrophoresis. This work demonstrates that the extension of those applications to GC/C/IRMS analysis of AICAR is possible.

Two types of PBA sorbents were initially tested, one silica-based available as cartridges and the second one PA-based available as a powder that forms a gel when immersed in water. Because of its application to urine samples, Szymańska et al.'s (2007) protocol was used to evaluate the performance of both the silica-based cartridges and the PA-based gel. Using aqueous standards,

the silica-based sorbent yielded a recovery of around 80% for AICAR. In contrast the gel gave quantitative or near-quantitative recovery percentages (> 90%) for AICAR and uridine. The PBA gel was therefore chosen for further method optimization.

### 3.2.3. PBA gel performance

Three parameters were considered to optimize the PBA-gel extraction: recovery, specificity and carry-over. Data for these tests are presented in the next sub-sections.

#### 3.2.3.1. Recovery

Using the same extraction protocol described in the “Materials and methods” section, recovery values for aqueous standards and urine are presented in Table 3.2. For the urine assay, a volunteer’s urine was spiked with high concentrations (15 µg/mL) of AICAR and uridine and four replicates were extracted. Recoveries were evaluated by comparing the gel extracts with the untreated urine. While quantitative percentages are observed for both compounds spiked in buffered water, lower recoveries are measured in urine (21% less for AICAR and 9% less for uridine). The PBA gel’s capacity reported by the supplier is very good at around 1 meq/g [186], which represents almost 26 mg of AICAR for one PBA gel (200 mg dry). However, it is possible that competition for the sorbent’s active sites by urinary matrix components influences extraction yields, which likely explains the difference in recovery between aqueous standards and urine. Despite this observation, the gel reproducibility was perfectly acceptable for urines treated individually and successfully allowed the extraction of AICAR and uridine for 44 out of the 46 urine samples analyzed in this work. The two remaining samples were later found to contain an insufficient quantity of AICAR or uridine.

Table 3.2: PBA gel recovery for AICAR and uridine in water and urine. Results are given as % ± SD.

<b>Matrix</b>	<b>AICAR</b>	<b>Uridine</b>
In water (n = 3)	96.9 ± 3.6	93.7 ± 1.6
In urine (n = 4)	76.1 ± 3.1	85.2 ± 4.5

### 3.2.3.2. PBA specificity

As mentioned in Chapter 1, PBA is deemed to be very specific to 1,2-cis-diols, including ribonucleotides, ribonucleosides and their analogs, removing any matrix constituents that do not contain these functionalities during the rinse steps of the extraction procedure. Alleviating the complexity of the matrix during the extraction step of the procedure facilitates and shortens the HPLC purification steps required to obtain pure GC/C/IRMS peaks. This specificity can be demonstrated by comparing the general aspect of UV-HPLC chromatograms originating from PBA gel extracts and other SPE protocols. Figure 3.6 compares a PBA-extract chromatogram with three others obtained after C18, MCX and HLB extraction. The specificity of the PBA gel for AICAR is obvious, as the AICAR peak can be discerned from other UV-absorbing compounds contrary to the other SPE cartridges.

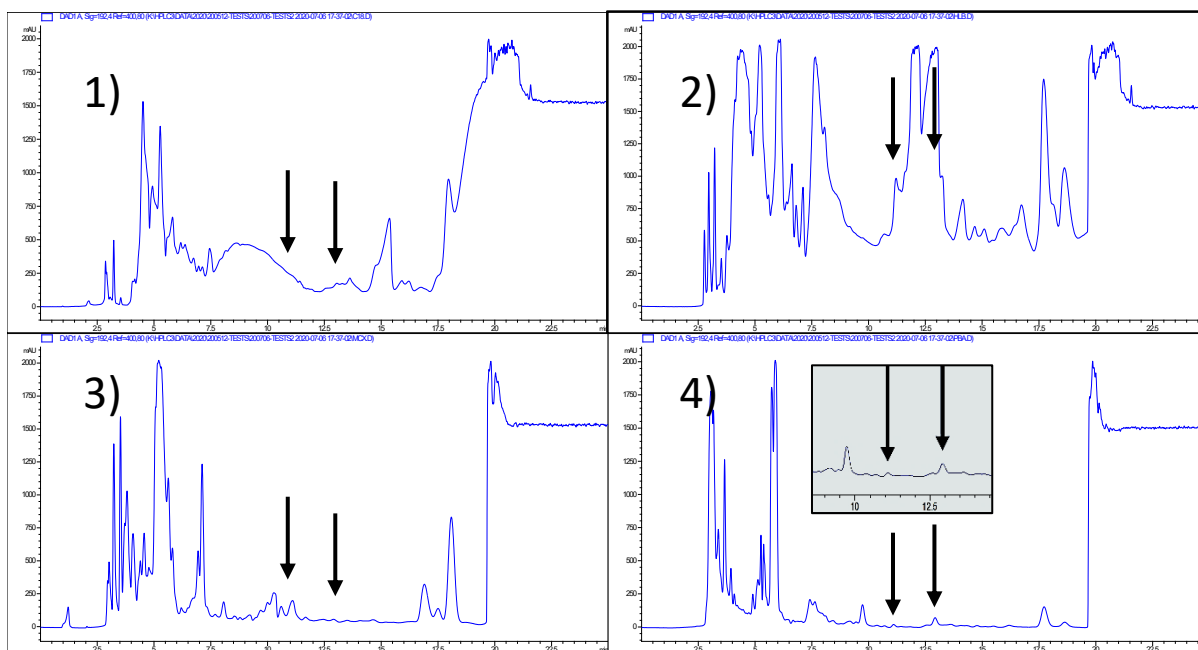


Figure 3.6: UV chromatogram for a urine extracted by SPE with 1) a C18 cartridge, 2) a HLB cartridge, 3) a MCX cartridge and 4) the PBA gel. The arrows point the expected elution time of uridine (left) and AICAR (right). Analyte concentrations were low in this sample, but peaks are visible in the PBA extract after zooming. Units are as in Figure 3.4.

### 3.2.3.3. Carry-over

PBA gels have been reported to be reusable multiple times. In the context of this work, it is crucial to make sure that no contamination from a previous extraction can alter the  $\delta^{13}\text{C}$  value of

a subsequent analysis. To test for possible carry-over, used PBA gels were washed with 0.1% formic acid before being re-conditioned. A blank buffer was then used to mimic a urine sample undergoing the entire protocol on the used gel and the eluates were evaluated by LC-MS/MS. For all four gels, the carry-over has been found to be < 0.5%. Using this last value, it can be calculated that to cause a  $\pm 1\%$  shift on a sample of equivalent concentration and possessing normal endogenous  $\delta^{13}\text{C}$  values, a contaminant would either have to have an isotopic signature that is < -210‰ or > +175‰, values that are completely outside the natural abundance isotopic range.

### **3.3. Semi-preparative HPLC**

Analyte purification by HPLC (often called semi-preparative HPLC) is a non-destructive technique in which targeted compounds can be selectively separated from the matrix they are dissolved in. It is strongly recommended by WADA as sample treatment prior to GC/C/IRMS analyses and many articles have been published on the topic [150, 158, 171]. Properly optimized, it is a powerful tool for the isolation of target analytes from complex matrices. In order to be performant, a semi-preparative HPLC method must effectively isolate AICAR and uridine from interfering compounds contained in a wide range of urinary matrices despite differences in composition and concentration.

It was decided early on that two HPLC purifications would be incorporated to the protocol created here, the first one after extraction on PBA gel and the second one after the acetylation step required for GC work. The intermediate acetylation step changes the chemical nature of each analyte and with it, its partitioning between the chromatography's stationary phase (SP) and mobile phase (MP), allocating a high degree of orthogonality to the overall HPLC cleanup and the global efficiency of the whole process. Efforts were made to minimize the adjustments made on the HPLC setup between the two purifications, which mostly meant keeping the same chromatographic column for both. This is easier from a manipulation point of view, but it also aids the method's general robustness as changes made to an instrument increase the probabilities of instrument malfunction (e.g., leaks) or human error. The first portion of method development, including the choice of mobile phase and column, was therefore done with the unacetylated molecules. Once the column was chosen, the second purification, done on the acetylated

molecules, was designed using the same column. The description of how the methods for both purifications were developed is presented accordingly in the following paragraphs.

### **3.3.1. Choice of solvents for the mobile phase**

As already mentioned, semi-preparative HPLC implies analyte recovery. This is typically done using a fraction collector connected downstream from the chromatography column and the UV detector. The fraction collector is programmed to collect the MP at specified times corresponding to analyte elution. The analyte is in solution when recovered, which implies that evaporation of the MP is required to move on to the next step of the method's protocol. This considerably limits the possible types of MP used, as any non-volatile salts, acids or alkaline buffers cannot be added to the MP to improve chromatography. As such, only pure solvents were tested, i.e., water (H<sub>2</sub>O), acetonitrile (ACN) and methanol (MeOH). MPs employed with reverse-phase (RP) chromatography are typically constituted of high percentages of H<sub>2</sub>O at the beginning of chromatography. H<sub>2</sub>O can then be progressively replaced during the course of the chromatographic run by one or more organic solvents (e.g., ACN and/or MeOH) through a concentration gradient to allow less polar analytes to elute as they are more likely to be retained by a non-polar RP SP. For AICAR and uridine, nearly 100% aqueous conditions as the initial solvent composition was necessary to increase retention. A large proportion of water is not an issue in itself, but does require a suitable HPLC column and does increase evaporation times in the context of fraction collection.

### **3.3.2. Choice of HPLC column**

HPLC columns were first evaluated using pure RM dissolved in water in order to remove any ambiguity caused by UV-active-matrix constituents in real urine samples. To optimize the odds of success when switching from pure standards to real samples, two elements were considered: 1. Longer retention times typically increase the odds of obtaining a pure peak, fanning out the analytes of interest from other crowding compounds at the moment of elution and 2. The difference in the retention times of AICAR and uridine was considered as an indicator of the capacity for a particular column to separate compounds with similar chemical properties. Molecules present in the PBA gel extracts subjected to HPLC purification are indeed similar as they all possess cis-diol moieties, therefore a column that can disperse the retention times of all of these cis-diol compounds is necessary to complement the specificity of the PBA gel extraction.

Since AICAR and uridine contain a high number of heteroatoms making them soluble in water, SPs displaying high affinity for high-polarity compounds were tested first. Hydrophilic Interaction Liquid Chromatography (HILIC, Macherey-Nagel, P/N 760532.20, 50 x 2 mm, 3  $\mu$ m) and normal-phase Fluophase PFP (Thermo, P/N 82705-154630, 150 x 4.6 mm, 5 $\mu$ m) columns were tested during method development, but eventually proved inefficient as almost no retention was observed (retention factors  $[k] \approx 0$ ). This held true no matter what percentage of organic MP was used. Better performances were achieved with conventional silica-base RPs when a high percentage of aqueous MP was present (i.e., 95-100%). This is in accordance with the choice of column made for the two published methods describing GC/C/IRMS analysis of AICAR, where a BETASIL Phenyl-Hexyl column was used to isolate underivatized AICAR [11]. This is why further testing was done using different types of RP columns, including C18 (Agilent, P/N 963967-902, 4.6 x 150 mm, 3.5  $\mu$ m) and C8 (Agilent, P/N 993967-906, 4.6 x 150, 3.5  $\mu$ m) SPs, as well as RP SPs functionalized with nitrile (Agilent, P/N 963967.905, 4.6 x 150, 3.5  $\mu$ m), amine (GL Sciences Inc., P/N 5020-05475, 3.0 x 150 mm, 3  $\mu$ m), amide (Agilent, P/N A2007150X046, 4.6 x 150 mm, 3  $\mu$ m) and phenyl (Agilent, P/N 963967-912, 4.6 x 150 mm, 3.5  $\mu$ m) groups.  $k$  values of AICAR and uridine were compared for each column by using an isocratic 100% H<sub>2</sub>O MP. All columns yielded  $k < 1$ , except for the C18 with values of 2.6 and 2.1 for AICAR and uridine, respectively. Even if this last result was interesting ( $k > 2$  is usually recommended [187]), most RP SPs are not designed to work under 100% aqueous conditions. Therefore, a column that could tolerate water without blocking or becoming unstable was purchased. An ACME<sup>®</sup> PLUS (hereafter abbreviated as ACME<sup>®</sup>) C18 column (Canadian Life Science, P/N ACMP-5-25046, 4.6 x 250, 5.0  $\mu$ m), containing a RP C18 SP and made to be functional at 100% water proved to be adequate. Results obtained for this column are presented in the following sections.

### 3.3.3. Performance of the ACME<sup>®</sup> PLUS column

The ACME<sup>®</sup> column provided even better retention and separation than the Agilent's C18 column. Figure 3.7 shows the nearly 1.5-minute separation gap achieved between AICAR ( $k = 2.9$ ) and uridine ( $k = 2.3$ ) in a mixture of RMs (A) and in a urine sample (B). Elution in 100% water occurred at around 11 minutes for uridine and 12.5 minutes for AICAR. Interestingly, the AICAR peak, barring concentrations too low for detection, was visible in all 46 analyzed

samples. This is of high value, since it allows detection of possible shifts in retention time giving more reliability to the method. Uridine was not always visually detectable, but was proven to be properly purified in all samples by further GC analysis. The main disadvantage of collecting analytes in 100% water is the time required to evaporate water. Here, this disadvantage was largely compensated by the performance of the method, both from a purity and a reliability point of view. The ACME<sup>®</sup> column was therefore used for the rest the work.

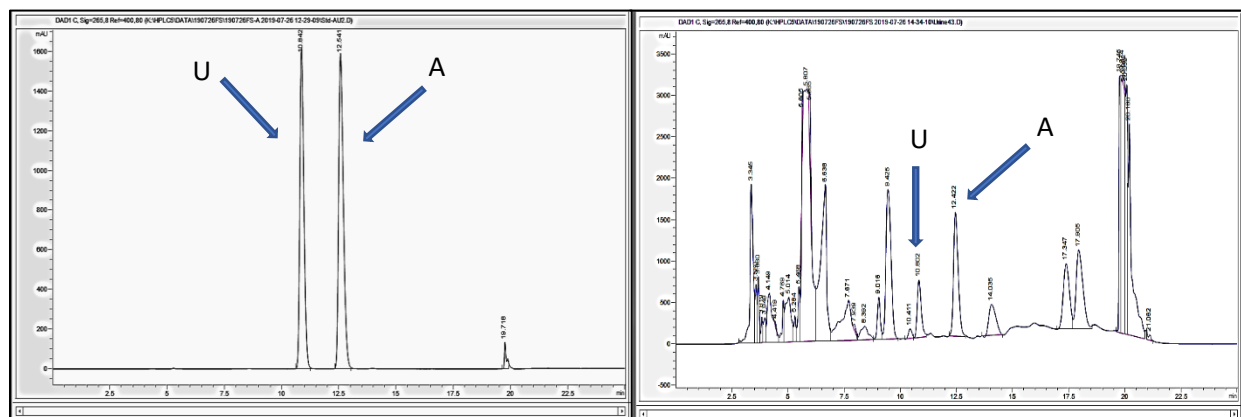


Figure 3.7: Examples of HPLC chromatograms obtained after PBA gel extraction with the ACME<sup>®</sup> column using the method's final version. Left: for a standard mix of AICAR and uridine and right: for a urine sample. A: AICAR and U: Uridine. Note the very distinctive AICAR peak in the sample and the >1-minute gap between AICAR and uridine.

### 3.3.4. Second HPLC: After acetylation

The ester groups created by acetylation are less polar and less reactive than hydroxyl groups. For this reason, acetylated AICAR and uridine were expected to display greater affinity for the RP SP than the unacetylated compounds. This was the case as retention times measured were much longer for the acetylated products. To make sure the method was not unnecessarily long, the proportion of organic MP at the start of chromatography was increased to 30% (15% ACN and 15% MeOH) to allow elution of uridine and AICAR at roughly 7.4 and 8.0 minutes, respectively. Such low retention times were possible since the chromatograms were much less loaded than during the first HPLC, a consequence of the two levels of purification to which the sample extracts had already been subjected to this stage. Efficient purification on the ACME<sup>®</sup> column was thus rapidly achieved. Examples of chromatograms can be seen in Figure 3.8.

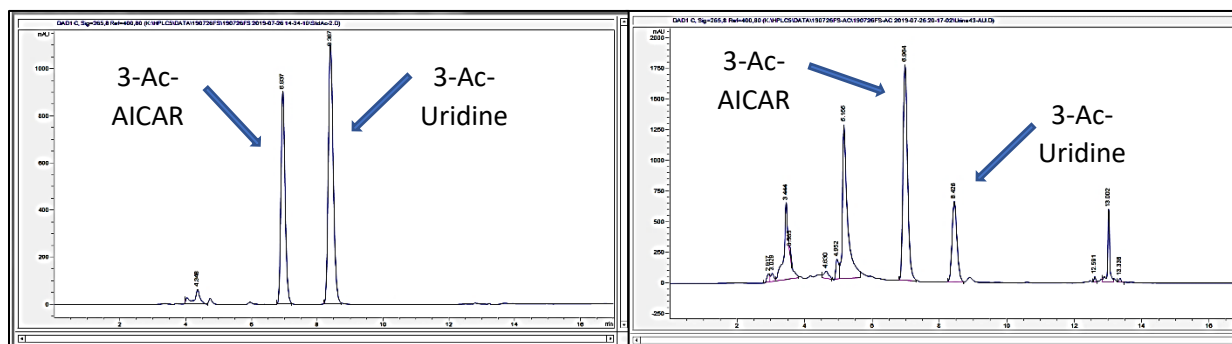


Figure 3.8: Examples of HPLC chromatograms obtained on ACME<sup>®</sup> column after acetylation. Left: for a standard mix of 3-Ac-uridine and 3-Ac-AICAR and right: for a urine sample. Note the interesting elution order swap between the free (Fig. 3.7) and acetylated forms of AICAR and uridine.

### 3.4. Acetylation

To make AICAR analyzable by GC, Piper et al. (2014) as well as Buisson et al. (2017) had to convert it to its tris-trimethylsilyl (TMS) derivative (Figure 3.9). TMS derivatization is a very common chemical reaction in organic and analytical chemistry, mostly used to protect alcohols, amines and ketones. TMS derivatives often show better volatility and/or chromatographic behavior than their underivatized counterpart, therefore explaining their utility for gas-phase analyses. TMS derivatives are however seldom used for GC/C/IRMS owing to the fact that silicon atoms in the reagent are known to be deposited as silicon carbide in combustion tubes during catalytic oxidation [164]. Buisson et al. (2017) have observed a deterioration in  $\delta^{13}\text{C}$  measurement reproducibility and accuracy as a result of this poisoning of the combustion catalyst. The idea of using TMS derivatization was therefore quickly rejected and a more convenient and reliable way to derivatize AICAR and uridine was investigated.

In contrast, acetylation is also a typical derivatization reaction used to protect alcohol and amine groups. It can simply be described as the introduction of an acetyl group on a molecule, transforming alcohols into esters (esterification) and amines into amides (Figure 3.10). Acetyl chloride ( $\text{AcCl}$ ) and acetic anhydride ( $\text{Ac}_2\text{O}$ ) are two widely used reagents to perform acetylation which are most often coupled to a basic catalyst such as pyridine (Pyr), dimethylaminopyridine (DMAP) or triethylamine ( $\text{Et}_3\text{N}$ ) [188-190]. The  $\text{S}_{\text{N}}1$ -type mechanism, with  $\text{Ac}_2\text{O}$  and Pyr as

reagents, can be seen in Figure 3.10. As a specific type of esterification, acetylation is reversible. Equilibrium toward the acetylated product is driven by adding a large excess of reagent (i.e.,  $\text{Ac}_2\text{O} \gg \text{AICAR}$  or uridine). This excess of reagent is created by using the mixture of acetylation reagent and catalyst as the solvent in which the reaction takes place. For that reason, this type of reaction can also be categorized as a solvolysis. Acetylation is widely used for anti-doping GC/C/IRMS analysis of AAS to improve chromatographic behavior, although some WADA-accredited laboratories prefer to analyze underivatized steroids.

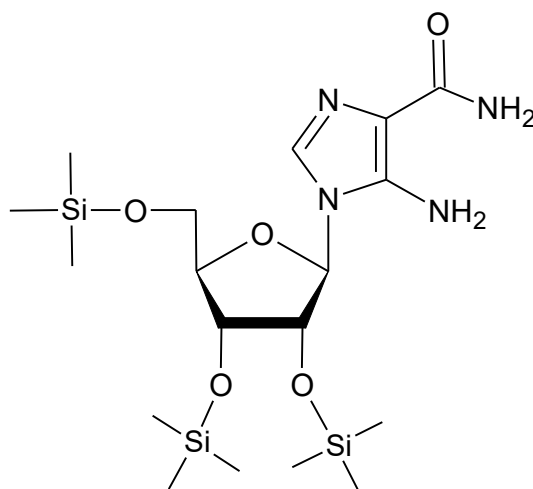


Figure 3.9: Trisilylated form of AICAR.

From a chemical structure point of view, AICAR can be regarded as a good candidate for acetylation. It bears three alcohol groups (one primary on C5' and two secondary on C2' and C3') and one primary amine on C5, all potential acetylation targets (Figure 1.1). The triacetylated product, 5-Amino-1-(2',3',5'-tri-O-acetyl- $\beta$ -D-ribofuranosyl)-imidazole-4-carboxamide (3-Ac-AICAR) has been used in several organic chemistry publications [191, 192] and is commercially available. AICAR's acetylation for GC/C/IRMS has been described as unfeasible in previous publications [11, 22], however those statements were not supported with data, which begs for more tests to be done. Thus, this work intends to show that AICAR can be acetylated to 3-Ac-AICAR and uridine to 3-Ac-uridine, two compounds that can be analyzed by GC/C/IRMS in an easy and robust way. A chromatogram and mass spectra are presented in Figures 3.20 and 3.21 of this chapter to support this affirmation.

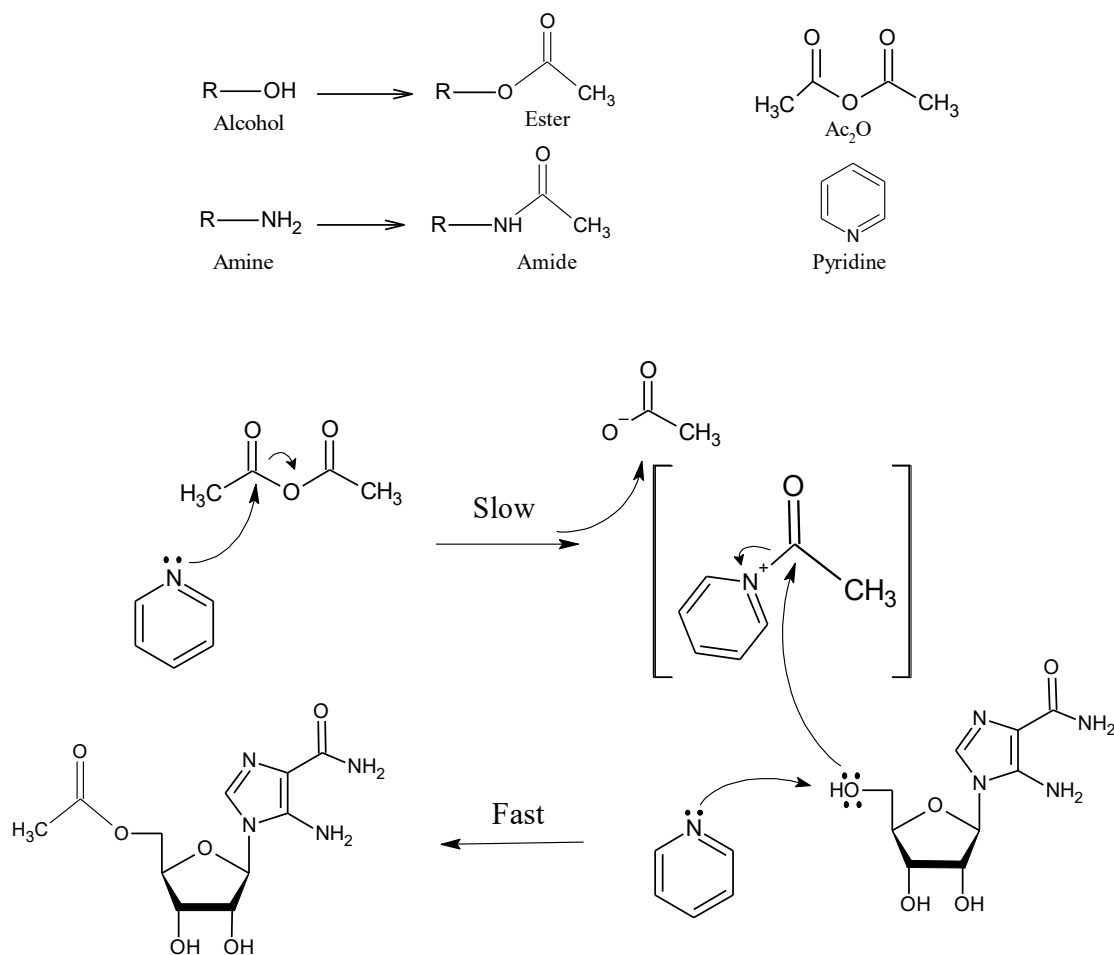


Figure 3.10: The acetylation reaction. A) General acetylation of an alcohol yielding an ester and of an amine yielding an amide. B) Chemical structures of Ac<sub>2</sub>O and Pyr. C) Acetylation mechanism of the C5'-OH of AICAR with Ac<sub>2</sub>O and Pyr.

### 3.4.1. Choice of reagents

Ac<sub>2</sub>O and AcCl were both considered for the reaction. Ac<sub>2</sub>O was eventually chosen over AcCl, as this last one is more reactive [193] and more likely to generate tetra-acetylated AICAR (4-Ac-AICAR), an undesirable by-product. AcCl's long-term stability was also an issue, since its reactivity with ambient humidity is also greater than Ac<sub>2</sub>O. Ac<sub>2</sub>O is also generally cheaper than AcCl.

As for the reaction's catalyst, choices were limited to compounds compatible with the subsequent HPLC purification. For this reason, strong or non-volatile acids or bases were discarded

straightaway. After review of the literature and of the different products available, two different catalysts were chosen for evaluation: Pyr and triethylamine (Et<sub>3</sub>N). For both of these compounds, the catalytic mechanism proceeds via the nucleophilic attack of the Ac<sub>2</sub>O acyl group (Figure 3.10).

After a few attempts with Et<sub>3</sub>N, two issues were eventually identified. The first one is the presence of 4-Ac-AICAR that was observed eluting just before 3-Ac-AICAR during GC analysis. This can be seen in Figure 3.11. Most of this peak could be removed by semi-preparative HPLC, but its presence meant dealing with lower reaction yields. In the worst cases, the 4-acetyl- to 3-Ac-AICAR ratio was almost 1 to 1. This peak was also detectable when using Pyr, however its intensity was consistently much lower and reproducible ( $\leq 10\%$  of the 3-Ac-AICAR peak). Another issue when using Et<sub>3</sub>N was the formation of a thick yellow-to-dark orange substance in the reaction vials. This product matches the description of tetraethylammonium acetate, formed by the reaction between Et<sub>3</sub>N and Ac<sub>2</sub>O. The presence of this substance thickened the reaction milieu and was difficult to dissolve after evaporation, a situation that is far from ideal for the following semi-preparative HPLC step. This problem was not encountered with Pyr, which was selected as the catalyst of the reaction.

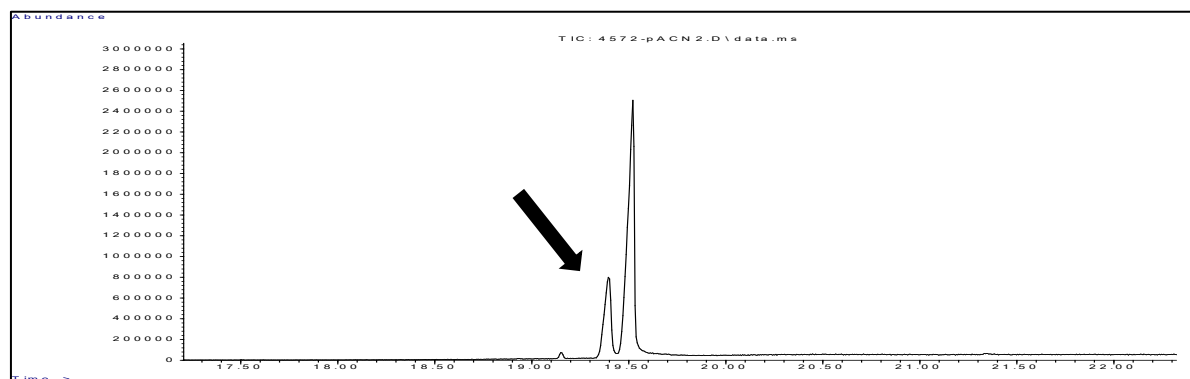


Figure 3.11: Total Ion Count GC-MS chromatogram of acetylated AICAR using Et<sub>3</sub>N. The arrow shows the peak with M<sup>+</sup> at  $m/z = 426$  corresponding to 4-Ac-AICAR.

### 3.4.2. Reaction parameters

The reaction's protocol was optimized to make sure the maximal yields were obtained. Following the choice of reagents, three other parameters were optimized: 1. reaction temperature, 2. reaction

time and 3. the stoichiometry of the reagents. After each acetylation test, the conditions under which the maximum signals were achieved for the acetylated products were identified using UV-HPLC at  $\lambda = 265$  nm. A second nucleoside was also added as an external standard (ES) when the reaction was over to account for small differences in the HPLC injection volume (either unacetylated cytidine or thymidine, depending on availability). For each experiment, the ratios of the surface areas of the analytes to the ES were determined. The highest ratio value was assigned a value of 100% and all the other results normalized accordingly. The parameter values yielding the higher results were then chosen for the reaction's final protocol. It must also be mentioned that the reaction was optimized using only RM, even though the ultimate goal of this work is the acetylation of urine extracts. This is justifiable since the combined cleanup effect of the PBA gel and the first HPLC allows for the acetylation to be performed in almost ideal conditions.

Two observations were made early on in the reaction's optimization process: 1. the reaction proceeded quickly and 2. without the need to heat the reaction medium. This somewhat came as a surprise, as most acetylation protocols are carried out at elevated temperatures (e.g., 60-70°C) and allow some time (e.g., 30 min) for the reaction to proceed. From a practical point of view however, this was good news, minimizing time and labor. Table 3.3 summarizes all the parameters and reagents tested, as well as the final choice of conditions used for method validation.

Table 3.3: Tested parameters and reagents for acetylation. < 1 minute corresponds to a 5-10 second stir on vortex before adding water to stop the reaction. RT: room temperature.

Parameter/Reagent	Tested	Chosen
Catalyst	Pyr, Et <sub>3</sub> N	Pyr
Time	< 1, 5, 10, 15, 20 and 30 minutes	< 1 minute
Ac <sub>2</sub> O : Pyr molar ratio	0.22, 0.30, 0.46, 0.63 and 0.72	0.5
Temperature	RT*, 30, 40, 50 and 60°C	RT

### 3.4.3. Yield and reproducibility

After the optimal conditions were determined, a quantitative assessment of the reaction yield was performed using the UV absorption at the retention time corresponding to the acetylated peaks on an HPLC chromatogram. Since no quantitative standard of the acetylated compounds was available for either AICAR or uridine at the time of experiment, equimolar solutions of the unacetylated compounds representing a 100% yield were used as reference against which the yield could be estimated. This is possible as the nitrogenous cycle of nucleosides and nucleotides is responsible for most of their UV absorption around  $\lambda \approx 260$  nm [194-196]. This region is left unchanged by acetylation so the absorbance of the acetylated and unacetylated molecules can then be considered as approximately equivalent. The precise wavelength was set to 265 nm after a UV scan of AICAR. Triplicate tests corresponding to 3 different masses of AICAR and uridine (5, 15 and 25  $\mu\text{g}$ ) were performed. Table 3.4 details the reaction yield in each case. Triplicates of 5 and 15  $\mu\text{g}$  all achieved yields over 90%. Results for the 25- $\mu\text{g}$  triplicate were slightly lower, ranging from 84 to 89%, however even in this case no trace of unacetylated AICAR or uridine was detectable on the UV chromatogram. The results were deemed satisfying since 1. the percentages obtained are still very close to being quantitative even at 25  $\mu\text{g}$ , a large mass to be acetylated that is rarely encountered in samples and 2.  $\delta^{13}\text{C}$  values are not expected to be altered for near quantitative results. In addition, the method was highly reproducible, with all SDs and relative standard deviations (%RSDs) being  $< 4\%$  for each individual triplicate measurement.

Results from Tables 3.3 and 3.4 confirm acetylation as a suitable alternative for AICAR CSIR analysis. In addition to the good yield and reproducibility values, the reaction proceeds very rapidly, does not require heat and is not known to be harmful for combustion catalysts. No issues were found after over 600 analyses made with the same catalyst. This last point gives acetylation a clear advantage over silylation for the chemical derivatization of AICAR for GC/C/IRMS analyses.

Table 3.4: Acetylation yields (%) for AICAR and uridine at three different masses.

Compound	AICAR			Uridine		
Mass	5 µg	15 µg	25 µg	5 µg	15 µg	25 µg
Mean for each mass n = 3 (%)	98	97	88	93	95	87
SD for each mass n = 3 (%)	1.4	2.5	2.1	0.2	2.9	2.5
%RSD for each mass n = 3 (%)	1.4	2.6	2.4	2.2	3.1	2.9
Mean yield for each compound n = 9 (%)	94			91		
SD for each compound n = 9 (%)	5.4			4.1		
%RSD for each compound n = 9 (%)	5.7			4.5		

### 3.5. GC/C/IRMS

Four aspects were considered for the development of the GC/C/IRMS method: gas chromatography, combustion, the correction of the isotopic measurements using RM and the correction for acetylation.

#### 3.5.1. Gas chromatography

The type of chromatographic column and GC parameters, including injector temperature, starting temperature and temperature ramp rate were all considered during method development. The choice of column has the greatest impact on peak symmetry, resolution and intensity, whereas GC parameters can be modulated to maximize peak intensity all in the goal of obtaining a sharp, resolved GC peak that is within the linear range of the IRMS.

##### 3.5.1.1. Choice of chromatographic column

As already mentioned in the “Material and methods” section, two different GC columns were tested. The first one was a DB-5MS from Agilent, a widely used GC column for mass spectrometric applications. The second was a CP Sil 8 CB for amines (CP Sil), also from Agilent.

This last column is less commonly used, but described by the manufacturer as very specific to non-volatile compounds bearing amine functionalities.

Peak symmetry was greatly influenced by the column type, as shown by the comparison of an AICAR peak eluting from both column types on Figure 3.12. The AICAR peak produced by the DB-5MS column exhibited a strong fronting behavior, even at small intensities, which is indicative of column saturation or a symptom of “mismatch” between the analyte and the SP (i.e., DB-5MS columns are possibly not made for AICAR analysis).

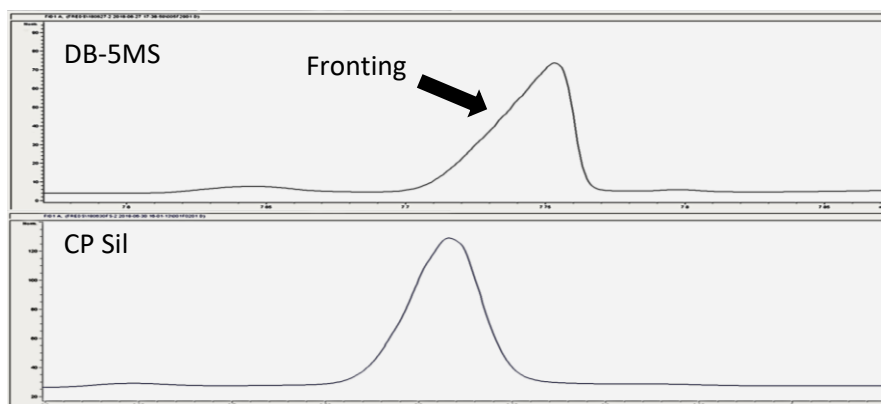


Figure 3.12: Peak shape comparison between the Agilent’s DB-5MS (top) CP Sil (bottom) columns.

The symmetry factor for DB-5MS and CP Sil peaks was computed by the ChemStation software (G2070BA) and plotted against its peak area in order to study the phenomenon in greater detail (Figure 3.13). A symmetry factor of 1 is the ultimate target as it indicates a Gaussian peak. Such symmetric peaks were possible over a wide range of peak areas on the CP Sil column, in contrast to the DB-5MS columns that generated fronting peaks that translated into larger and larger symmetry factors with increasing peak area.

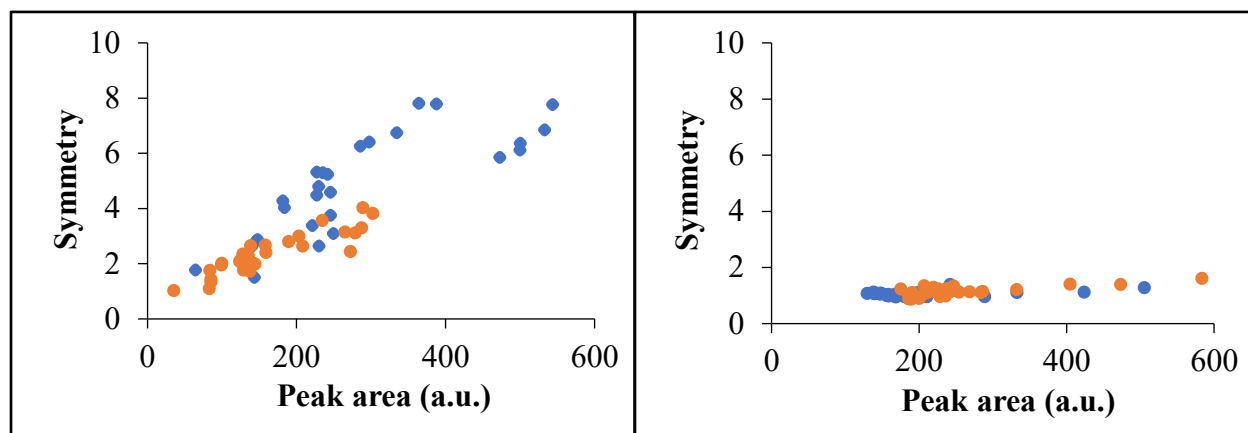


Figure 3.13: Symmetry factor (no units) comparison between the DB-5MS (left) and the CP Sil (right) columns. Orange dots: 3-Ac-AICAR and blue dots: 3-Ac-uridine.

DB-5MS column performance was also shown to degrade from irreversible sorption and decomposition of semi-volatile compounds on the column's active sites. Over time, column damage became evident from decreasing peak intensity and worsening peak shapes. Sorbitol was used as a column protectant in the attempt to prolong column life [169, 170], however the positive effect was short-lived and unpredictable. Sorbitol was also used on the CP Sil columns, but tests demonstrated that only a few injections were necessary to condition a new column after which the column was useable for at least 600 injections without any visible deterioration in chromatographic performance.

In summary, the CP Sil column was much better suited to the analysis of triacetylated AICAR and uridine. The DB-5MS column was therefore left aside and the CP Sil used for the rest of method development.

### 3.5.1.2. GC temperature parameters

The GC temperature parameters can be broken down into three main components: the injector's temperature, the oven's initial temperature and the rate at which the temperature of the oven increases (called temperature ramp). Optimizing these parameters in terms of the analyte's signal intensity can be tricky though, mostly because it is impossible to isolate the influence of each parameter from other sources of signal variations, such as small instrumental errors associated to injection volume, day to day variations in signal intensity on one instrument or inter-instrument

variations in signal intensities. The use of any other compound as an internal reference is also ineffective since the signal of such a reference is also dependant on GC parameters. The strategy that was therefore adopted was to make as many analyte injections as possible in one sequence of injection using a GC equipped with a flame ionization detector (FID). All injections were made from the same solution (a large volume solution was used to minimize effects of solvent evaporation), each one with a given value of the tested parameter and in a given order (e.g., ascending order). The experiment was then repeated, but this time by either reversing or shuffling the order of the tested values to make sure injection order had no impact on the outcome of the analytes' signal. For each experiment, results were normalized to the highest surface area obtained which as assigned a value of 100%. An example is given in Figure 3.14 for the GC injector's temperature.

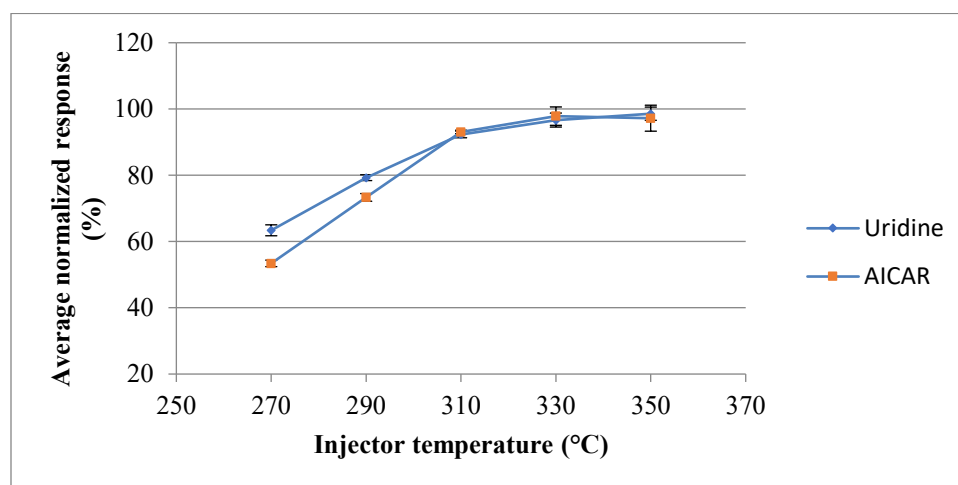


Figure 3.14: Influence of the injector temperature on the GC-FID signal for 3-Ac-AICAR (orange squares) and 3-Ac-uridine (blue triangles). For each point  $n = 2$  and error bars are  $\pm 1$  SD. Results obtained with a DB-5MS column.

The injector temperature was the only parameter tested solely on the DB-5MS column. This was possible since it is independent from the GC column. All the other parameters were optimized on both the CP Sil and the DB-5MS column despite our choice to use the CP Sil, as this could potentially provide important information on the columns' performances. Results can be found in Table 3.5 and show that the largest impact observed was from the oven's initial temperature on

the DB-5MS. Maximal surface areas were obtained at 100°C, but average losses of 33% for AICAR and 38% for uridine were measured when this temperature was increased to 200°C.

After selecting the optimal GC oven parameters and the injector temperature based solely on the maximal peak intensity, some changes were eventually made to account for new observations made after analyzing numerous samples. This explains the discrepancies between the “optimal” GC parameters (Table 3.5) and the method’s final version in the "Material and methods” section. Keeping the injector temperature above 300°C caused the accumulation of soot in the GC’s injection liner, visible as dark material encrusted in the liner’s glass wool. This mostly occurred after long injection sequences and impacted chromatography by broadening the peaks. A compromise temperature of 290°C was eventually chosen. As for the oven’s parameters, since only minor impacts were noticed on the analytes’ signal, values were set to optimize the method’s total time duration while ensuring that this did not increase the likelihood of co-eluting peaks.

Table 3.5: Optimal GC parameter values.

Parameter	Values tested	Optimal value
Injector’s temperature	270, 290, 310, 330 and 350°C	≥ 310°C
Oven’s initial temperature	100, 150 and 200°C	DB-5MS: 100°C CP Sil: No impact
Temperature ramp	DB-5MS: 10, 15 and 20°C/min CP Sil: 10, 15, 20, 25 and 30 20°C/min	DB-5MS: No impact CP Sil: Small impact (always < 10% from maximal value)

### 3.5.2. Combustion

Complete transformation of the analytes into CO<sub>2</sub> is very important in GC/C/IRMS analyses, not only to ensure that sufficient signal is detected by the IRMS, but also to avoid potential KIE associated with incomplete combustion. Undesirable chemical reactions between the catalyst and the analytes (e.g. formation of silicon carbide upon combustion of TMS derivatives [164]) can also cause KIE. The combustion process can be described for the most part by two general

parameters: the type of catalyst used and the composition of the carrying gas going through the combustion chamber.

A typical catalyst suggested by Isoprime and already present in a lot of GC/C/IRMS instruments is copper (II) oxide (CuO), available as small pellets that fit inside a hollow quartz tube through which the carrier gas flows. More specialized catalyst setups are sometimes used for more elaborate applications, for example to measure N stable isotopes which requires NO<sub>x</sub> reduction to N<sub>2</sub> [197] or to combust methane [198]. These typically include nickel (II) oxide and small amounts of platinum to increase the speed at which oxygen is transferred during combustion [199]. Such catalysts were considered since AICAR and uridine are N-bearing compounds likely difficult to combust, however installing a new combustion quartz tube is a relatively long and painstaking process that requires the instrument to be shut down for at least a few hours and often resulting in the breakage of some instrument consumables (e.g., quartz tubes, capillaries). To minimize frequent instrument interventions and because NO<sub>x</sub> reduction was not considered essential here since N stable isotopes are not of interest, the usual catalyst - CuO - was therefore the favoured option provided it performed sufficiently well for the combustion of triacetylated AICAR and uridine.

When using CuO, the oxygen involved in the oxidation of analytes can either originate from within the catalyst's lattice (the lattice is unstable when heated to 850°C) or from reactive oxygen species at the catalyst's surface [199]. Monitoring of the O<sub>2</sub> signal at the exit of the combustion chamber during analysis showed a relatively narrow negative signal depletion as analyte elution occurs (data not shown), suggesting the consumption of readily available oxygen at the catalyst's surface, followed by the replenishment of these reactive oxygen species through adsorption from the carrier gas. During this project, an O<sub>2</sub> tank was connected to the stream of helium carrier gas carrying the analytes to the IRMS. This allows for the reactive oxygen coating the catalyst particles to remain stable and maintain catalytic oxidation all throughout long injection sequences. Additionally, CuO can be re-oxidized by lowering the furnace's temperature [200], something very convenient making possible catalyst's "regeneration" over the course of a few hours. Here, this was done at 600°C.

As already mentioned, combustion of N-bearing compounds using CuO as a catalyst produces NO<sub>x</sub>, mostly NO, NO<sub>2</sub> and N<sub>2</sub>O [201]. Generating N<sub>2</sub>O and NO<sub>2</sub> can be problematic as these

species are isobaric to  $^{16}\text{O}^{12}\text{C}^{16}\text{O}$  ( $m/z = +44$ ) and  $^{18}\text{O}^{12}\text{C}^{16}\text{O}$  ( $m/z = +46$ ) [202]. At high  $\text{O}_2$  content (e.g., after catalyst regeneration at  $600^\circ\text{C}$ ), very depleted  $\delta^{13}\text{C}$  values ( $< -40\text{‰}$ ) were obtained due to the artefactual amplification of the mass 46 signal which is used by the IRMS's software in the attribution of  $^{18}\text{O}$ ,  $^{17}\text{O}$ ,  $^{16}\text{O}$ ,  $^{13}\text{C}$  and  $^{12}\text{C}$  content to what it assumes is a pure  $\text{CO}_2$  peak.  $^{17}\text{O}^{12}\text{C}^{16}\text{O}$  and  $^{13}\text{C}^{16}\text{O}_2$  both contribute to  $m/z = 45$  though the former is much less significant; the proportion of  $^{17}\text{O}^{12}\text{C}^{16}\text{O}$  is calculated using the  $m/z = 46$  signal ( $^{18}\text{O}^{12}\text{C}^{16}\text{O}$ ) since the expected proportion of  $^{18}\text{O}/^{17}\text{O}$  in  $\text{CO}_2$  is known (referred to as the Craig correction, [203]). Figure 3.15 shows what happens when multiple injections of 3-Ac-AICAR are done on a freshly regenerated catalyst after the oxygen supply is suspended. The  $\delta^{13}\text{C}$  values are very low for the first few 3-Ac-AICAR injections, whereas  $\delta^{18}\text{O}$  measurements (corresponding to the masses 46/44 ratio) were artificially inflated by the presence of  $\text{NO}_2$ . In contrast, the raw  $\delta^{13}\text{C}$  CSIR values (noted  $^{45}\delta$ ) that is not corrected for the contribution of  $^{17}\text{O}$  in the  $m/z = 45$  signal, were found to be very stable throughout all the 29 injections ( $\text{SD} < 0.2\text{‰}$ ). Conditioning the system through multiple injections is therefore necessary to establish a proper oxygen balance in the combustion system that does not allow for  $\text{NO}_2$  to be generated but that is sufficiently high to completely combust C containing compounds.

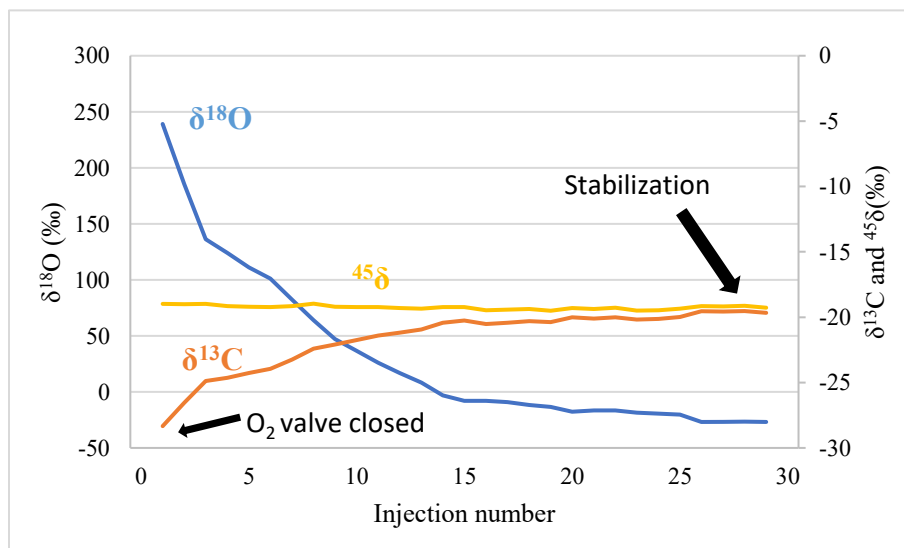


Figure 3.15: Increase in the  $\delta^{13}\text{C}$  value (orange) values and decrease in the  $\delta^{18}\text{O}$  values (blue) as the  $\text{O}_2$  level decreases in the GC/C/IRMS combustion chamber. CSIR values uncorrected for  $^{17}\text{O}$  ( $^{45}\delta$ , yellow) are stable throughout the test.

The morning following the experiment described in Figure 3.15, another series of injections was made using 3-Ac-AICAR and 3-Ac-uridine to see if  $\delta^{13}\text{C}$  values were still stable. SDs of 0.12 and 0.04 were obtained respectively for acetylated AICAR and uridine, as shown in Table 3.6. A comparison with EA-IRMS values demonstrates that the results are accurate. It is likely that a decrease in the amount of available oxygen stoichiometrically favors the formation of NO ( $m/z = 30$ ) over  $\text{NO}_2$ , which does not interfere with the assignment of a  $\delta^{13}\text{C}$  value to AICAR or uridine.

Table 3.6: Precision achieved by the GC/C/IRMS instrument under suitable  $\text{O}_2$  levels. The measured  $\delta^{13}\text{C}$  values were corrected with the MG only.

Compound	n	Average (‰)	Std Dev (‰)	EA-IRMS (‰)
AICAR	7	-15.4	0.12	-15.53
Uridine	7	-24.6	0.04	-25.21

This  $\text{O}_2$ -related effect was found to happen not only after catalyst regeneration, but also when oxygen levels added to the helium in the combustion chamber were high. Figure 3.16 displays the  $\delta^{13}\text{C}$  value measured for 3-Ac-AICAR at different  $\text{O}_2$  intensities (measured as nanoamperes [nA] reaching the IRMS detector). Artificially depleted  $\delta^{13}\text{C}$  values clearly corresponded to higher  $\text{O}_2$  signals, something that could be adjusted by closing the oxygen supply or decreasing it.

Pinpointing precise levels at which CSIR were unaffected proved to be difficult and are expected to differ from one instrument to another (the intensity of the oxygen signal depends on the tuning of the ion source) or when the catalyst is replaced. Since stable values on Figure 3.16 were achieved with  $\text{O}_2$  signals around 3 nA, which is close to the baseline levels usually measured without any external sources, the decision was made to simply turn off the  $\text{O}_2$  supply before the start of all analyses and verify that the oxygen level remained under 5 nA. Even without an external  $\text{O}_2$  supply during analysis, the CuO catalyst provided good stability even for analytical sequences of over 50 injections. Table 3.7 shows how stable values were for RMs analyzed at the beginning, within and at the end of a sequence lasting 50 hours; all measured SDs were  $< 0.50\%$ .

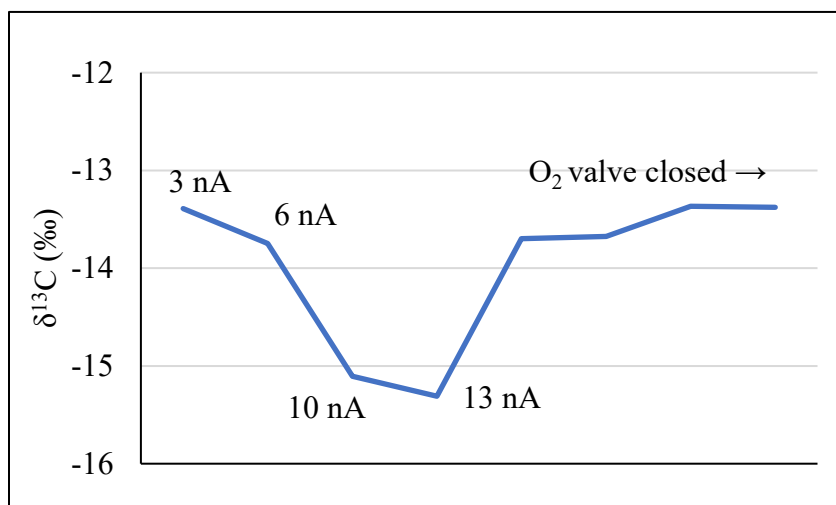


Figure 3.16: Influence of the approximate O<sub>2</sub> levels on the δ<sup>13</sup>C (‰) values of a 3-Ac-AICAR standard.

Table 3.7: Precision results over a 50-hour long sequence for RMs bought already acetylated (no in-house acetylation) and acetylated during the course of this work.

Compound	In-house acetylation?	n	Average (‰)	Std Dev (‰)
3-Ac-AICAR	No	5	-16.25	0.47
	Yes	4	-19.87	0.43
3-Ac-uridine	No	5	-25.56	0.35
	Yes	4	-24.29	0.24

### 3.5.3. Correction of δ<sup>13</sup>C values with reference material

RM of known isotopic composition that can be analyzed under identical conditions as the samples are required for CSIR analyses [125]. Ideally, three RMs bracketing the range of expected measured δ<sup>13</sup>C values should be analyzed. This is to allow the correction to be δ<sup>13</sup>C-specific as it is plausible that a correction, for example at -15‰, is different from one at -30‰.

When RMs of different isotopic composition are used in an analysis, the known and the measured

values can then be plotted against one another and act as a “multipoint isotopic correction”, a linear calibration line whose slope and intercept are used to normalize measured stable isotopic compositions to the VPDB scale. It is also important for GC/C/IRMS work that the RM be structurally similar to the targets as chromatographic behavior, ease of combustion and the presence of certain heteroatoms (e.g., N, as discussed earlier) may influence the  $\delta^{13}\text{C}$  measurement. Peak width for example, should be similar for targets and references so as to ensure similar background corrections for both. It is not always possible to find structurally similar RM with contrasting isotopic compositions however; availability of such materials is therefore a common issue.

As already discussed, only two different acetylated RMs were available for the work covered by this thesis: a 3-Ac-AICAR and a 3-Ac-uridine standard, both having been analyzed externally by EA-IRMS at respective values of  $-15.53 \pm 0.05\text{‰}$  ( $n = 6$ ) and  $-25.21 \pm 0.02\text{‰}$  ( $n = 5$ ), respectively. The isotopic range covered is acceptable, given that the measured values for the acetylated products in natural samples ranged from roughly -20 to -30‰. However, despite not going against IRMS “good practices” [125], a two-point correction results in a significant increase in the method’s uncertainty, as each point has considerable “weight” on the outcome of the isotopic correction.

To make sure no bias was introduced by a limited range of  $\delta^{13}\text{C}$  values, the 3-Ac-AICAR and 3-Ac-uridine standards were injected onto the GC/C/IRMS with other commercially available acetylated molecules to see if the isotopic calibration curve was linear over a broader range of  $\delta^{13}\text{C}$  values. Other commercially available nucleosides that were amenable to GC work once acetylated were also tested (e.g., thymidine and 2'-deoxycytidine), but their C isotopic signatures were not significantly different from the one of the uridine standard. Therefore, dissimilar standards including triacetin and sorbitol hexaacetate, as well as a certified mix of four acetylated steroids referred to as the CU/USADA-33-1 [204] mix were used, thus covering a range extending roughly from -15 to -36‰. All these standards had been either analyzed by EA-IRMS or bought with a certificate of analysis including  $\delta^{13}\text{C}$  values (designated as “external” values and

available in Appendix 1. GC/C/IRMS results, designated as “internal” values, were then plotted against the external ones. The resulting graph can be seen in Figure 3.17.

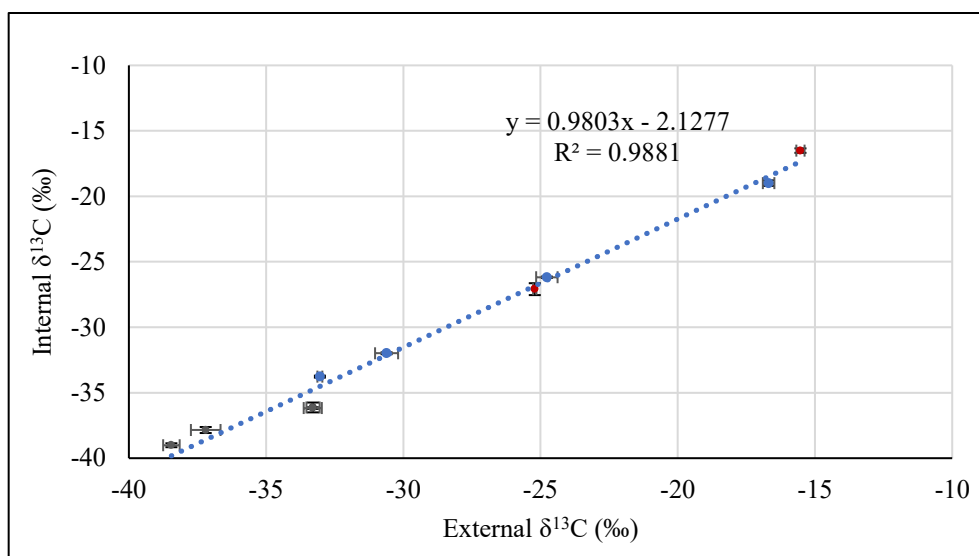


Figure 3.17: Relation for various molecules between their external and internal  $\delta^{13}\text{C}$  values. Red: triacetylated AICAR and uridine, blue: steroid acetates and grey: triacetin and glycerol hexaacetate.

The rather low  $r^2$  of 0.9881 obtained is not surprising as the different materials behave differently chromatographically and during combustion. Here, the two points the furthest away from their external values were the ones of the two sorbitol hexaacetate standards. Without those two points,  $r^2$  equalled 0.9970. Most importantly, no deviation was observed for AICAR and uridine when compared to the other standards' response pattern, indicating that using a restricted range of  $\delta^{13}\text{C}$  values does not cause any important bias since the instrument's response was linear on all the range of  $\delta^{13}\text{C}$  values.

With that information in hand, data from method validation were compiled to evaluate the reproducibility of the different QCs using the two-point correction. Values uncorrected for acetylation were considered here, as they are the ones directly affected by the correction made with RM. Mean and SD values for the Mix-AU, QCN and were calculated and are available in Table 3.8. All SDs were  $< 0.50\text{‰}$  which is deemed satisfactory to demonstrate the method's reliability, especially considering that those results were acquired over many sample batches analyzed over the course of almost a year.

Table 3.8: Long-term precision for 3-Ac-AICAR and 3-Ac-uridine in the Mix-AU, QCN and QCP. The SDs obtained are all < 0.50‰ and demonstrate the good performance of the two-point calibration method.

QCs	Compound	Average $\delta^{13}\text{C}$ (‰)	SD (‰)
Mix-AU (n = 11)	AICAR	-19.95	0.34
	Uridine	-24.78	0.46
QCN (n = 6)	AICAR	-26.56	0.32
	Uridine	-27.34	0.25
QCP (n = 6)	AICAR	-20.32	0.45
	Uridine	-27.51	0.47

#### 3.5.4. Correction for acetylation

In CSIR analysis, chemical derivatizations that introduce new C atoms onto the analytes inevitably alter the C isotopic composition of the targeted molecules. The mathematical relation between the derivatized (in this case, acetylated) molecule, the analyte molecule (hereafter designated as the “target” molecule) and the derivatization reagent (here  $\text{Ac}_2\text{O}$ ) is expressed by the general mass balance formula (Equation 3a) [11, 158, 205, 206]:

$$n_{\text{TD}} \delta^{13}\text{C}_{\text{TD}} = n_{\text{T}} \delta^{13}\text{C}_{\text{T}} + n_{\text{D}} \delta^{13}\text{C}_{\text{D}} \quad (\text{Equation 3a})$$

where,

- $n_{\text{TD}}$  is the number of C atoms for the derivatized molecule (in the case of 3-Ac-AICAR and 3-Ac-uridine, this number is 15);
- $\delta^{13}\text{C}_{\text{TD}}$  is the  $\delta^{13}\text{C}$  of the derivatized molecule;
- $n_{\text{T}}$  is the number of C atoms of the target molecule (9 for AICAR and uridine);
- $\delta^{13}\text{C}_{\text{T}}$  is the  $\delta^{13}\text{C}$  value of the target molecule;
- $n_{\text{D}}$  is the number of C atoms added to the target molecule from the derivatization reagent (here, this number is 6, since 3 acetate groups with 2 C atoms/acetate are added to the target molecule) and;
- $\delta^{13}\text{C}_{\text{D}}$  is the  $\delta^{13}\text{C}$  value of the added C atoms from the derivatization reagent.

When introducing the right number of C atoms in the context of this thesis, Equation 3a can be rewritten as Equation 3b:

$$15 \delta^{13}\text{C}_{\text{TD}} = 9 \delta^{13}\text{C}_{\text{T}} + 6 \delta^{13}\text{C}_{\text{D}} \quad (\text{Equation 3b})$$

In Equations 3a and 3b,  $\delta^{13}\text{C}_{\text{T}}$  and  $\delta^{13}\text{C}_{\text{D}}$ , are unknowns; they are determined by the following protocol:

1. The underivatized material (a high purity material is required) is analyzed by EA-IRMS to obtain its  $\delta^{13}\text{C}$  value. This value will act as  $\delta^{13}\text{C}_{\text{T}}$  for point 2.
2. The same material from point 1 is derivatized (here, acetylated) and analyzed by GC/C/IRMS. The obtained  $\delta^{13}\text{C}$  value then represents  $\delta^{13}\text{C}_{\text{TD}}$  that will be needed for point 3.
3. The measured  $\delta^{13}\text{C}$  signature is first normalized using the isotopic calibration line (Section 3.5.3).
3.  $\delta^{13}\text{C}_{\text{D}}$  is then determined algebraically using equation 3b.
4. Unknown samples derivatized with the same batch of reagent are analyzed by GC/C/IRMS. Once the isotopic calibration is applied, the measured  $\delta^{13}\text{C}_{\text{TD}}$  value and the calculated  $\delta^{13}\text{C}_{\text{D}}$  value are used in combination to find the sample's  $\delta^{13}\text{C}_{\text{T}}$ .

$\delta^{13}\text{C}_{\text{D}}$  is not the  $\delta^{13}\text{C}$  value of the derivatization reagent, but rather the “effective”  $\delta^{13}\text{C}$  value of the C atoms added to the molecule during derivatization [206, 207]. This is a crucial distinction, as KIE favor the inclusion of  $^{12}\text{C}$  over  $^{13}\text{C}$  in the derivatized material compared to the anhydride constituting the acetylation medium. KIE are linked to the difference in the carbonyl  $^{12}\text{C}$ -N versus  $^{13}\text{C}$ -N bond strength in the anhydride/pyr intermediate (bracketed in Figure 3.10) which breaks upon formation of the acetylated compound. To give an idea of how important the KIE involved are, the  $\delta^{13}\text{C}_{\text{D}}$  values calculated in this work were roughly in the -40 to -45‰ range, whereas EA-IRMS analysis made directly on the bulk  $\text{Ac}_2\text{O}$  used for acetylation yielded a value of  $-21.78 \pm 0.11\text{‰}$  ( $n = 5$ ) and so only indirectly-determined  $\delta^{13}\text{C}_{\text{D}}$  are valid. Moreover, KIE associated with its determination can be compound-specific, as even molecules with similar structures can possess different experimental values for  $\delta^{13}\text{C}_{\text{D}}$ . Having two different  $\delta^{13}\text{C}_{\text{D}}$  values, one for AICAR and one for uridine, is therefore possible.

Some specialized publications on the topic put forward the need for compound-specific  $\delta^{13}\text{C}_\text{D}$  values [206], whereas others reported negligible differences for structurally similar molecules [207], opening the door for the use of a single  $\delta^{13}\text{C}_\text{D}$  value for more than one molecule. From the experimental perspective of this work, accurate  $\delta^{13}\text{C}_\text{D}$  determination is also challenging since mathematically, a 1‰ error in the measured  $\delta^{13}\text{C}_\text{TD}$  value for AICAR or uridine translates to a 2.5‰ error in the determined  $\delta^{13}\text{C}_\text{D}$  value through error propagation (deducted from Equation 3b). It is therefore mathematically impossible to determine  $\delta^{13}\text{C}_\text{D}$  with better precision than the IRMS measurement itself, underlining the importance of reducing measurement error at the source.

To determine if different  $\delta^{13}\text{C}_\text{D}$  values for AICAR and uridine were necessary, an experiment was designed with different compounds bearing primary and secondary hydroxyl groups. Each compound used had related RM traceable to an externally measured EA-IRMS value to improve measurement accuracy. Detailed results as well as a further theoretical justification to this section are given in Appendix 1.  $\delta^{13}\text{C}_\text{D}$  values were measured at  $-44.80 \pm 0.13\text{‰}$  and  $-42.26 \pm 0.08\text{‰}$  for AICAR and uridine, respectively. With values sitting more than five SDs away from each other, this experiment supplied very strong evidence for the need of specific  $\delta^{13}\text{C}_\text{D}$  values for AICAR and uridine. Other polyol compounds, like D-sorbitol and glycerol also displayed statistically different  $\delta^{13}\text{C}_\text{D}$  values. Compound-specific correction was therefore used to account for acetylation during method validation. Since the  $\delta^{13}\text{C}_\text{D}$  values determined over the course of the validation process showed larger variation than other values (SDs were higher),  $\delta^{13}\text{C}_\text{D}$  values specific to every batch of samples analyzed or for every new experiment performed were used. This allowed for inter-day variations due to local reaction conditions to be compensated for.

### **3.6. Mandatory method characteristics**

The technical documentation available for GC/C/IRMS of AAS (known as the TD2019IRMS technical document [158]) specifies “method characteristics” that must be included in all CSIR methods implemented by WADA-accredited laboratories. These requirements have so far unfortunately been limited to the analysis of steroid compounds. Of course, AICAR’s analysis is expected to require a minimum of adaptation, but Table 3.9 shows that this was possible for each requirement from WADA’s technical document to meet a realistic equivalent.

Table 3.9: Characteristics to be included in the method as stated in the TD2019IRMS [158].

Method characteristics	Requirements for AAS	In this work
CO <sub>2</sub> monitoring gas stability	Must be checked before each analysis	10 CO <sub>2</sub> pulses evaluated before each batch. The SD for the measured $\delta^{13}\text{C}$ value (45/44) had to be < 0.10‰.
Linearity of the ion source	Must be checked regularly.	The linearity of the 45/44 and 46/44 ratio of CO <sub>2</sub> pulses based on an evaluation of the slope of the $\delta^{13}\text{C}$ and $\delta^{18}\text{O}$ of the reference gas pulses versus the major height (1.5 to 15 nA) shall be $\leq 0.1\%$ .
Sample preparation	Sample purification by HPLC and/or SPE and/or equivalent is recommended.	Samples were purified by PBA gel and two HPLC purification steps – one before and one after the acetylation step.
“Negative/Positive” samples	A “negative” and a “positive” sample have to be analyzed with each batch. They shall meet the applicable criteria and be monitored.	Pooled anonymous urines with [AICAR] $\approx 1 \mu\text{g/mL}$ were used as the negative control (QCN). A volunteer’s urine was spiked with $10 \mu\text{g/mL}$ of synthetic AICAR and used as the positive control sample (QCP).
System calibration	Must be done periodically and after major revisions of the instrument. A CIRM traceable to an international RM shall be used.	The system was calibrated during each analysis. The CIRMs used (3-Ac-AICAR and 3-Ac-uridine) had values traceable to international RM.
Use of RM	Steroid RM with traceable values must be analyzed with each batch, underivatized or acetylated, as appropriate.	AICAR and uridine standards, bought unacetylated and with traceable $\delta^{13}\text{C}$ values determined by EA-IRMS, were analyzed with each batch along with the calibration RMs.
ERCs	Pd must be used as principal ERC. A second ERC must be available when Pd cannot be analyzed.	Uridine is the principal ERC here for reasons discussed earlier. AAS have also been analyzed for comparison purposes.
Correction for acetylation	Steroids can be analyzed underivatized or acetylated. Values must be reported after correction using the mass balance formula.	The correction for AICAR and uridine acetylation was done with the mass balance formula and corrected values were used for statistical evaluation.

### **3.7. Method validation**

WADA-accredited laboratories are subject to strict method requirements, as they are regulated by the International Organization for Standardization/International Electrotechnical Commission 17025 (ISO/IEC 17025) [208] standard and WADA's ISL [166]. The ISL can be seen as an extension of the ISO/IEC standard applying specifically to anti-doping laboratories. It dictates, among other things, the requirements of method validation to be evaluated by laboratories. There is no technical document published by WADA so far specifically about the validation of a method for the CSIR of AICAR. The TD2019IRMS was therefore used as a starting point. Two elements - "AICAR and uridine stability in urine" and "Peak purity and identification" - were not specifically covered by the TD2019IRMS and are described in the two following sub-sections. Section 3.7.3 then lists in the form of a table the elements of method validation that were either excerpt or adapted from the TD2019IRMS.

#### **3.7.1. AICAR and uridine stability in stored urine**

When it comes to sample storage, WADA-accredited laboratories have to follow strict protocols to ensure the sample integrity [166]. Long-term storage is always done at -20°C as compounds, including nucleic acid-like molecules are likely to degrade overtime in liquid urine [209, 210]. Nonetheless partial degradation of analytes is expected to happen to a small extent, as frozen urines obviously need to be thawed to be analyzed.

To evaluate the analytes' stability in urine, two samples (Sample 1 and Sample 2) from volunteers were stored at +4°C and -20°C over a period of 87 days. Both urines had been spiked with the equivalent of 5 µg/mL of AICAR and uridine with a known isotopic composition. Each urine was divided into aliquots as follows:

- To evaluate possible impact on AICAR and uridine concentration: 11 aliquots of 1 mL each, one stored at -80°C, five stored at -20°C and five stored at +4°C. Once every two to three weeks, an aliquot stored at -20°C and one stored at +4°C were transferred at -80°C. On the 87<sup>th</sup> day, all aliquots were therefore stored at -80°C until LC-MS/MS analysis. Those aliquots were used to record concentration variations during storage at different temperatures.

- To evaluate possible impact on  $\delta^{13}\text{C}$  values: three aliquots of 3 mL each, one stored at -80°C, one stored at -20°C and one at +4°C for 87 days were measured by GC/C/IRMS.

Concentration results can be seen in Figure 3.18 and showed altogether that AICAR and uridine are stable in urine, with most variations not discernible from measurement uncertainty (%RSD ranging from 1.2 to 6.6%). However, one notable exception occurred with AICAR in Sample 2 stored at +4°C. The %RSD for all the measurements was 14.4% and a decrease in concentration of roughly 25% between the beginning and the end of the experiment. As for the isotopic values, the differences measured in  $\delta^{13}\text{C}$  (‰) values between the analytes stored at -80° and the ones stored at +4°C or -20 °C are given in Table 3.10. The maximum variation (+1.01‰) was measured for AICAR, this time in Sample 1 stored at +4°C. All other values were <0.50‰, even after correcting the values for acetylation, which is well within the method's measurement uncertainty.

The decrease in AICAR concentration in Sample 2 stored at +4°C (a loss of roughly 25% on the 87<sup>th</sup> day relatively to the initial concentration) is likely due to degradation as the descending trend is progressive and relatively constant as of the 17<sup>th</sup> day of storage. However, no variation in the isotopic values was associated with this decrease. The difference in  $\delta^{13}\text{C}$  value for AICAR in Sample 1 is somewhat more difficult to explain as no obvious trend was measured in terms of concentration variation (%RSD of 5.5% for all data points). It is possible that this minor enrichment in  $^{13}\text{C}$  is a reflection of measurement uncertainty as the difference between the two aliquots before correction for acetylation is only 0.71‰.

Be that as it may, possible AICAR degradation and minor changes in isotopic signature were only observed when urines were stored at +4°C over a relatively long period of time. AICAR and uridine concentrations were stable at -20°C and no significant variation was observed for the measured  $\delta^{13}\text{C}$  values. Therefore, all urines used in this work as well as urine extracts (e.g., after PBA gel extraction) were stored at -20°C. Storage at +4°C was only used for short periods of time (i.e., <48 hours). Since esters are subject to hydrolysis in aqueous environments, acetylated fractions recovered after the second HPLC were only stored dry after immediate solvent evaporation.

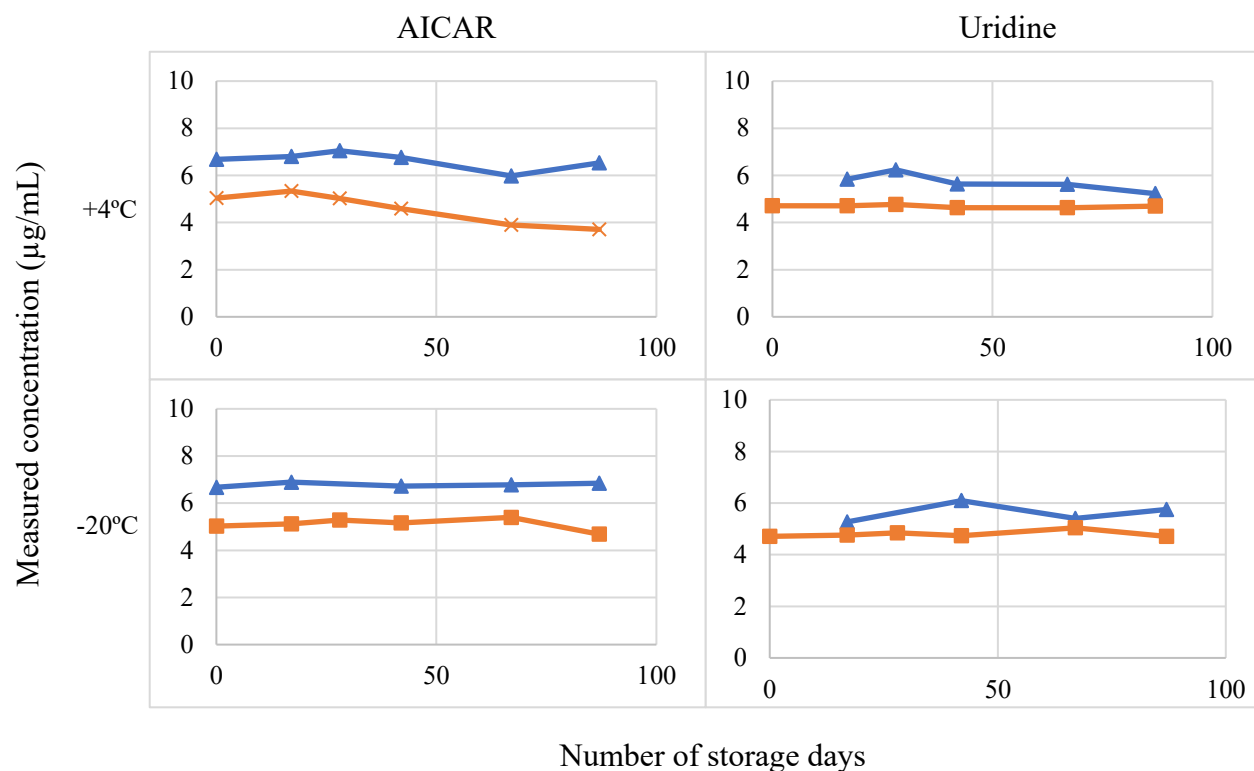


Figure 3.18: AICAR (left) and uridine (right) long-term stability in urine when stored at +4°C (top) and -20°C (bottom) for two urine samples spiked with 5 µg/mL of both substances. Blue triangles: Sample 1 and orange squares: Sample 2. Missing points were not determined.

Table 3.10: Effect of long-term (87 days) storage on  $\delta^{13}\text{C}$  values of AICAR and uridine corrected for acetylation. Values in parenthesis express the difference from urine stored at -80°C.

Compound	Sample	$\delta^{13}\text{C}$ (‰)	$\delta^{13}\text{C}$ (‰)	$\delta^{13}\text{C}$ (‰)
		Urine at -80°C	Storage at -20°C	Storage at +4°C
AICAR	1	-6.24	-6.61 (-0.37)	-5.23 (+1.01)
	2	-4.22	-4.68 (-0.46)	-4.27 (-0.05)
Uridine	1	-13.91	-13.99 (-0.08)	-14.03 (-0.07)
	2*	n/d	n/d	n/d

\*n/d: not determined. Uridine was lost for Sample 2 during sample preparation for GC/C/IRMS.

### 3.7.2. Peak purity and identification

Since analytes are combusted to CO<sub>2</sub> when performing CSIR analyses, the information related to the molecular structure is lost. There is consequently no way to formally establish the identity of the peak on which a measurement is made apart than from using its sole retention time, something not totally reliable as interferent compounds can mimic the analyte peak by eluting at the same moment. Given the exhaustivity of the above exposed purification protocol, interferent peaks – and therefore analyte peak purity - were not expected to be an issue for the current method. Nevertheless, formally demonstrating that this is indeed the case is important. WADA also demands for peak identification of TCs to be made by GC-MS analysis every time an abnormal result is detected. Peak purity and identification were therefore evaluated as follows:

The chromatographic progression of the  $m/z = 45$  to  $m/z = 44$  ratio within an analyte peak can be screened to visually detect any incongruity and monitor peak purity. The monitoring of this ratio usually displays a distinct “isotopic swing” profile, starting at a baseline value, swinging up, then down (or vice-versa) before returning to baseline. A shift in the baseline value or a disruption in the "shape" of the isotopic swing is likely indicative of a co-eluting peak. An example of such a contaminant is given in the right panel of Figure 3.19, in comparison to clean peak in the left panel. All the 45/44 ratio of urinary references and samples were screened throughout the different analyses done for this thesis and no interference pattern was ever detected.

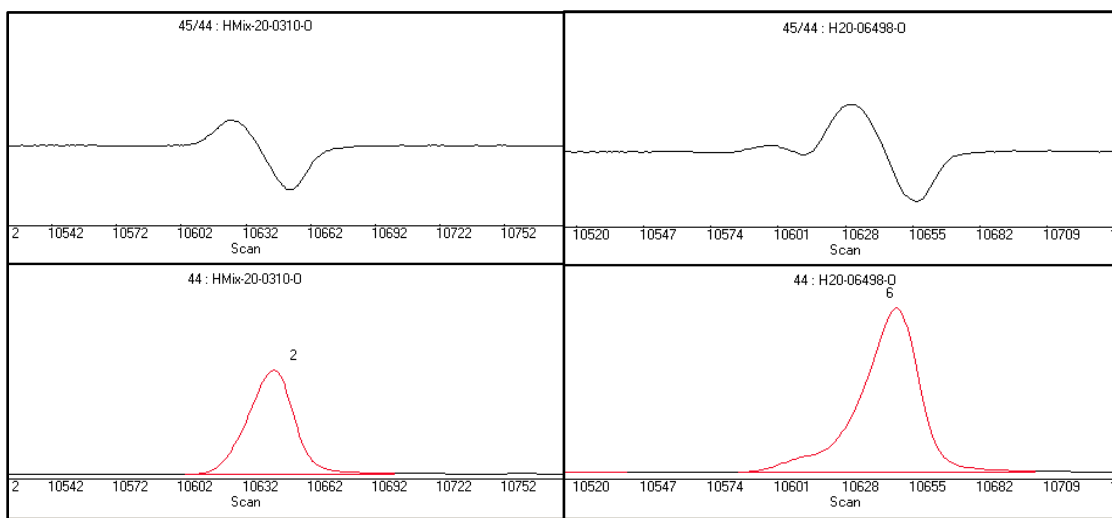


Figure 3.19: Examples of the 45/44 ratio pattern for a pure peak (left) and a peak co-eluting with an interference (right) possibly altering the  $\delta^{13}\text{C}$  value.

To properly identify analyte peaks, a GC-MS analysis of the sample using the same chromatographic conditions as with the GC/C/IRMS (i.e., same GC column and parameters) can be done. The TD2015IDCR is the technical document describing how such analyte identification must be made [211]. Examples of GC-MS spectra for 3-Ac-AICAR and 3-Ac-uridine are shown in Figure 3.20. The peaks of interest are firstly identified in unknown samples using mass spectra and retention time by comparison with a relevant RM analyzed in the same sample sequence. The ion fragments used for GC-MS identification are given in Table 3.11. Figure 3.21 shows the ion-extracted chromatogram of the target analytes for each of these ions. Analyte peaks can also be searched for possible interfering ions from peak onset to peak tail or using the Chemstation software peak purity feature.

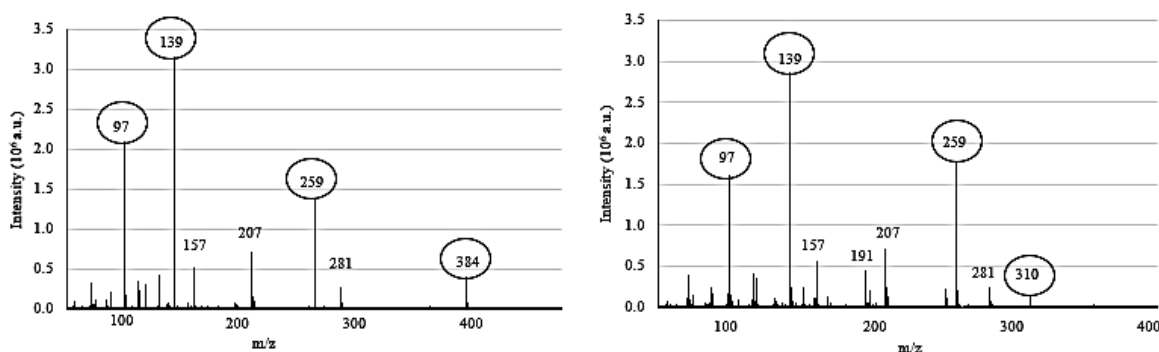


Figure 3.20: Examples of mass spectra for 3-Ac-AICAR (left) and 3-Ac-uridine (right). Circled  $m/z$  values are the ones suggested in this work for analyte identification.

Table 3.11: Proposed  $m/z$  values for -3Ac-AICAR and 3-Ac-uridine GC-MS identification

Compound	$m/z$ retained for identification
AICAR	384, 259, 139, 97
Uridine	310, 259, 139, 97

The spectrum for both compounds displayed common ions at  $m/z = 259, 139$  and  $97$ , very likely originating from their ribose moiety ( $m/z = 259$  corresponds to triacetylated ribose). The

3-Ac-AICAR spectrum contained a distinctive molecular ion at  $m/z = 384$ . This was not the case of uridine however, for which the molecular ion was only observed at very high signal intensity. For that reason, the  $m/z = 310$  value - which matches the loss of an acetic acid molecule (60 amu) - was used instead.

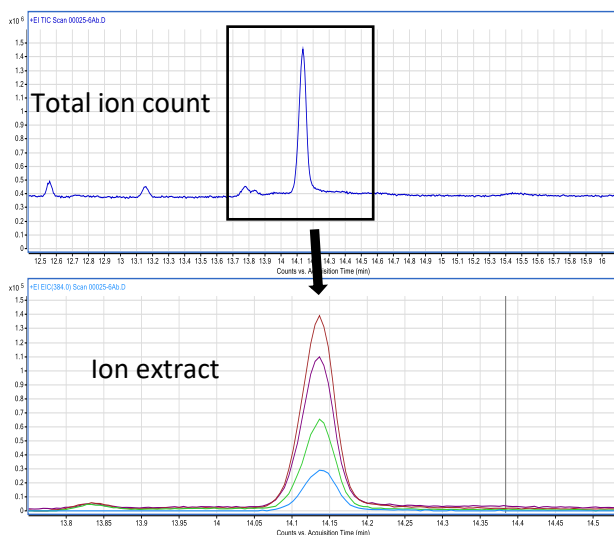


Figure 3.21: 3-Ac-AICAR total ion count (TIC) chromatogram from a sample (upper panel) and ion extract chromatography of the same peak (lower panel) using  $m/z = 384, 259, 137$  and  $97$ .

### 3.7.3. Validated parameters

Table 3.12 contains all the method validation elements that could be excerpt or adapted from the TD2019IRMS document and applied to AICAR CSIR analysis, as well as the results that were obtained. Supplemental information is also available in Appendix 2.

It is important to remember that although this method was developed based on technical documents related to AAS, the validation results should be evaluated relatively to what is essential for AICAR CSIR analysis. Notable highlights from Table 3.12, such as the good combined uncertainty associated to the method and the possibility of analyzing samples with concentration lower than average as well as the good precision results reported in Section 3.5.3 are all indicators that the method does what it is intended to and is therefore fit for purpose.

Table 3.12: WADA requirements [158] for parameters assessed during method validation that could be adapted to AICAR CSIR analysis.

Parameter to be included in method validation	Definition/Mean of evaluation in the context of this work	Results
Linearity of the ion source	Determined using CO <sub>2</sub> pulses of different intensities.	SD ≤ 0.1 for δ <sup>13</sup> C values of peaks ranging from 1 to 15 nA.
Linearity of the instrument	Determined in a similar manner by many injections of AICAR and uridine at different intensities.	0.3 to 16 nA for AICAR and uridine.
Linearity of the analytical method/Limit of quantification (LOQ)	Extrapolated using the intensities of analytes versus their concentrations and data from the impact of the acetylated mass of analyte.	AICAR: 0.25 to 30 µg/mL and uridine: 0.02 to 30 µg/mL
Estimated combined standard Measurement Uncertainty (u <sub>c</sub> )	Must be determined for each TC and ERC. The u <sub>c</sub> shall be not greater than 1.0 ‰ (u <sub>c_Max</sub> ). Technical documents supply guidelines to estimate u <sub>c</sub> using in-house intermediate precision data (TD2019DL [212]), in this work the QCN.	0.8‰ for AICAR and 0.6‰ for uridine.
Δδ <sub>TC-ERC</sub> values from urine samples to demonstrate method performance	AICAR and uridine CSIR were measured in a total of 44 urine samples from athletes and from out of which 7 (16%) were from women.	The mean Δδ <sup>13</sup> C <sub>A-U</sub> value was 2.0‰ with a SD of 2.0‰ (mean + 3SDs = 8.0‰).

## 4. Results and discussion

As demonstrated in the previous chapter, it is possible to accurately and reproducibly make CSIR measurements on urinary AICAR using the protocol described in the previous chapters. As per the fourth objective of this thesis, the purpose of this next chapter is to evaluate the method's ability to differentiate between "positive" (i.e., containing any proportion of exogenous AICAR) and "negative" samples (i.e., containing only endogenous AICAR) using the data from the 46 urines (identified hereafter as U1 to U46) that were analyzed during this project. In addition to the results presented in this chapter, all isotopic measurements for individual samples are available in Appendix 3 as well as concentration estimates determined by LC-MS/MS for AICAR and uridine in Appendix 4.

### 4.1. CSIR of synthetic AICAR

Doping detection by CSIR is facilitated when the endogenous and exogenous forms of the targeted molecule possess  $\delta^{13}\text{C}$  values that are far apart from each other. One of the most impactful results obtained by Piper et al. (2014) was the enriched  $\delta^{13}\text{C}$  values associated to AICAR's commercial origins. Samples from certified sources (i.e., bought from a laboratory with a certificate of analysis) and from unofficial suppliers found on the Internet were all located in the -5 to -3‰ region. The  $\delta^{13}\text{C}$  values measured for synthetic AICAR in this work, presented in Table 4.1, are in line with Piper et al.'s values.

Table 4.1: All published  $\delta^{13}\text{C}$  values for AICAR bought from commercial sources, either certified or not. The mean value is -4.1‰ and the SD 0.8‰.

Supplier	$\delta^{13}\text{C} \pm \text{SD}$ (‰)	Reference
Sigma	$-5.2 \pm 0.3$ (n = 6)	Piper et al. (2014)
	$-3.3 \pm 0.3$ (n = 6)	Piper et al. (2014)
TRC	$-3.4 \pm 0.3$ (n = 6)	Piper et al. (2014)
	$-4.44 \pm 0.02$ (n = 5)	This work
	$-4.34 \pm 0.04$ (n = 5)	This work
Unofficial sources	$-5.3 \pm 0.2$ (n = 3)	This work
	$-3.5 \pm 0.3$ (n = 6)	Piper et al. (2014)
	$-3.7 \pm 0.3$ (n = 6)	Piper et al. (2014)

Good knowledge of the CSIR of synthetic AICAR is essential as it gives some insight on the characteristics of a potential “AICAR-positive” sample. As such, provided that a minimal proportion of the administered compound is reaching the bladder unmodified, a urine sample containing exogenous AICAR is anticipated to have its  $\delta^{13}\text{C}$  value shifted toward -5‰ whereas other endogenous compounds present in the urinary matrix - including the ERCs - are expected to remain unchanged; within the -25 to -15‰ range, depending on the athlete’s baseline CSIR. AICAR’s  $\delta^{13}\text{C}$  shift is expected to be most significant when the amount of excreted exogenous AICAR is large relative to the endogenous AICAR naturally present in urine as the CSIR of the overall pool of AICAR will then approach the exogenous value. Piper et al. (2014) have shown that this is indeed the case after oral ingestion of a large amount of AICAR (10 g) when performing an excretion study on a volunteer, with the exogenous AICAR values sitting at least 11.0‰ away from the endogenous ones obtained from urine samples containing no synthetic AICAR (from -25.8‰ to -16.2‰ in their publication) [11]. However, because of the large AICAR dose administered, Piper et al.’s experimental conditions represent an extreme case that favored the easy detection of AICAR doping by the laboratory. Their administration protocol is not necessarily representative of how an athlete would ingest or inject AICAR.

#### **4.2. Sample results and comparison with existing literature**

To evaluate the efficiency of a CSIR method for anti-doping purposes, the results of “AICAR-positive” samples (such as the ones obtained after an AICAR excretion study) have to be compared to the normal values from a population of “AICAR-negative” urines (i.e., not containing any synthetic AICAR). This is why Piper et al.’s (2014) analyzed urines from 63 volunteers that were all students and staff members of the German Sport University in Köln, Germany, and thus dwelled exclusively in the Köln area. They were unpaid and had attested to the non-use of AICAR or any other dietary supplements. Performing this study under controlled conditions is a good way to isolate the natural CSIR values of AICAR from undesired external factors such as the presence of synthetic AICAR in a sample, for instance. A similar experiment is currently being conducted at the *Laboratoire de contrôle du dopage* of the *INRS-AFSB* to see if Piper et al.’s results can be replicated (data not available yet). However, it is also possible that such controlled conditions introduce a bias in the measurements as they exclude some factors normally affecting anti-doping urine samples. Restricting the origin of the samples to one single

geographical origin may for example artificially minimize natural variability between samples compared to a population composed of routine anti-doping samples which are collected and imported globally. The objective which this work was aiming at by analyzing a sample population was therefore less to obtain CSIR values from a “AICAR-negative” population than to probe the values from real-life anti-doping samples which possess much more diverse origins than Piper et al.’s volunteers. Since European CSIR are known to be lower when compared to e.g., North-American ones, it was expected that the 11.0‰ gap between AICAR endogenous and exogenous  $\delta^{13}\text{C}$  values as observed by Piper et al. would be reduced in this work. As shown in Table 4.2, this was the case with values on average more than 5‰ more enriched in  $^{13}\text{C}$  (n = 43) than what was reported by Piper et al. Some notable examples of samples that contained AICAR with a particularly enriched values are sample U1 at -9.3‰, U42 at -10.4‰, U20 at -11.6‰, U31 at -12.5‰ and U35 at -12.9‰ (Appendix 3) which were initially suspected to contain synthetic AICAR.

Table 4.2: Summary of all  $\delta^{13}\text{C}$  measurements for this work and Piper et al. (2014).

Compound (n for this work)	Mean $\delta^{13}\text{C}$ (‰)		SD $\delta^{13}\text{C}$ (‰)		Minimum $\delta^{13}\text{C}$ (‰)		Maximum $\delta^{13}\text{C}$ (‰)	
	This work	Piper et al. n = 63	This work	Piper et al. n = 63	This work	Piper et al. n = 63	This work	Piper et al. n = 63
AICAR (n = 44)	-15.6	-20.9	2.08	1.96	-18.5	-25.8	-9.3	-16.2
Uridine (n = 44)	-17.5	/	1.75	/	-21.6	/	-13.1	/
Pd (n = 35)	-19.8	-22.9	1.21	0.73	-23.5	-24.5	-17.1	-21.2
Et (n = 35)	-21.0	-23.9	1.26	0.67	-24.5	-25.2	-18.6	-22.4
Andro (n = 35)	-20.0	-22.9	1.17	0.72	-23.1	-24.8	-17.7	-21.5

There is probably more than one reason explaining the differences in terms of  $\delta^{13}\text{C}$  values between this work and Piper et al. (2014). The fact that most samples analyzed here originated from North-, Central- and South America is certainly one of them as shown by the steroid values which were  $^{13}\text{C}$ -enriched by roughly 3‰ in this work relatively to Piper et al. However, the mean 5.3‰ enrichment for AICAR is difficult to explain entirely with the origin of the samples as only factor. The different methodologies used by Piper et al. and in this work may have an additional influence on the results and this needs to be examined.

The possible presence of synthetic AICAR in urine samples used to gather information on the compound has been mentioned in at least one previous study [13]. A lot of the samples analyzed for this thesis were chosen for their high AICAR concentration. Since increased urinary AICAR concentration is a marker of exogenous administration [11, 15, 16], those samples rose more interests as they increased the probability of finding a rare and scientifically valuable abnormal result. This also gave maximum chances of getting satisfactory analyte GC/C/IRMS signal. The decision of analyzing this type of sample was based on Piper et al.'s (2014) optimistic tone about the efficiency of CSIR to differentiate between endogenous and exogenous AICAR in urine and the premise of an easy differentiation between the two. It was assumed a potential AICAR-positive sample could be identified and put aside as its inclusion with negative samples would bias the data. As it will be discussed in more details in the following section however, this work supports the idea that the interpretation of CSIR results in order to differentiate between AICAR-negative and -positive samples might be more complicated than assumed based on Piper et al.'s work. Since AICAR-positive samples were more difficult than expected to identify, it is therefore possible that one or more samples from this work is "contaminated" by exogenous AICAR. Nevertheless, the probability that such an occurrence has a large influence on the data is low, even for high-concentration samples. This is first supported by Piper et al.'s (2014) investigation of suspicious samples with concentrations  $> 3.5 \mu\text{g/mL}$ , in which no abnormal CSIR results were found. Second, AICAR as a doping substance is very expensive. A single "treatment" is expected to cost over 1 000 \$ US per day [86]. This considerably limits the class of athlete having financial capability to afford such a product and therefore the number of concerned samples is expected to be small. Finally, no distinguishable difference in terms of the absolute  $\delta^{13}\text{C}$  of AICAR or  $\Delta\delta^{13}\text{C}_{\text{A-U}}$  values ( $\delta^{13}\text{C}$  between AICAR and uridine, its ERC) between samples of low and high concentrations were found in this work (Figure 4.1). This result does not prove without a doubt

the absence of synthetic AICAR in all samples, but the similarity between high- and low-concentration samples does support the idea that if any sample containing exogenous AICAR is present, its impact on the overall results is altogether small.

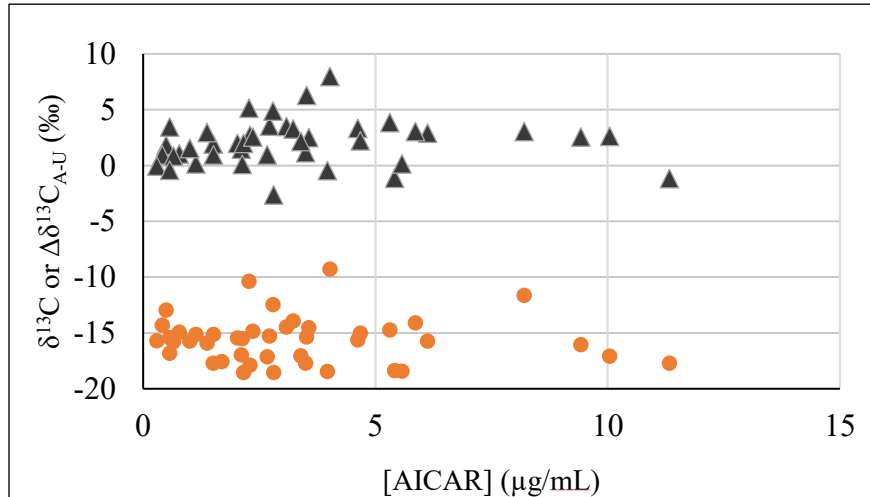


Figure 4.1: AICAR  $\delta^{13}\text{C}$  (orange circles) and  $\Delta\delta^{13}\text{C}_{\text{A-U}}$  (grey triangles) values versus AICAR concentration for all samples in which AICAR and uridine could be analyzed ( $n = 43$ ).

Aside from the possible presence of synthetic AICAR, another parameter controlled by Piper et al. (2014) that can easily be overlooked is the absence of dietary supplements in their urine population. Some of those supplements can, in principle, be incorporated into the metabolic chain upstream of AICAR's (and uridine's) *de novo* formation so it is plausible to expect an influence on its CSIR. Examples of such supplements include ribose, amino acids and folic acid. These supplements are not prohibited by WADA, which means they might be part of the factors to take into consideration when evaluating normal urinary AICAR CSIR. To support this idea, the declaration filled out by the athletes whose samples were analyzed here were investigated (when available) to look if such supplements had been mentioned. A case was found for sample U1 (at -9.3‰, the most enriched result herein) who had declared the use of ribose. Ribose has been demonstrated to help restore muscle ATP levels after exercise [213] and can be legitimately used by athletes. It is industrially synthesized from glucose by bacterial fermentation [210]. Most commercial glucose is from corn starch and therefore expected to bear high  $\delta^{13}\text{C}$  values [214, 215] which could explain sample U1 high CSIR value.

Since at this point it is only possible to make hypotheses on the distinctive impact of undeclared synthetic AICAR or dietary supplements, it is difficult to establish what a real negative urine population would look like for AICAR in terms of CSIR. On one hand, Piper et al. (2014) have made sure their samples did not contain synthetic AICAR which gives reliability to their data. On the other hand, the absence of non-prohibited dietary supplements in their population might also introduce a bias in their reported values. For this reason, more work is needed to isolate the influence of each of those factors on the CSIR of AICAR. As already mentioned, some of this work has already been initiated at the *INRS-AFSB* (data not yet available). This topic is discussed in the “Future work” section of this thesis.

#### **4.3. The influence of the origins of the C atoms in AICAR and uridine**

One result shared by this work as well as by Piper et al. (2014) and likely inherent to the natural CSIR of AICAR is its general  $^{13}\text{C}$  enrichment relatively to endogenous steroids. In this work, AICAR was more  $^{13}\text{C}$ -enriched than steroids in all samples analyzed for both. In addition to this, the  $\delta^{13}\text{C}$  values of AICAR covered a very wide range - almost 10‰ for this work as well as in Piper et al.’s publication. The spread of AICAR  $\delta^{13}\text{C}$  is even more striking for Piper et al. who compared their values to a very narrow population range for steroid  $\delta^{13}\text{C}$  values (a difference of roughly 3‰ between their minimum and maximum values for all steroids, Table 4.2), owing to the fact that their volunteers were all dwelling in the same area. The precise reasons for the high and scattered CSIR of AICAR and - to a lesser extent - uridine in this work are not explicitly stated in the literature. Explaining the CSIR of an endogenous compound entails establishing the origins of each of its C atoms and their own individual  $\delta^{13}\text{C}$  values. Anti-doping authorities are inexperienced when facing cases such as AICAR, as current anti-doping analyses using CSIR deal exclusively with AAS. All endogenous steroids analyzed are linked to cholesterol and share a steroidal backbone (e.g., androstane, estrane) representing a pool of roughly 20 C atoms for the most part left unmodified by phase-I metabolic reactions [216]. In the absence of synthetic AAS, steroid CSIR values originating from a single sample are very close to each other owing to the common origin of the carbon atoms in the steroidal backbone. Nucleic acids and their analogs are more complex as they are assembled *de novo* or by salvage. As it can be seen in Table 4.3, AICAR’s and uridine’s C atoms have origins much more diverse than endogenous AAS making their CSIR difficult to predict.

Table 4.3: Origins of the different C atoms for AICAR and uridine molecules. Information was obtained using the KEGG [47-49]. Atom numbering can be better understood using Figures 1.1 and 3.2.

Compound	C atoms identification	Number of atoms	“Upstream” molecule of origin
AICAR	C1' to C5' (ribose)	5	PRPP
	C4 and C5	2	Glycine
	C2	1	10-formyltetrahydrofolate
	4-carboxamide	1	CO <sub>2</sub>
Uridine	C1' to C5' (ribose)	5	PRPP
	C4, C5 and C6	3	L-aspartate
	C2	1	Carbamoyl-phosphate

Further investigation made on the compounds given in Table 4.3 reveals that 6 out of the 9 C atoms present in AICAR and uridine molecules are likely to originate from glucose. This is the case for the ribose moiety from PRPP, as pentose-phosphate (PRPP's precursor), is synthesized from glucose conversion (KEGG [47-49]). The salvaged CO<sub>2</sub> molecule used for the “4-carboxamide” C atom of AICAR is derived from glucose consumption during cellular respiration [217] and carbamoyl-phosphate for uridine's C2 atom is made via a HCO<sub>3</sub><sup>-</sup> ion also originating from CO<sub>2</sub> through the blood carbonate buffer system [218]. Since glucose is supplied to the human body by three processes: polysaccharide breakdown (with starch or glycogen as a starting point) [219], glycogenolysis (breakdown of stored glycogen) [220] or by gluconeogenesis when glucose reserves become low [221], this yields a plausible explanation on why the values are so diverse as every individual's specific diet and the proportion of each of the glucose-producing mechanisms taking place at a given time both have an influence on AICAR and uridine CSIR.

#### 4.4. Evaluation of steroids and uridine as ERCs

Enriched and variable  $\delta^{13}\text{C}$  values, such as the ones described for AICAR thus far, are not necessarily problematic to detect doping by CSIR since doping cases are built on the  $\delta^{13}\text{C}$  value of the TC relative to the one of an ERC (noted  $\Delta\delta^{13}\text{TC-ERC}$ ). However for the ERC method to work, the CSIR of the TC and the ERC have to be naturally similar. Moreover, this isotopic “proximity” has to be reproducible among urine samples. As a result of the wide scattering of the AICAR CSIR values when compared to steroids, Piper et al. (2014) have shown that the  $\Delta\delta^{13}\text{A-Steroids}$  values are not as reproducible from one sample to another than what is usually documented for the  $\Delta\delta^{13}\text{TC-ERC}$  values of AAS. Since a wide range of AICAR  $\delta^{13}\text{C}$  values was also observed in this work, it was expected that the  $\Delta\delta^{13}\text{A-Steroids}$  values calculated would possess distribution similar to the one of Piper et al. and it was indeed the case. This can be seen in Table 4.4 where mean  $\Delta\delta^{13}\text{A-U}$  and  $\Delta\delta^{13}\text{A-Steroids}$  ( $\Delta\delta^{13}\text{A-Pd}$ ,  $\Delta\delta^{13}\text{A-Et}$  and  $\Delta\delta^{13}\text{A-Andro}$ ), with their respective SD, are presented. As a consequence of the  $^{13}\text{C}$ -enriched values reported in Table 4.2,  $\Delta\delta^{13}\text{C}_{\text{A-ERC}}$  values reported herein are higher by roughly 2‰ for every AICAR-ERC pair analyzed by both works. Nevertheless, the scattering of those values, based on the SDs, is very similar.

Table 4.4:  $\Delta\delta^{13}\text{C}_{\text{A-ERC}}$  values presented as mean  $\pm$  SD from this work from and Piper et al. (2014).

$\Delta\delta^{13}\text{C}_{\text{A-ERC}}$	Mean $\pm$ SD (‰)	
	This work	Piper (2014) n = 63
$\Delta\delta^{13}\text{C}_{\text{A-U}}$	2.04 $\pm$ 1.99 (n = 43)	
$\Delta\delta^{13}\text{C}_{\text{A-Pd}}$	4.20 $\pm$ 2.20 (n = 34)	2.06 $\pm$ 1.90
$\Delta\delta^{13}\text{C}_{\text{A-Et}}$	5.40 $\pm$ 2.08 (n = 34)	2.94 $\pm$ 2.04
$\Delta\delta^{13}\text{C}_{\text{A-Andro}}$	4.33 $\pm$ 2.12 (n = 34)	1.94 $\pm$ 2.11

Results such as the ones in Table 4.4 can be useful to evaluate the suspiciousness of a sample by evaluating the deviation of its  $\Delta\delta^{13}\text{C}_{\text{A-ERC}}$  values relative to the statistical distribution of normal samples. Assuming a normal distribution, Piper et al. (2014) estimated the so called “reference limits” values for AICAR – defined as the thresholds at which a  $\Delta\delta^{13}\text{TC-ERC}$  result is considered abnormal – by using the average  $\Delta\delta^{13}\text{C}_{\text{A-ERC}}$  values from their work to which they added three SDs for each ERC they had tested (therefore encompassing roughly 99.7% of the values). For comparison purposes, this 3-fold SD method was also applied to the data from this work. The results obtained, along with the ones of Piper et al. (2014) are presented in Table 4.5.

Table 4.5: Reference limit values reported by Piper et al. (2014) for three different ERCs: Pd, Et and Andro with five samples for which  $\Delta\delta^{13}\text{C}_{\text{A-ERC}}$  results were high in this work.

$\Delta\delta^{13}\text{C}_{\text{A-ERC}}$	Piper et al. (2014) Mean + 3SDs (%) n = 63	This work Mean + 3SDs (%) n = 43	$\Delta\delta^{13}\text{TC-ERC}$ (%)				
			U1	U13	U20	U26	U31
$\Delta\delta^{13}\text{C}_{\text{A-U}}$		8.0	8.0	6.3	3.1	3.0	4.9
$\Delta\delta^{13}\text{C}_{\text{A-Pd}}$	7.8	10.8	10.6	6.1	7.3	7.6	7.7
$\Delta\delta^{13}\text{C}_{\text{A-Et}}$	9.1	11.6	11.0	6.9	8.0	8.6	9.0
$\Delta\delta^{13}\text{C}_{\text{A-Andro}}$	8.3	10.7	10.3	6.1	7.0	7.3	7.6

Biometric measurements, such as CSIR of AAS, are often considered to be normally distributed, however this distribution can be skewed [148]. Piper et al. (2014) did report their  $\Delta\delta^{13}\text{C}_{\text{A-ERC}}$  value distributions to be Gaussian - albeit without supplying any information on whether or not this was determined formally using any statistical means. As seen in Figure 4.2, the  $\Delta\delta^{13}\text{C}_{\text{A-U}}$  values from this work approached the typical bell-shaped curve of a normal distribution, however this was much more difficult to observe for other  $\Delta\delta^{13}\text{C}_{\text{A-ERC}}$  distributions like  $\Delta\delta^{13}\text{C}_{\text{A-Pd}}$  for example (also in Figure 4.2).

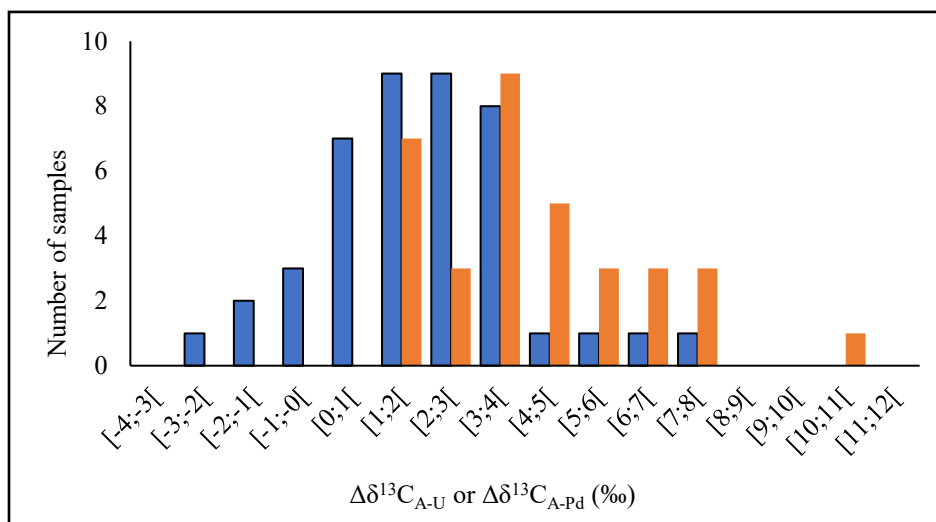


Figure 4.2:  $\Delta\delta^{13}\text{C}_{\text{A-U}}$  (blue) and  $\Delta\delta^{13}\text{C}_{\text{A-Pd}}$  (orange) value distribution ( $n = 43$  for  $\Delta\delta^{13}\text{C}_{\text{A-U}}$  and  $34$  for  $\Delta\delta^{13}\text{C}_{\text{A-Pd}}$ ). Values on the x axis represent  $\Delta\delta^{13}\text{C}$  values (in ‰) distributed in 1‰ half-open intervals with the first number included and the second one excluded.

High and dispersed  $\Delta\delta^{13}\text{C}$  values, such as the ones in Table 4.4 and Figure 4.2, point to potential issues regarding the proximity between endogenous and exogenous  $\delta^{13}\text{C}$  values for AICAR. For example, the highest measurement made for uridine in this work was  $-13.1\text{‰}$  for U32. For a sample such as this, the range of possible normal values for AICAR would extend all the way to  $5.1\text{‰}$  if the  $8.0\text{‰}$   $\delta^{13}\text{C}_{\text{A-U}}$  reference limit (Table 4.5) is applied, causing an overlap between the possible endogenous values and the expected exogenous values (Table 4.1).

Table 4.5 also contains the  $\Delta\delta^{13}\text{C}_{\text{A-ERC}}$  for the five samples with highest  $\Delta\delta^{13}\text{C}_{\text{A-ERC}}$  values. With the exception of U1, all of them are located inside the reference limits comprising endogenous samples for both works. Sample U1 - an interesting case already discussed in Section 4.2 - is the only one that could be considered abnormal based on Piper et al.'s (2014) data as its  $\Delta\delta^{13}\text{C}_{\text{A-Pd}}$ ,  $\Delta\delta^{13}\text{C}_{\text{A-Et}}$  and  $\Delta\delta^{13}\text{C}_{\text{A-Andro}}$  values are all outside their respective reference limit. Its  $\Delta\delta^{13}\text{C}_{\text{A-U}}$  was also the highest of all samples analyzed. In spite of these results, it is impossible to determine without a reasonable doubt if this sample is indeed AICAR-positive. Reference limits presented here are the only ones estimated thus far and they were extracted from a relatively small set of samples (especially when compared to what is available for AAS). These results can by no means be considered as gold standard by anti-doping authorities. It must also be stressed again that

despite synthetic AICAR potentially being present among the samples from this work, it is also plausible that the controlled environment under which Piper et al. have collected their samples (i.e., no dietary supplements) might have introduced a bias in the distribution of their values. Some supplements not prohibited by WADA could in principle have an effect on AICAR CSIR as they are part of their precursors (e.g., amino acids, folic acid and ribose). Analogously, there are examples of supplements that are known to affect AAS  $\delta^{13}\text{C}$  (e.g., pregnenolone [222]).

The results conveyed so far shed light to divergences between the metabolisms of AICAR, uridine and steroids which should be carefully taken into consideration in our way of assessing AICAR doping diagnosis in anti-doping testing. In short, the rules that apply to steroids may indeed not apply to AICAR. The steroid pool is replenished slowly in the human body (roughly 1% every 5 hour), therefore changes in the CSIA of steroids are anticipated to happen over the course of weeks or even months [223]. As part of the purine and pyrimidine pathways, respectively, AICAR and uridine are expected to cycle through the human body at a much faster rate. ZMP, from which endogenous AICAR is believed to be derived, is excreted at baseline levels by cells, meaning that it is consumed at the same speed it is produced (evidence for this have been shown in *C. Elegans* [224]). Uridine is also synthesized and degraded continuously by the liver [51, 225]. These high turnover rates potentially impact the way in which anti-doping tests can be conducted by laboratories.

Neither Piper et al. (2014) nor Buisson et al. (2017) have properly evaluated the impact of using compounds that cycle slowly in the human body such as steroid as ERCs for assessing potential doping with a high turnover compound such as AICAR. Instead, both publications highlight the convenience of using steroids in the context of anti-doping analyses where the end user will necessarily have a great deal of experience with the analysis of such compounds. In line with this, many publications consider the distribution of isotopic signatures within a given organism as roughly uniform to facilitate, for instance, the elaboration of models that describe the isotopic distribution at different trophic levels [226]. Contrary to this type of bulk analysis however, this assumption does not necessarily hold true for CSIA as large variations can be observed between different compounds within a single organism [161].

In order for an ERC to be suitable for a given analysis, its  $\delta^{13}\text{C}$  value must be correlated with that of the TC. This can be seen when using Andro and Pd measured in this work as examples. During

AAS analysis, Andro is a marker for T doping and can be analyzed using Pd as its ERC [158]. Plotting Andro and Pd  $\delta^{13}\text{C}$  values from the same urine against one another for all measurements available gives a relatively high  $r^2$  of 0.772, as shown in Figure 4.3. In simplistic terms, since Andro and Pd come from the same precursors, enriched Andro  $\delta^{13}\text{C}$  values are associated with enriched Pd  $\delta^{13}\text{C}$  values for any given sample and depleted Andro  $\delta^{13}\text{C}$  values are expected to be associated with depleted Pd  $\delta^{13}\text{C}$  values. For that reason, large inter-sample  $\Delta\delta^{13}\text{C}_{\text{TC-ERC}}$  variations potentially mean that the ERC is not suitable for the analysis. As also shown in Figure 4.3, AICAR and Pd  $\delta^{13}\text{C}$  values from the urines analyzed in this work are essentially not correlated ( $r^2 = 0.097$ ), calling into question the use of steroids as ERCs for AICAR.

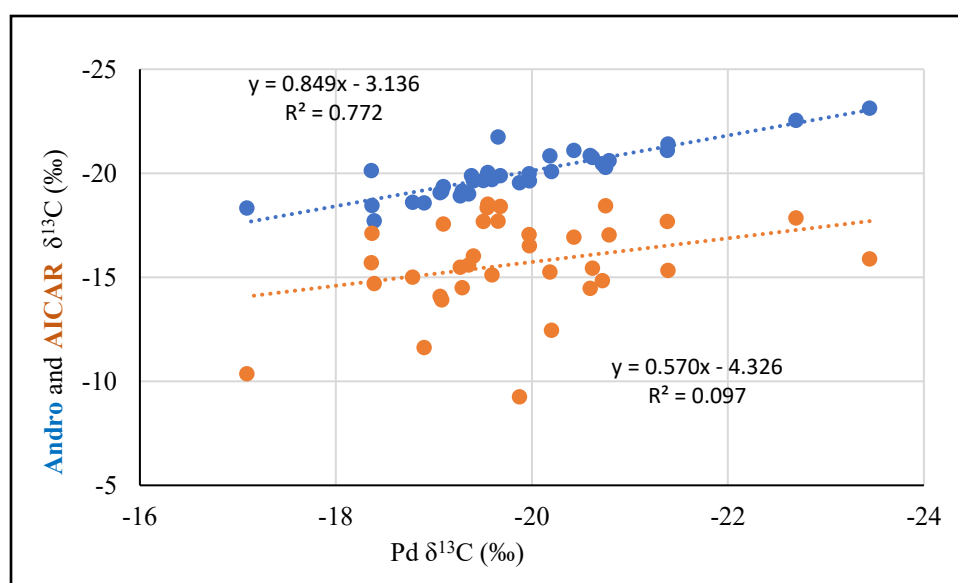


Figure 4.3: Correlation between Andro and Pd  $\delta^{13}\text{C}$  values (blue circles,  $n = 34$ ) as well as AICAR and Pd  $\delta^{13}\text{C}$  values (orange circles,  $n = 44$ ).

One of the goals of this thesis was to evaluate the use of an ERC that is more closely related to AICAR, uridine. Uridine's  $\delta^{13}\text{C}$  values were on average closer to the ones of AICAR when compared to the steroids (Tables 4.2 and 4.4), however as shown in Figure 4.4, the correlation factor of 0.199 between AICAR and uridine is hardly better than the one linking AICAR to Pd, demonstrating that uridine is also far from being an ideal candidate.

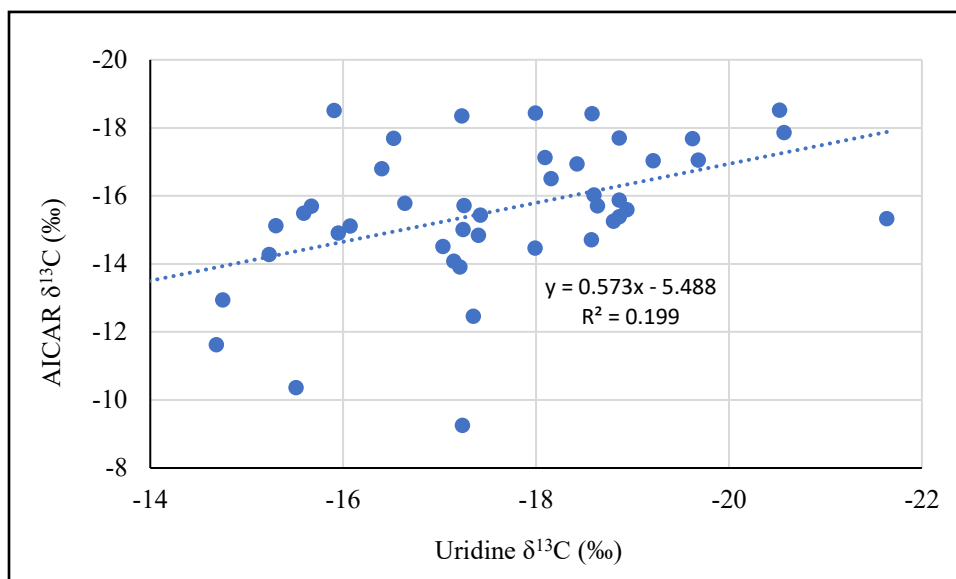


Figure 4.4: Correlation between AICAR and uridine  $\delta^{13}\text{C}$  values measured for this work ( $n = 43$ ).

Despite what they have in common (e.g., a ribose moiety obtained from PRPP), AICAR and uridine are also part of separate metabolisms influenced by specific factors. Recovery of uridine as a nucleoside is part of the pyrimidine salvage pathway [227]. This is a fundamental distinction between AICAR and uridine metabolisms. AICAR's C isotopic signature likely depends mostly on precursors available at the moment of synthesis whereas salvaged uridine molecules might introduce a “memory effect” that stabilizes the  $\delta^{13}\text{C}$  value over time. This work may unexpectedly give evidence for this hypothesis as the correlation between the CSIR of uridine and steroids (known to bear rather stable  $\delta^{13}\text{C}$  values [223]) is higher than between uridine and AICAR, supporting the idea that the cycle time of uridine is intermediate between the ones of AICAR and steroids. This can be seen in Figure 4.5 with Andro as an example ( $r^2 = 0.327$ ).

Aside from their turnover rates and pathways of synthesis, some of the C atoms in AICAR and uridine have unshared origins (Table 4.3) which could also be a cause for their different  $\delta^{13}\text{C}$  values. Glycine, from which the C4 and C5 atoms of AICAR are derived, has been reported to possess higher CSIR values than most of other amino acids in vertebrates. For instance, the prevalence of glycine in hair proteins has been linked to 1-2‰ enrichment in  $^{13}\text{C}$  when compared to other body tissues [228]. This could explain why AICAR is on average more enriched in  $^{13}\text{C}$  than uridine (+1.7‰ on average in this work, Table 4.2). The remaining C atoms, C2 for AICAR

and C4, C5 and C6 for uridine, have more than one possible origin [229-231], which makes it difficult to predict their CSIR values.

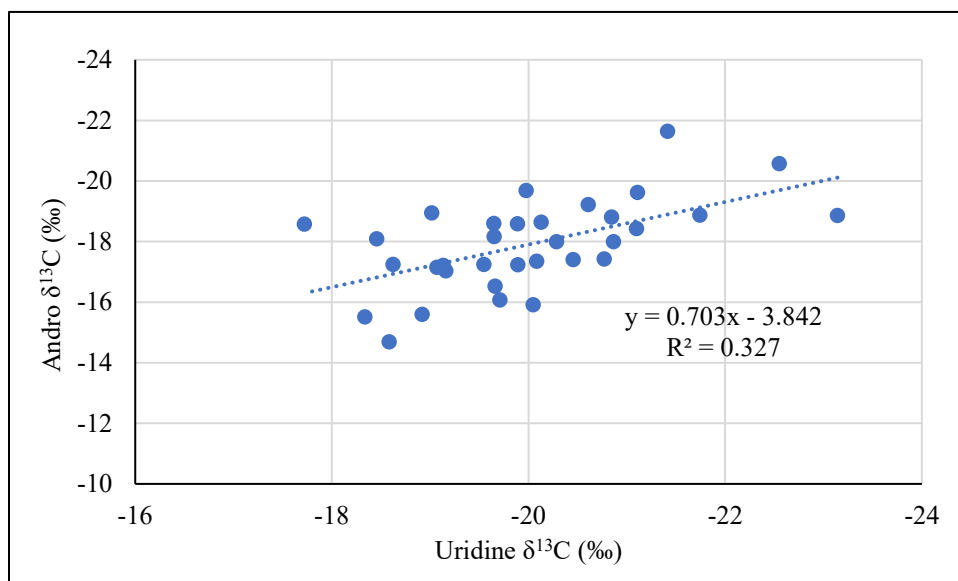


Figure 4.5: Correlation between uridine and Andro  $\delta^{13}\text{C}$  values measured for this work ( $n = 34$ ).

The results reported in this thesis therefore somewhat invalidate using steroids or uridine as ERCs for AICAR, simply because the information gathered thus far on AICAR tends to suggest that the compound possesses a unique isotopic signature that can hardly be related to another compound of similar composition - at least in terms of CSIR. This does not mean GC/C/IRMS tests are totally useless to detect eventual doping cases involving AICAR as there is still a notable difference in absolute  $\delta^{13}\text{C}$  value between the synthetic material analyzed so far and the reported endogenous values (roughly 4‰). AICAR's absolute  $\delta^{13}\text{C}$  value could be used as a marker for its exogenous origin, something possible based on the actual WADA technical documentation albeit in very specific cases for AAS when the TC's isotopic signature is outside the normal endogenous range [158]. More subtle doping cases cannot be detected with such a method.

ERCs are useful to anti-doping analyses as they account for natural variations in isotopic compositions so that variations caused by the administration of the exogenous substance are highlighted. Finding a more suitable ERC for AICAR analysis would be ideal as this would narrow the  $\Delta\delta^{13}\text{C}_{\text{A-ERC}}$  distribution and highlight abnormalities that are not seen using uridine or

steroids as ERCs. Such an ERC is yet to be identified, but further discussion on this topic is provided in the next chapter.

## 5. Conclusion

### 5.1 Future work

This work has uncovered some interesting findings but also raised a lot of questions about the CSIR of AICAR in urine. The following elements are based on the questions left unanswered in the previous section and are proposed here as new potential research avenues:

1. *The CSIR analysis of more AICAR of commercial origins.* Precise reasons explaining commercial AICAR's high CSIR values are not known, mainly because a lot of information about the precursor compounds and routes of synthesis is unavailable. Efficient production of AICAR by a genetically modified strain of *Bacillus Subtilis* has been reported using glucose and a source of amino acids or purines (e.g., yeast RNA) [232]. Corn starch being a cheap source of glucose, its location on the  $\delta^{13}\text{C}$  scale is expected to be in the C4-plant range (i.e., -7 to -15‰). This could in part explain why AICAR  $\delta^{13}\text{C}$  values are high, but not completely as none of the commercial values measured so far were lower than -5.3‰. It seems however unlikely that small underground laboratories have access to the cutting-edge technology of genetically modified micro-organisms. Conventional organic chemistry approaches to synthesize AICAR can also be found in the literature as the molecule has been used as a precursor for the development of cancer therapy drugs, for example [191, 233, 234]. This suggests a lot of "home made recipes" could have been developed and might be in use in many laboratories, official or not. Since the amount of material tested so far is obviously very scarce, more data is needed to determine if the  $\delta^{13}\text{C}$  values of the exogenous molecule are always different from the endogenous one.
2. *The analysis of more samples to get a better idea of the statistical distribution of AICAR  $\delta^{13}\text{C}$  values in an "AICAR-negative population".* Some results in this work suggest that dietary supplements such as ribose should be taken into consideration when establishing a negative reference population. The first step to be initiated is to undertake our own reference population to compare to Piper et al.'s study, in order to establish if their data - especially the  $\Delta\delta^{13}\text{C}_{\text{A-ERC}}$  values - are reproducible when performed on a controlled population. As already mentioned, this experiment is already under way at the *INRS-AFSB* where voluntary laboratory workers provided the necessary samples.
3. *The influence of dietary supplements on AICAR's CSIR.* This is the next logical step as a follow-up on (2). Since it is plausible that some results from this work (e.g., U1) are actually

caused by non-prohibited food supplements (e.g., ribose), excretion studies made with a volunteer before and after the intake of a supplement would provide critical information. Prior to the excretion study, GC- or EA-IRMS analysis of the supplement would be performed in order to understand the potential impact that the administration of this supplement might have on isotopic signature.

4. *Longitudinal data on AICAR (and uridine)  $\delta^{13}\text{C}$  values.* Aside from the excretion study made by Piper et al. (2014), no longitudinal data on the CSIR of AICAR have ever been acquired. The extent of natural variation of the compound's  $\delta^{13}\text{C}$  values over time is therefore not known. Based on statistical results, it has been hypothesized that physical exercise could increase AICAR's production [12]. Even though the data from this work do not bring any evidence for this as no specific relation was observed between AICAR concentration and  $\delta^{13}\text{C}$  values (Figure 4.1), a sudden increase in AICAR excretion could in principle influence its CSIR. It is possible that owing to its metabolism, AICAR naturally displays more variations in its  $\delta^{13}\text{C}$  values than e.g., AAS which are known to have relatively stable CSIR within a single individual [223]. The athletes' diet, a factor having a certain influence overtime on the CSIR of AICAR and uridine, should also be incorporated in those studies. This type of research is rare, but examples exist [223, 235]. Studies with volunteers consuming different diets (e.g., vegetarian, vegan, keto) or modifying their diet overtime would also supply precious information about the influence of food on the isotopic composition of urinary AICARs. Just like for (2), this kind of information would help in establishing a better understanding of how normal urinary AICAR CSIR behave, this time within a single individual. Excretion studies made on a few persons and over the course of different amount of time (e.g., intra-day variation or over a few weeks) and with subjects with different lifestyles (e.g., athletic versus sedentary) could provide useful data on this matter.
5. *The search for a better ERC for AICAR.* As stated at the end of the previous section, more research should be done to identify a suitable ERC for AICAR. Some of this research is already planned to be carried out at the *Laboratoire de contrôle du dopage* of the *INRS-AFSB*. ERCs are difficult to identify as they must fulfil many requirements and the possibility that in fact no ideal ERC exists at all for AICAR should be considered. Such an ERC should have a CSIR naturally similar to AICAR, but not affected by an intake of the exogenous compound. Its urinary concentration should be in the same ballpark as AICAR to make sure

sufficient amounts are always available for analysis. Its chemistry should also be similar to AICAR's in order to allow identical treatment during extraction and purification of the molecules as well as for the compound to be GC-amenable.

6. *Site-specific CSIR could be used as an experimental way to determine the contributions of different C atoms on the AICAR molecule.* This could be useful to determine what component added to the molecules during *de novo* synthesis influences the most AICAR's carbon isotopic signature. The cleavage of the glycosidic bond between AICAR's ribose and nitrogenous base, for example, could allow for the individual CSIR analysis of both moieties. Enzymes performing this specific reaction are commercially available. Such analyses could also give information on the component of synthetic AICAR that has the most influence on its high  $\delta^{13}\text{C}$  values and perhaps eventually help in identifying a more suitable ERC for AICAR.
7. *The identification of better biomarkers related to the presence of exogenous AICAR during sample screening.* GC/C/IRMS procedures are not typically performed on all samples received by an anti-doping laboratory as they are time-consuming and the percentage of abnormal findings they yield is small when compared to the total number of samples. Efficient screening of the samples in order to detect the suspicious ones prior to their isotopic analysis is therefore important. AICAR urinary concentration itself has been shown to be an indicator of synthetic AICAR administration [11, 15, 16], however the many samples of high concentration analyzed in this work and for which the results were normal suggest that other markers could be used to improve sample screening. Other molecular markers, perhaps part of the purine pathway or related to ZMP could be studied and used in as additional information to AICAR concentration. It is also possible that a method for the detection of exogenous AICAR in urine rely on the combination of GC/C/IRMS with another analytical technique (e.g., LC-MS/MS of ZMP in RBC [17]).

## 5.2 General conclusions

A method for the extraction, the purification and the GC/C/IRMS analysis of urinary AICAR and uridine has been developed and applied to over 40 samples. The same method was also used for the analysis of QC urine samples as well as synthetic AICAR purchased on the Internet.

Acetylation was used for the first time as a chemical derivatization for this type of analysis. As per the first two objectives of this thesis, every step of the method was optimized individually in order to yield maximal analyte recovery while focusing on method robustness and specificity.

GC/C/IRMS measurements were precise as demonstrated by the analysis of QCs which yielded SDs ranging from 0.25 to 0.47‰ before correction for acetylation and 0.37 to 1.28‰ after correction for acetylation.

The results obtained from the CSIR analysis of urine samples yielded results somewhat unexpected as the  $\delta^{13}\text{C}$  values obtained for AICAR were 5.3‰ more  $^{13}\text{C}$ -enriched than for Piper et al.'s (2014) sample population. Those  $\delta^{13}\text{C}$  values were also very dispersed, from -9.3 to -18.5‰. This scattering, also observed by Piper et al., made difficult the use of an ERC to better diagnose the origin of AICAR in urine samples.  $\Delta\delta^{13}\text{C}_{\text{A-ERC}}$  values for all ERC candidates tested (Pd, Andro, Et, and uridine) showed low inter-sample reproducibility. As an important consequence of this, reference limit values - thresholds at which an AICAR-positive sample can be detected based on its  $\Delta\delta^{13}\text{C}_{\text{A-ERC}}$  result - were much higher (around 10‰ for each AICAR-ERC duo evaluated in this work) than the ones applying for steroid analyses (generally 3‰ [158]). Such high values can make difficult the detection of exogenous AICAR, especially in urine samples with ERCs known to be naturally  $^{13}\text{C}$ -enriched when compared to European ones (e.g., North-American ones) as the range of values considered normal for such samples can get close and even overlap with the range of  $\delta^{13}\text{C}$  values known for synthetic AICAR. The main conclusion to be drawn from those results is that the ERCs evaluated thus far for AICAR's GC/C/IRMS analysis, despite being the only ones available at the moment, are far from being ideal. Even though Piper et al. had also reported high reference limit values that could have allowed them to anticipate possible complications associated with samples displaying higher natural  $\delta^{13}\text{C}$  values, they did not mention this possibility. The results presented here demonstrate that this potential issue has to be taken into account when performing CSIR analyses of AICAR.

This work has also brought into light the impact of the type of population used to determine the natural distribution of AICAR  $\delta^{13}\text{C}$  values. Some factors, such as the use of non-prohibited dietary supplements, were not discussed by Piper et al. (2014) and might interfere with normal AICAR CSIR values. This possibility should be further investigated in order to evaluate its impact on urinary AICAR  $\delta^{13}\text{C}$  values, something that could have important consequences on the values considered normal by WADA for AICAR GC/C/IRMS analysis. The study of another urine population under controlled conditions (i.e., without supplements) is also being conducted at the moment to verify if Piper et al.'s (2014) results can be replicated. This could allow WADA

to eventually gather enough information about AICAR to publish relevant guidelines and technical documentation about the compound. As many questions are obviously yet to be answered about AICAR and anti-doping testing, more research should therefore be promoted by WADA on AICAR among the whole community of their accredited laboratories.

This thesis highlights very well how some assumptions made in anti-doping sciences should not be taken for granted. Notably, the uniform distribution of CSIR within an organism should never be assumed when performing CSIA. This has important consequences on the choice of ERC for a given TC, not only for AICAR but also for any substance that could be analyzed by GC/C/IRMS in the future. As mentioned in the first lines of this thesis, anti-doping regulations are conceived to be updated overtime as new scientific information becomes available. This thesis is therefore entirely in line with this concept as the results it contains could one day help establish better guidelines for the analysis of urinary AICAR by GC/C/IRMS.

## Bibliography

1. World Anti-Doping Agency website, "Who we are". Available from: <https://www.wada-ama.org/en/who-we-are>, accessed 2020-10-09.
2. World Anti-Doping Agency, World Anti-doping Code 2015 with 2019 amendments. Available from: [https://www.wada-ama.org/sites/default/files/resources/files/wada\\_anti-doping\\_code\\_2019\\_english\\_final\\_revised\\_v1\\_linked.pdf](https://www.wada-ama.org/sites/default/files/resources/files/wada_anti-doping_code_2019_english_final_revised_v1_linked.pdf), accessed 2020-10-12.
3. World Anti-Doping Agency, The 2020 Prohibited List. Available from: [https://www.wada-ama.org/sites/default/files/wada\\_2020\\_english\\_prohibited\\_list\\_0.pdf](https://www.wada-ama.org/sites/default/files/wada_2020_english_prohibited_list_0.pdf), accessed 2020-10-09.
4. World Anti-Doping agency, THE 2009 PROHIBITED LIST. Available from: [https://www.wada-ama.org/sites/default/files/resources/files/WADA\\_Prohibited\\_List\\_2009\\_EN.pdf](https://www.wada-ama.org/sites/default/files/resources/files/WADA_Prohibited_List_2009_EN.pdf), accessed 2020-10-09.
5. Benkimoun, P., *Police find range of drugs after trawling bins used by Tour de France cyclists*. BMJ, 2009. 339: p. b4201.
6. Stokes, S., *Colombian doctor Beltrán Niño arrested with AICAR and TB-500 doping products*, in *Velonation*. 2012.
7. Sobolevsky, T., et al., *Detection of PPAR $\delta$  agonists GW1516 and GW0742 and their metabolites in human urine*. Drug Test Anal, 2012. 4(10): p. 754-60.
8. Thevis, M., et al., *Characterization of two major urinary metabolites of the PPAR $\delta$ -agonist GW1516 and implementation of the drug in routine doping controls*. Anal Bioanal Chem, 2010. 396(7): p. 2479-91.
9. Pokrywka, A., et al., *Metabolic modulators of the exercise response: doping control analysis of an agonist of the peroxisome proliferator-activated receptor  $\delta$  (GW501516) and 5-aminoimidazole-4-carboxamide ribonucleotide (AICAR)*. J Physiol Pharmacol, 2014. 65(4): p. 469-76.
10. U.S. Securities and Exchange Commission, QUARTERLY REPORT PURSUANT TO SECTION 13 OR 15(d) OF THE SECURITIES EXCHANGE ACT OF 1934 For the quarterly period ended June 30, 2010 Merck & Co., Inc. Available from: <https://www.sec.gov/Archives/edgar/data/310158/000095012310074336/y83714e10vq.htm#002>, accessed 2020-10-12.
11. Piper, T., et al., *Determination of  $^{13}C/^{12}C$  ratios of endogenous urinary 5-aminoimidazole-4-carboxamide  $1\beta$ -D-ribofuranoside (AICAR)*. Rapid Communications in Mass Spectrometry, 2014. 28(11): p. 1194-1202.
12. Thomas, A., et al., *Quantification of urinary AICAR concentrations as a matter of doping controls*. Anal Bioanal Chem, 2010. 396(8): p. 2899-908.
13. Sobolevsky, T. and B. Ahrens, *Urinary concentrations of AICAR and mannitol in athlete population*. Drug Testing and Analysis, 2019. 11(3): p. 530-535.
14. Mendler, M., et al., *Urine levels of 5-aminoimidazole-4-carboxamide riboside (AICAR) in patients with type 2 diabetes*. Acta Diabetologica, 2018. 55(6): p. 585-592.
15. Dixon, R., et al., *AICA-Riboside: Safety, Tolerance, and Pharmacokinetics of a Novel Adenosine-Regulating Agent*. The Journal of Clinical Pharmacology, 1991. 31(4): p. 342-347.
16. Dixon, R., et al., *Acadesine (AICA-Riboside): Disposition and Metabolism of an Adenosine-Regulating Agent*. The Journal of Clinical Pharmacology, 1993. 33(10): p. 955-958.

17. Thomas, A., et al., *Quantification of AICAR-ribotide concentrations in red blood cells by means of LC-MS/MS*. Anal Bioanal Chem, 2013. 405(30): p. 9703-9.
18. Nicoli, R., et al., *Analytical Strategies for Doping Control Purposes: Needs, Challenges, and Perspectives*. Analytical chemistry, 2015. 88.
19. Hemmersbach, P., *History of mass spectrometry at the Olympic Games*. Journal of Mass Spectrometry, 2008. 43(7): p. 839-853.
20. Cawley, A.T. and U. Flenker, *The application of carbon isotope ratio mass spectrometry to doping control*. Journal of Mass Spectrometry, 2008. 43(7): p. 854-864.
21. Piper, T., et al., *Nitrogen isotope ratios of endogenous urinary AICAR*, in *Recent advances in doping analysis (22)*, T.M.G.H.M.U. Schänzer W, Editor. 2014, Sportverlag Strauß. p. 150-153.
22. Buisson, C., et al., *Implementation of AICAR analysis by GC-C-IRMS for anti-doping purposes*. Drug Testing and Analysis, 2017. 9(11-12): p. 1704-1712.
23. Lowy, B.A. and M.K. Williams, *Lesch-Nyhan syndrome: the synthesis of inosine 5'-phosphate in the hypoxanthine-guanine phosphoribosyltransferase-deficient erythrocyte by alternate biochemical pathways*. Pediatr Res, 1977. 11(5): p. 691-4.
24. Stouthamer, A.H., P.G. de Haan, and H.J.J. Nijkamp, *Mapping of purine markers in Escherichia coli K 12*. Genetical Research, 1965. 6(3): p. 442-453.
25. Love, S.H. and P.D. Boyles, *Studies on the synthesis of 5-amino-4-imidazolecarboxamide ribotide by cell-free extracts of Escherichia coli*. Biochim Biophys Acta, 1959. 35: p. 374-80.
26. NISHIKAWA, H., H. MOMOSE, and I. SHIIO, *Pathway of Purine Nucleotide Synthesis in Bacillus Subtilis\**. The Journal of Biochemistry, 1968. 63(2): p. 149-155.
27. Moyed, H.S. and B. Magasanik, *THE ROLE OF PURINES IN HISTIDINE BIOSYNTHESIS I*. Journal of the American Chemical Society, 1957. 79(17): p. 4812-4813.
28. Lowy, B.A., M.K. Williams, and I.M. London, *Enzymatic Deficiencies of Purine Nucleotide Synthesis in the Human Erythrocyte*. Journal of Biological Chemistry, 1962. 237(5): p. 1622-1625.
29. Lowy, B.A. and M.K. Williams, *The presence of a limited portion of the pathway de novo of purine nucleotide biosynthesis in the rabbit erythrocyte in vitro*. J Biol Chem, 1960. 235: p. 2924-7.
30. Zimmerman, T.P. and R.D. Deeproose, *Metabolism of 5-amino-1-β-d-ribofuranosyl-imidazole-4-carboxamide and related five-membered heterocycles to 5'-triphosphates in human blood and L5178Y cells*. Biochemical Pharmacology, 1978. 27(5): p. 709-716.
31. Sabina, R.L., D. Patterson, and E.W. Holmes, *5-Amino-4-imidazolecarboxamide riboside (Z-riboside) metabolism in eukaryotic cells*. Journal of Biological Chemistry, 1985. 260(10): p. 6107-14.
32. Hardie, D.G. and S.A. Hawley, *AMP-activated protein kinase: the energy charge hypothesis revisited*. BioEssays, 2001. 23(12): p. 1112-1119.
33. Hardie, D.G., et al., *Management of cellular energy by the AMP-activated protein kinase system*. FEBS Letters, 2003. 546(1): p. 113-120.
34. Sullivan, J.E., et al., *Characterization of 5'-AMP-Activated Protein Kinase in Human Liver Using Specific Peptide Substrates and the Effects of 5'-AMP Analogues on Enzyme Activity*. Biochemical and Biophysical Research Communications, 1994. 200(3): p. 1551-1556.

35. Sullivan, J.E., et al., *Inhibition of lipolysis and lipogenesis in isolated rat adipocytes with AICAR, a cell-permeable activator of AMP-activated protein kinase*. FEBS Letters, 1994. 353(1): p. 33-36.
36. Medicine, N.L.o., *PubMed*.
37. Hardie, D.G., D. Carling, and M. Carlson, *THE AMP-ACTIVATED/SNF1 PROTEIN KINASE SUBFAMILY: Metabolic Sensors of the Eukaryotic Cell?* Annual Review of Biochemistry, 1998. 67(1): p. 821-855.
38. Kjøbsted, R., et al., *AMPK in skeletal muscle function and metabolism*. Faseb j, 2018. 32(4): p. 1741-1777.
39. Chen, Z.-P., et al., *Effect of Exercise Intensity on Skeletal Muscle AMPK Signaling in Humans*. Diabetes, 2003. 52(9): p. 2205-2212.
40. Reilly, S.M. and C.H. Lee, *PPAR delta as a therapeutic target in metabolic disease*. FEBS Lett, 2008. 582(1): p. 26-31.
41. Reznick, R.M. and G.I. Shulman, *The role of AMP-activated protein kinase in mitochondrial biogenesis*. The Journal of Physiology, 2006. 574(1): p. 33-39.
42. Ceschin, J., et al., *Identification of yeast and human 5-aminoimidazole-4-carboxamide-1- $\beta$ -D-ribofuranoside (AICAR) transporters*. J Biol Chem, 2014. 289(24): p. 16844-54.
43. Daignan-Fornier, B. and B. Pinson, *5-Aminoimidazole-4-carboxamide-1-beta-D-ribofuranosyl 5'-Monophosphate (AICAR), a Highly Conserved Purine Intermediate with Multiple Effects*. Metabolites, 2012. 2(2): p. 292-302.
44. Dolinar, K., et al., *Nucleosides block AICAR-stimulated activation of AMPK in skeletal muscle and cancer cells*. American Journal of Physiology-Cell Physiology, 2018. 315(6): p. C803-C817.
45. Daignan-Fornier, B. and B. Pinson, *Yeast to Study Human Purine Metabolism Diseases*. Cells, 2019. 8(1).
46. Yin, J., et al., *Potential Mechanisms Connecting Purine Metabolism and Cancer Therapy*. Frontiers in Immunology, 2018. 9(1697).
47. Kanehisa, M., et al., *New approach for understanding genome variations in KEGG*. Nucleic Acids Res, 2019. 47(D1): p. D590-d595.
48. Kanehisa, M., *Toward understanding the origin and evolution of cellular organisms*. Protein Sci, 2019. 28(11): p. 1947-1951.
49. Kanehisa, M. and S. Goto, *KEGG: kyoto encyclopedia of genes and genomes*. Nucleic Acids Res, 2000. 28(1): p. 27-30.
50. Rébora, K., B. Laloo, and B. Daignan-Fornier, *Revisiting purine-histidine cross-pathway regulation in Saccharomyces cerevisiae: a central role for a small molecule*. Genetics, 2005. 170(1): p. 61-70.
51. Zhang, Y., et al., *Uridine Metabolism and Its Role in Glucose, Lipid, and Amino Acid Homeostasis*. BioMed Research International, 2020. 2020: p. 7091718.
52. Xi, H., B.L. Schneider, and L. Reitzer, *Purine catabolism in Escherichia coli and function of xanthine dehydrogenase in purine salvage*. J Bacteriol, 2000. 182(19): p. 5332-41.
53. Malykh, E.A., et al., *Specific features of L-histidine production by Escherichia coli concerned with feedback control of AICAR formation and inorganic phosphate/metal transport*. Microb Cell Fact, 2018. 17(1): p. 42.
54. Pinson, B., et al., *Metabolic intermediates selectively stimulate transcription factor interaction and modulate phosphate and purine pathways*. Genes & development, 2009. 23(12): p. 1399-1407.

55. Hartman, S.C. and J.M. Buchanan, *The biosynthesis of the purines*. Ergebnisse der Physiologie Biologischen Chemie und Experimentellen Pharmakologie, 1959. 50(1): p. 75-121.
56. Moat, A.G. and H. Friedman, *The biosynthesis and interconversion of purines and their derivatives*. Bacteriol Rev, 1960. 24(3): p. 309-39.
57. Lowy, B.A., J.L. Cook, and I.M. London, *The Biosynthesis of Purine Nucleotides de Novo in the Rabbit Reticulocyte in Vitro*. Journal of Biological Chemistry, 1961. 236(5): p. 1442-1445.
58. Wagner, C. and M.E. Levitch, *The utilization of formate by human erythrocytes*. Biochimica et Biophysica Acta (BBA) - General Subjects, 1973. 304(3): p. 623-633.
59. Sell, H., et al., *Cytokine secretion by human adipocytes is differentially regulated by adiponectin, AICAR, and troglitazone*. Biochemical and Biophysical Research Communications, 2006. 343(3): p. 700-706.
60. Du, J.-H., et al., *AICAR stimulates IL-6 production via p38 MAPK in cardiac fibroblasts in adult mice: A possible role for AMPK*. Biochemical and Biophysical Research Communications, 2005. 337(4): p. 1139-1144.
61. Golubitzky, A., et al., *Screening for Active Small Molecules in Mitochondrial Complex I Deficient Patient's Fibroblasts, Reveals AICAR as the Most Beneficial Compound*. PLOS ONE, 2011. 6(10): p. e26883.
62. Spangenburg, E.E., K.C. Jackson, and R.A. Schuh, *AICAR inhibits oxygen consumption by intact skeletal muscle cells in culture*. J Physiol Biochem, 2013. 69(4): p. 909-17.
63. Nagata, D., et al., *AMP-Activated Protein Kinase Inhibits Angiotensin II-Induced Stimulated Vascular Smooth Muscle Cell Proliferation*. Circulation, 2004. 110(4): p. 444-451.
64. Blanco, C.L., et al., *Effects of intravenous AICAR (5-aminoimidazole-4-carboximide riboside) administration on insulin signaling and resistance in premature baboons, Papio sp.* PLoS One, 2018. 13(12): p. e0208757.
65. Huang, Y., et al., *AICAR Administration Attenuates Hemorrhagic Hyperglycemia and Lowers Oxygen Debt in Anesthetized Male Rabbits*. Front Physiol, 2017. 8: p. 692.
66. Idrovo, J.P., et al., *AICAR attenuates organ injury and inflammatory response after intestinal ischemia and reperfusion*. Mol Med, 2015. 20(1): p. 676-83.
67. Pold, R., et al., *Long-Term AICAR Administration and Exercise Prevents Diabetes in ZDF Rats*. Diabetes, 2005. 54(4): p. 928-934.
68. Iglesias, M.A., et al., *AICAR Administration Causes an Apparent Enhancement of Muscle and Liver Insulin Action in Insulin-Resistant High-Fat-Fed Rats*. Diabetes, 2002. 51(10): p. 2886-2894.
69. Suwa, M., H. Nakano, and S. Kumagai, *Effects of chronic AICAR treatment on fiber composition, enzyme activity, UCP3, and PGC-1 in rat muscles*. Journal of Applied Physiology, 2003. 95(3): p. 960-968.
70. Swain, J.L., et al., *Accelerated repletion of ATP and GTP pools in postischemic canine myocardium using a precursor of purine de novo synthesis*. Circulation Research, 1982. 51(1): p. 102-105.
71. Mauser, M., et al., *Influence of ribose, adenosine, and "AICAR" on the rate of myocardial adenosine triphosphate synthesis during reperfusion after coronary artery occlusion in the dog*. Circulation Research, 1985. 56(2): p. 220-230.

72. Hoffmeister, H.M., M. Mauser, and W. Schaper, *Effect of adenosine and AICAR on ATP content and regional contractile function in reperfused canine myocardium*. Basic Research in Cardiology, 1985. 80(4): p. 445-458.
73. Sabina, R.L., et al., *Metabolism of 5-amino-4-imidazolecarboxamide riboside in cardiac and skeletal muscle. Effects on purine nucleotide synthesis*. Journal of Biological Chemistry, 1982. 257(17): p. 10178-10183.
74. Narkar, V.A., et al., *AMPK and PPARdelta agonists are exercise mimetics*. Cell, 2008. 134(3): p. 405-15.
75. Kjøbsted, R., et al., *Prior AICAR Stimulation Increases Insulin Sensitivity in Mouse Skeletal Muscle in an AMPK-Dependent Manner*. Diabetes, 2015. 64(6): p. 2042-2055.
76. Halseth, A.E., et al., *Acute and chronic treatment of ob/ob and db/db mice with AICAR decreases blood glucose concentrations*. Biochemical and Biophysical Research Communications, 2002. 294(4): p. 798-805.
77. Babraj, J.A., et al., *Blunting of AICAR-induced human skeletal muscle glucose uptake in type 2 diabetes is dependent on age rather than diabetic status*. American Journal of Physiology-Endocrinology and Metabolism, 2009. 296(5): p. E1042-E1048.
78. Bosselaar, M., et al., *Intravenous AICAR During Hyperinsulinemia Induces Systemic Hemodynamic Changes but Has No Local Metabolic Effect*. The Journal of Clinical Pharmacology, 2011. 51(10): p. 1449-1458.
79. Boon, H., et al., *Intravenous AICAR administration reduces hepatic glucose output and inhibits whole body lipolysis in type 2 diabetic patients*. Diabetologia, 2008. 51(10): p. 1893.
80. Cuthbertson, D.J., et al., *5-Aminoimidazole-4-Carboxamide 1- $\beta$ -Ribofuranoside Acutely Stimulates Skeletal Muscle 2-Deoxyglucose Uptake in Healthy Men*. Diabetes, 2007. 56(8): p. 2078-2084.
81. Guerrieri, D., H.Y. Moon, and H. van Praag, *Exercise in a Pill: The Latest on Exercise-Mimetics*. Brain Plast, 2017. 2(2): p. 153-169.
82. Hürlimann, H.C., et al., *Physiological and toxic effects of purine intermediate 5-amino-4-imidazolecarboxamide ribonucleotide (AICAR) in yeast*. J Biol Chem, 2011. 286(35): p. 30994-1002.
83. Marie, S., et al., *AICA-ribosiduria: a novel, neurologically devastating inborn error of purine biosynthesis caused by mutation of ATIC*. Am J Hum Genet, 2004. 74(6): p. 1276-81.
84. López, J.M., *Is ZMP the toxic metabolite in Lesch–Nyhan disease?* Medical Hypotheses, 2008. 71(5): p. 657-663.
85. Aschenbach, W.G., et al., *Effect of AICAR Treatment on Glycogen Metabolism in Skeletal Muscle*. Diabetes, 2002. 51(3): p. 567-573.
86. ZAREMBO, A., *'Exercise pill' could take the work out of workouts*, in Los Angeles Times. 2008.
87. *Exercise in a pill? Yes, if you're a mouse*. 2008 Available from: <https://www.cbc.ca/news/technology/exercise-in-a-pill-yes-if-you-re-a-mouse-1.723876>, accessed 2020-10-20.
88. Roberts, M.D., *Exercise In A Pill: Are We There Yet?* 2019 Available from: <https://www.bodybuilding.com/content/exercise-in-a-pill-are-we-there-yet.html>, accessed 2020-10-20.
89. Retsin, F., *Quand l'Aicar revient sur le tapis...*, in La Voix du Nord. 2019.
90. *Direct SARMS*. Available from: <https://belgium.direct-sarms.com/product/aicar-peptide-vial/>, accessed 2020-10-20.

91. *SARMS World*. Available from: <https://www.sarmsworld.com/aicar/>, accessed 2020-10-20.
92. *Peptides Worldwide*. Available from: <https://peptidesworldwide.com/product/aicar/>, accessed 2020-10-20.
93. Roberts, B., Available from: <http://fr.thinksteroids.com/profils-steroides/aicar/>, accessed
94. *Southern SARMS*. Available from: <http://www.southernsarms.com/aicar-cardarine-combo.html>, accessed 2020-10-20.
95. Sharp, Z., *Principles of Stable Isotope Geochemistry, 2nd Edition*. 2017.
96. Chokkathukalam, A., et al., *Stable isotope-labeling studies in metabolomics: new insights into structure and dynamics of metabolic networks*. *Bioanalysis*, 2014. 6(4): p. 511-24.
97. Hiller, K., C. Metallo, and G. Stephanopoulos, *Elucidation of Cellular Metabolism Via Metabolomics and Stable-Isotope Assisted Metabolomics*. *Current Pharmaceutical Biotechnology*, 2011. 12(7): p. 1075-1086.
98. Ehleringer, J. and S.M. Matheson, *STABLE ISOTOPES AND COURTS*. *Utah law review*, 2010. 2010.
99. Neveu, M., C.H. House, and S.T. Wieman, *Phoebe's carbon isotope composition as evidence for self-shielding in the solar nebula*. *Icarus*, 2020. 345: p. 113714.
100. Goderis, S., et al., *Isotopes in cosmochemistry: recipe for a Solar System*. *Journal of Analytical Atomic Spectrometry*, 2016. 31(4): p. 841-862.
101. Tomascak, P.B., T. Magna, and R. Dohmen, *Advances in Lithium Isotope Geochemistry*. *Advances in Isotope Geochemistry*. 2016: Springer International Publishing.
102. Abrams, S.A., *Using stable isotopes to assess mineral absorption and utilization by children*. *The American Journal of Clinical Nutrition*, 1999. 70(6): p. 955-964.
103. Halicz, L., et al., *Strontium stable isotopes fractionate in the soil environments?* *Earth and Planetary Science Letters*, 2008. 272(1): p. 406-411.
104. Anbar, A.D., *Iron stable isotopes: beyond biosignatures*. *Earth and Planetary Science Letters*, 2004. 217(3): p. 223-236.
105. Shouakar-Stash, O., R.J. Drimmie, and S.K. Frape, *Determination of inorganic chlorine stable isotopes by continuous flow isotope ratio mass spectrometry*. *Rapid Communications in Mass Spectrometry*, 2005. 19(2): p. 121-127.
106. Aregbe, Y., et al., *Detection of reprocessing activities through stable isotope measurements of atmospheric noble gases*. *Fresenius' Journal of Analytical Chemistry*, 1997. 358(4): p. 533-535.
107. Rozanski, K., et al., *Reconstruction of past climates from stable isotope records of palaeo-precipitation preserved in continental archives*. *Hydrological Sciences Journal*, 1997. 42(5): p. 725-745.
108. Gourcy, L.L., M. Groening, and P.K. Aggarwal, *Stable Oxygen and Hydrogen Isotopes in Precipitation*, in *Isotopes in the Water Cycle: Past, Present and Future of a Developing Science*, P.K. Aggarwal, J.R. Gat, and K.F.O. Froehlich, Editors. 2005, Springer Netherlands: Dordrecht. p. 39-51.
109. Ehleringer, J.R., et al., *Hydrogen and oxygen isotope ratios in human hair are related to geography*. *Proceedings of the National Academy of Sciences*, 2008. 105(8): p. 2788-2793.
110. Xia, C., et al., *Characteristics of hydrogen and oxygen stable isotopes in precipitation and the environmental controls in tropical monsoon climatic zone*. *International Journal of Hydrogen Energy*, 2019. 44(11): p. 5417-5427.

111. Thornton, S.F. and J. McManus, *Application of Organic Carbon and Nitrogen Stable Isotope and C/N Ratios as Source Indicators of Organic Matter Provenance in Estuarine Systems: Evidence from the Tay Estuary, Scotland*. Estuarine, Coastal and Shelf Science, 1994. 38(3): p. 219-233.
112. Huang, J., et al., *Detection of corn oil in adulterated olive and soybean oil by carbon stable isotope analysis*. Journal of Consumer Protection and Food Safety, 2017. 12(3): p. 201-208.
113. Çınar, S.B., A. Ekşi, and İ. Coşkun, *Carbon isotope ratio ( $^{13}\text{C}/^{12}\text{C}$ ) of pine honey and detection of HFCS adulteration*. Food Chemistry, 2014. 157: p. 10-13.
114. Cawley, A., *Stable isotope ratio analysis in sports anti-doping*. Drug Test Anal, 2012. 4(12): p. 891-2.
115. Meier-Augenstein, W., *Applied gas chromatography coupled to isotope ratio mass spectrometry*. J Chromatogr A, 1999. 842(1-2): p. 351-71.
116. Bartelink, E.J. and L.A. Chesson, *Recent applications of isotope analysis to forensic anthropology*. Forensic Sci Res, 2019. 4(1): p. 29-44.
117. Idoine, F.A., J.F. Carter, and R. Sleeman, *Bulk and compound-specific isotopic characterisation of illicit heroin and cling film*. Rapid Communications in Mass Spectrometry, 2005. 19(22): p. 3207-3215.
118. Chahartaghi, M., et al., *Feeding guilds in Collembola based on nitrogen stable isotope ratios*. Soil Biology and Biochemistry, 2005. 37(9): p. 1718-1725.
119. Symes, C.T. and S.M. Woodborne, *Trophic level delineation and resource partitioning in a South African afro-montane forest bird community using carbon and nitrogen stable isotopes*. African Journal of Ecology, 2010. 48(4): p. 984-993.
120. Zehr, J.P. and B.B. Ward, *Nitrogen cycling in the ocean: new perspectives on processes and paradigms*. Appl Environ Microbiol, 2002. 68(3): p. 1015-24.
121. Seal, R.R., II, *Sulfur Isotope Geochemistry of Sulfide Minerals*. Reviews in Mineralogy and Geochemistry, 2006. 61(1): p. 633-677.
122. Taylor, P.D.P., P. De Bièvre, and S. Valkiers, *Chapter 41 - The Nature and Role of Primary Certified Isotopic Reference Materials: A Tool to Underpin Isotopic Measurements on a Global Scale*, in *Handbook of Stable Isotope Analytical Techniques*, P.A. de Groot, Editor. 2004, Elsevier: Amsterdam. p. 907-927.
123. Gröning, M., *Chapter 40 - International Stable Isotope Reference Materials*, in *Handbook of Stable Isotope Analytical Techniques*, P.A. de Groot, Editor. 2004, Elsevier: Amsterdam. p. 874-906.
124. Meier-Augenstein, W., *Chapter 8 - GC and IRMS Technology for  $^{13}\text{C}$  and  $^{15}\text{N}$  Analysis on Organic Compounds and Related Gases*, in *Handbook of Stable Isotope Analytical Techniques*, P.A. de Groot, Editor. 2004, Elsevier: Amsterdam. p. 153-176.
125. Dunn, P. and J.F. Carter, *Good Practice Guide for Isotope Ratio Mass Spectrometry Second Edition 2018*. 2018.
126. Smith, B.N. and S. Epstein, *Two Categories of  $^{13}\text{C}/^{12}\text{C}$  Ratios for Higher Plants*. Plant Physiology, 1971. 47(3): p. 380-384.
127. O'Leary, M.H., *Carbon Isotopes in Photosynthesis*. BioScience, 1988. 38(5): p. 328-336.
128. Torres, I.C., et al., *Stable isotope ( $\delta^{13}\text{C}$  and  $\delta^{15}\text{N}$ ) values of sediment organic matter in subtropical lakes of different trophic status*. Journal of Paleolimnology, 2012. 47(4): p. 693-706.
129. Nier, A.O. and E.A. Gulbransen, *Variations in the Relative Abundance of the Carbon Isotopes*. Journal of the American Chemical Society, 1939. 61(3): p. 697-698.

130. Craig, H., *The geochemistry of the stable carbon isotopes*. *Geochimica et Cosmochimica Acta*, 1953. 3(2): p. 53-92.
131. Sieper, H.-P., et al., *A measuring system for the fast simultaneous isotope ratio and elemental analysis of carbon, hydrogen, nitrogen and sulfur in food commodities and other biological material*. *Rapid Communications in Mass Spectrometry*, 2006. 20(17): p. 2521-2527.
132. Barber, A., et al., *The role of iron in the diagenesis of organic carbon and nitrogen in sediments: A long-term incubation experiment*. *Marine Chemistry*, 2014. 162: p. 1-9.
133. Heinzle, E., et al., *Analysis of  $^{13}\text{C}$  labeling enrichment in microbial culture applying metabolic tracer experiments using gas chromatography–combustion–isotope ratio mass spectrometry*. *Analytical Biochemistry*, 2008. 380(2): p. 202-210.
134. Southan G, et al. *Misuse of testosterone in sport: an approach to detection by measurement of isotopic abundance using GC-IRMS*. in *Programme and Abstracts of The 2nd International Symposium on Applied Mass Spectrometry in the Health Sciences*. 1990. Barcelona, Spain.
135. Becchi, M., et al., *Gas chromatography/combustion/isotope-ratio mass spectrometry analysis of urinary steroids to detect misuse of testosterone in sport*. *Rapid Communications in Mass Spectrometry*, 1994. 8(4): p. 304-308.
136. Tykot, R.H., *Stable isotopes and diet: You are what you eat*. 2004. 154.
137. DeNiro, M.J. and S. Epstein, *Influence of diet on the distribution of carbon isotopes in animals*. *Geochimica et Cosmochimica Acta*, 1978. 42(5): p. 495-506.
138. Thomas, P.J., et al., *Isotope discrimination by form IC RubisCO from *Ralstonia eutropha* and *Rhodobacter sphaeroides*, metabolically versatile members of 'Proteobacteria' from aquatic and soil habitats*. *Environmental Microbiology*, 2019. 21(1): p. 72-80.
139. Cassar, N., et al., *Bicarbonate uptake by Southern Ocean phytoplankton*. *Global Biogeochemical Cycles*, 2004. 18(2).
140. Kennedy, B.V. and H.R. Krouse, *Isotope fractionation by plants and animals: implications for nutrition research*. *Canadian Journal of Physiology and Pharmacology*, 1990. 68(7): p. 960-972.
141. Yamori, W., K. Hikosaka, and D.A. Way, *Temperature response of photosynthesis in C3, C4, and CAM plants: temperature acclimation and temperature adaptation*. *Photosynthesis Research*, 2014. 119(1): p. 101-117.
142. Bishop, M.B. and C.B. Bishop, *Photosynthesis and carbon dioxide fixation*. *Journal of Chemical Education*, 1987. 64(4): p. 302.
143. Ehleringer, J. and T. Cerling, *C3 and C4 Photosynthesis*. *Encyclopedia of Global Environmental Change*, 2002. 2.
144. Leegood, R.C., *C4 photosynthesis: principles of CO2 concentration and prospects for its introduction into C3 plants*. *Journal of Experimental Botany*, 2002. 53(369): p. 581-590.
145. Farquhar, G., *On the Nature of Carbon Isotope Discrimination in C 4 Species*. *Australian Journal of Plant Physiology*, 1983. 10: p. 205-226.
146. Bräutigam, A., et al., *On the Evolutionary Origin of CAM Photosynthesis*. *Plant Physiology*, 2017. 174(2): p. 473-477.
147. de la Torre, X., et al.,  *$^{13}\text{C}/^{12}\text{C}$  Isotope ratio MS analysis of testosterone, in chemicals and pharmaceutical preparations*. *Journal of Pharmaceutical and Biomedical Analysis*, 2001. 24(4): p. 645-650.
148. Cawley, A.T., et al., *Carbon isotope ratio ( $\delta^{13}\text{C}$ ) values of urinary steroids for doping control in sport*. *Steroids*, 2009. 74(3): p. 379-392.

149. Ueki, M. and M. Okano, *Analysis of exogenous dehydroepiandrosterone excretion in urine by gas chromatography/combustion/isotope ratio mass spectrometry*. Rapid Commun Mass Spectrom, 1999. 13(22): p. 2237-43.
150. Ouellet, A., N. LeBerre, and C. Ayotte, *A simplified and accurate method for the analysis of urinary metabolites of testosterone-related steroids using gas chromatography/combustion/isotope ratio mass spectrometry*. Rapid Communications in Mass Spectrometry, 2013. 27(15): p. 1739-1750.
151. de la Torre, X., et al., *Metabolism of boldione in humans by mass spectrometric techniques: detection of pseudoendogenous metabolites*. Drug Test Anal, 2013. 5(11-12): p. 834-42.
152. Torre, X., et al., *Nandrolone criteria for 19-norandrosterone Isotope Ratio Mass Spectrometric confirmation*. 2015.
153. de la Torre, X., et al., *Development and validation of a GC-C-IRMS method for the confirmation analysis of pseudo-endogenous glucocorticoids in doping control*. Drug Test Anal, 2015. 7(11-12): p. 1071-8.
154. Buisson, C., et al., *Isotope ratio mass spectrometry analysis of the oxidation products of the main and minor metabolites of hydrocortisone and cortisone for antidoping controls*. Steroids, 2009. 74(3): p. 393-397.
155. Iannella, L., et al., *Development and validation of a method to confirm the exogenous origin of prednisone and prednisolone by GC-C-IRMS*. Drug Test Anal, 2019. 11(11-12): p. 1615-1628.
156. Zhang, Y., et al., *Calibration and data processing in gas chromatography combustion isotope ratio mass spectrometry*. Drug Test Anal, 2012. 4(12): p. 912-22.
157. de la Torre, X., et al., *Isotope ratio mass spectrometry in antidoping analysis: The use of endogenous reference compounds*. Rapid Communications in Mass Spectrometry, 2019. 33(6): p. 579-586.
158. World Anti-Doping Agency, *Detection of Synthetic Forms of Endogenous Anabolic Androgenic Steroids by GC/C/IRMS*. Available from: [https://www.wada-ama.org/sites/default/files/td2019irms\\_final\\_eng\\_clean.pdf](https://www.wada-ama.org/sites/default/files/td2019irms_final_eng_clean.pdf), accessed 2020-10-09.
159. Van Renterghem, P., et al., *Development of a GC/C/IRMS method--confirmation of a novel steroid profiling approach in doping control*. Steroids, 2012. 77(11): p. 1050-60.
160. de la Torre, X., et al., *A comprehensive procedure based on gas chromatography–isotope ratio mass spectrometry following high performance liquid chromatography purification for the analysis of underivatized testosterone and its analogues in human urine*. Analytica Chimica Acta, 2012. 756: p. 23-29.
161. McCullagh, J.S.O., D. Juchelka, and R.E.M. Hedges, *Analysis of amino acid  $^{13}\text{C}$  abundance from human and faunal bone collagen using liquid chromatography/isotope ratio mass spectrometry*. Rapid Communications in Mass Spectrometry, 2006. 20(18): p. 2761-2768.
162. Howland, M.R., et al., *Expression of the dietary isotope signal in the compound-specific  $\delta^{13}\text{C}$  values of pig bone lipids and amino acids*. International Journal of Osteoarchaeology, 2003. 13(1-2): p. 54-65.
163. Walsh, R.G., S. He, and C.T. Yarnes, *Compound-specific  $\delta^{13}\text{C}$  and  $\delta^{15}\text{N}$  analysis of amino acids: a rapid, chloroformate-based method for ecological studies*. Rapid Communications in Mass Spectrometry, 2014. 28(1): p. 96-108.

164. Shinebarger, S.R., M. Haisch, and D.E. Matthews, *Retention of carbon and alteration of expected  $^{13}\text{C}$ -tracer enrichments by silylated derivatives using continuous-flow combustion-isotope ratio mass spectrometry*. *Anal Chem*, 2002. 74(24): p. 6244-51.
165. Piper, T., et al., *Determination of  $^{13}\text{C}/^{12}\text{C}$  ratios of endogenous urinary steroids: method validation, reference population and application to doping control purposes*. *Rapid Communications in Mass Spectrometry*, 2008. 22(14): p. 2161-2175.
166. World Anti-Doping Agency, International Standard for Laboratories. Available from: [https://www.wada-ama.org/sites/default/files/resources/files/isl\\_nov2019.pdf](https://www.wada-ama.org/sites/default/files/resources/files/isl_nov2019.pdf), accessed 2020-10-09.
167. Szymańska, E., et al., *Development and validation of urinary nucleosides and creatinine assay by capillary electrophoresis with solid phase extraction*. *Journal of Pharmaceutical and Biomedical Analysis*, 2007. 44(5): p. 1118-1126.
168. Caimi, R.J. and J.T. Brenna, *Quantitative evaluation of carbon isotopic fractionation during reversed-phase high-performance liquid chromatography*. *Journal of Chromatography A*, 1997. 757(1): p. 307-310.
169. Anastassiades, M., K. Mastovska, and S. Lehotay, *Evaluation of Analyte Protectants to Improve Gas Chromatographic Analysis of Pesticides*. *Journal of chromatography. A*, 2003. 1015: p. 163-84.
170. Mastovská, K., S.J. Lehotay, and M. Anastassiades, *Combination of analyte protectants to overcome matrix effects in routine GC analysis of pesticide residues in food matrixes*. *Anal Chem*, 2005. 77(24): p. 8129-37.
171. Lalonde, K., A. Barber, and C. Ayotte, *Two-dimensional HPLC purification of underivatized urinary testosterone and metabolites for compound specific stable carbon isotope analysis*. *Drug Test Anal*, 2020.
172. Gohlke, C., *Molecular Mass Calculator*. Available from: <https://www.lfd.uci.edu/~gohlke/molmass/>, accessed 2020-12-01.
173. Huang, L.-f., et al., *Simultaneous determination of adenine, uridine and adenosine in cordyceps sinensis and its substitutes by LC/ESI-MS*. *Journal of Central South University of Technology*, 2004. 11(3): p. 295-299.
174. Werner, R.A. and W.A. Brand, *Referencing strategies and techniques in stable isotope ratio analysis*. *Rapid Communications in Mass Spectrometry*, 2001. 15(7): p. 501-519.
175. Carter, J.F. and B. Fry, *Ensuring the reliability of stable isotope ratio data—beyond the principle of identical treatment*. *Analytical and Bioanalytical Chemistry*, 2013. 405(9): p. 2799-2814.
176. Jimmerson, L.C., et al., *A LC-MS/MS Method for Quantifying Adenosine, Guanosine and Inosine Nucleotides in Human Cells*. *Pharmaceutical research*, 2017. 34(1): p. 73-83.
177. Bonnefous, J.L., et al., *Determination of Six Thioguanine Nucleotides in Human Red Blood Cells Using Solid-Phase Extraction Prior to High Performance Liquid Chromatography*. *Journal of Liquid Chromatography*, 1992. 15(5): p. 851-861.
178. Contreras-Sanz, A., et al., *Simultaneous quantification of 12 different nucleotides and nucleosides released from renal epithelium and in human urine samples using ion-pair reversed-phase HPLC*. *Purinergic Signal*, 2012. 8(4): p. 741-51.
179. Czarnecka, J., M. Cieślak, and K. Michał, *Application of solid phase extraction and high-performance liquid chromatography to qualitative and quantitative analysis of nucleotides and nucleosides in human cerebrospinal fluid*. *Journal of Chromatography B*, 2005. 822(1): p. 85-90.

180. Phenomenex, *The Complete Guide to Solid Phase Extraction (SPE)*. Available from: <https://phenomenex.blob.core.windows.net/documents/13868f78-8e68-4e8f-8eb7-d36ec8787b93.pdf>, accessed 2020-11-21.
181. Chatterjee, S., et al., *The chemical nature of the 2'-substituent in the pentose-sugar dictates the pseudoaromatic character of the nucleobase (pKa) in DNA/RNA*. *Organic & Biomolecular Chemistry*, 2006. 4(9): p. 1675-1686.
182. Furikado, Y., et al., *Universal Reaction Mechanism of Boronic Acids with Diols in Aqueous Solution: Kinetics and the Basic Concept of a Conditional Formation Constant*. *Chemistry – A European Journal*, 2014. 20(41): p. 13194-13202.
183. Davis, G.E., et al., *High-performance liquid chromatographic separation and quantitation of nucleosides in urine and some other biological fluids*. *Clinical Chemistry*, 1977. 23(8): p. 1427-1435.
184. Bullinger, D., et al., *Metabolic signature of breast cancer cell line MCF-7: profiling of modified nucleosides via LC-IT MS coupling*. *BMC Biochemistry*, 2007. 8(1): p. 25.
185. Willmann, L., et al., *Exometabolom analysis of breast cancer cell lines: Metabolic signature*. *Sci Rep*, 2015. 5: p. 13374.
186. Bio-Rad, *Affi-Gel® Boronate Affinity Gel to Separate Ribonucleotides, Ribonucleosides, Sugars, Catecholamines and Coenzymes*. Bulletin 1066 US Rev B]. Available from: [https://www.bio-rad.com/webroot/web/pdf/lsr/literature/Bulletin\\_1066B.pdf](https://www.bio-rad.com/webroot/web/pdf/lsr/literature/Bulletin_1066B.pdf), accessed 2020-11-21.
187. *Commission Decision 2002/657/EC*. Official Journal of the European Communities, 2002. L221(8).
188. Bonner, T.G. and P. McNamara, *The pyridine-catalysed acetylation of phenols and alcohols by acetic anhydride*. *Journal of the Chemical Society B: Physical Organic*, 1968(0): p. 795-797.
189. Xu, S., et al., *The DMAP-Catalyzed Acetylation of Alcohols—A Mechanistic Study (DMAP=4-(Dimethylamino)pyridine)*. *Chemistry – A European Journal*, 2005. 11(16): p. 4751-4757.
190. Roncaglia, F., et al., *Acetic Anhydride/Et<sub>3</sub>N/DMAP: An Effective Acetylating System for Hemiacetals*. *Synthetic Communications*, 2011. 41(8): p. 1175-1180.
191. Scudiero, O., et al., *New synthetic AICAR derivatives with enhanced AMPK and ACC activation*. *Journal of Enzyme Inhibition and Medicinal Chemistry*, 2016. 31(5): p. 748-753.
192. Shuto, S., et al., *Synthesis of sugar-modified analogs of bredinin (mizoribine), a clinically useful immunosuppressant, by a novel photochemical imidazole ring-cleavage reaction as the key step I*. *Journal of the Chemical Society, Perkin Transactions 1*, 2000(21): p. 3603-3609.
193. Clayden, J., et al., *Chimie Organique*. 1re édition ed, ed. D. Boeck. 2003.
194. Voet, D., et al., *Absorption spectra of nucleotides, polynucleotides, and nucleic acids in the far ultraviolet*. *Biopolymers*, 1963. 1(3): p. 193-208.
195. Middleton, C.T., et al., *DNA Excited-State Dynamics: From Single Bases to the Double Helix*. *Annual Review of Physical Chemistry*, 2009. 60(1): p. 217-239.
196. Nwokeoji, A.O., et al., *Accurate Quantification of Nucleic Acids Using Hypochromicity Measurements in Conjunction with UV Spectrophotometry*. *Analytical Chemistry*, 2017. 89(24): p. 13567-13574.
197. Hofmann, D., et al., *Using Natural Isotope Variations of Nitrogen in Plants as an Early Indicator of Air Pollution Stress*. *Journal of Mass Spectrometry*, 1997. 32(8): p. 855-863.

198. Moritz, A., et al., *Methane Baseline Concentrations and Sources in Shallow Aquifers from the Shale Gas-Prone Region of the St. Lawrence Lowlands (Quebec, Canada)*. Environmental Science & Technology, 2015. 49(7): p. 4765-4771.
199. Spivey, J.J., *Complete catalytic oxidation of volatile organics*. Industrial & Engineering Chemistry Research, 1987. 26(11): p. 2165-2180.
200. Merritt, D.A., et al., *Performance and Optimization of a Combustion Interface for Isotope Ratio Monitoring Gas Chromatography/Mass Spectrometry*. Analytical Chemistry, 1995. 67(14): p. 2461-2473.
201. Glarborg, P., et al., *Modeling nitrogen chemistry in combustion*. Progress in Energy and Combustion Science, 2018. 67: p. 31-68.
202. Dautraix, S., et al., *<sup>13</sup>C Isotopic analysis of an acetaminophen and diacetylmorphine mixture*. Journal of Chromatography A, 1996. 756(1): p. 203-210.
203. Brand, W., S. Assonov, and T. Coplen, *Correction for the <sup>17</sup>O interference in d(<sup>13</sup>C) measurements when analyzing CO<sub>2</sub> with stable isotope mass spectrometry (IUPAC Technical Report)*. Pure and Applied Chemistry, v.82, 1719-1733 (2010), 2010. 82.
204. Zhang, Y., H.J. Tobias, and J.T. Brenna, *Steroid isotopic standards for gas chromatography-combustion isotope ratio mass spectrometry (GCC-IRMS)*. Steroids, 2009. 74(3): p. 369-378.
205. Piper, T. and M. Thevis, *Chapter Fourteen - Applications of Isotope Ratio Mass Spectrometry in Sports Drug Testing Accounting for Isotope Fractionation in Analysis of Biological Samples*, in *Methods in Enzymology*, M.E. Harris and V.E. Anderson, Editors. 2017, Academic Press. p. 403-432.
206. Docherty, G., V. Jones, and R.P. Evershed, *Practical and theoretical considerations in the gas chromatography/combustion/isotope ratio mass spectrometry  $\delta^{13}\text{C}$  analysis of small polyfunctional compounds*. Rapid Communications in Mass Spectrometry, 2001. 15(9): p. 730-738.
207. Angelis, Y.S., et al., *Examination of the kinetic isotopic effect to the acetylation derivatization for the gas chromatographic-combustion-isotope ratio mass spectrometric doping control analysis of endogenous steroids*. Drug Test Anal, 2012. 4(12): p. 923-7.
208. International Organization for Standardization/International Electrotechnical Commission 17025, *ISO/IEC 17025:2017(E) General requirements for the competence of testing and calibration laboratories*. 2017: Switzerland.
209. Van Eenoo, P., et al., *Results of stability studies with doping agents in urine*. J Anal Toxicol, 2007. 31(9): p. 543-8.
210. Kuenen, J.G. and W.N. Konings, *The importance of cooling of urine samples for doping analysis*. Accreditation and Quality Assurance, 2010. 15(2): p. 133-136.
211. World Anti-Doping Agency, *Minimum criteria for chromatographic-mass spectrometric confirmation of the identity of analytes for doping control purposes* Available from: [https://www.wada-ama.org/sites/default/files/resources/files/td2015idcr\\_-\\_eng.pdf](https://www.wada-ama.org/sites/default/files/resources/files/td2015idcr_-_eng.pdf), accessed 2020-10-09.
212. World Anti-Doping Agency, *Decision limits for the confirmatory quantification of threshold substances*. Available from: [https://www.wada-ama.org/sites/default/files/td2019dl\\_final\\_eng\\_clean.pdf](https://www.wada-ama.org/sites/default/files/td2019dl_final_eng_clean.pdf), accessed 2021-01-28.
213. Hellsten, Y., L. Skadhauge, and J. Bangsbo, *Effect of ribose supplementation on resynthesis of adenine nucleotides after intense intermittent training in humans*. Am J Physiol Regul Integr Comp Physiol, 2004. 286(1): p. R182-8.

214. Hii, S.L., et al., *Pullulanase: Role in Starch Hydrolysis and Potential Industrial Applications*. Enzyme Research, 2012. 2012: p. 921362.
215. Fellows, P., *Food processing technology : principles and practice*. 2016.
216. Schiffer, L., et al., *Human steroid biosynthesis, metabolism and excretion are differentially reflected by serum and urine steroid metabolomes: A comprehensive review*. J Steroid Biochem Mol Biol, 2019. 194: p. 105439.
217. Patel, S., et al., *Physiology, Carbon Dioxide Retention*, in *StatPearls*. 2020, StatPearls Publishing Copyright © 2020, StatPearls Publishing LLC.: Treasure Island (FL).
218. Kothe, M., et al., *Direct demonstration of carbamoyl phosphate formation on the C-terminal domain of carbamoyl phosphate synthetase*. Protein Sci, 2005. 14(1): p. 37-44.
219. Lin, A.H.-M., et al., *Starch Source Influences Dietary Glucose Generation at the Mucosal  $\alpha$ -Glucosidase Level*. Journal of Biological Chemistry, 2012. 287(44): p. 36917-36921.
220. Paredes-Flores, M.A. and S.S. Mohiuddin, *Biochemistry, Glycogenolysis*, in *StatPearls*. 2020, StatPearls Publishing Copyright © 2020, StatPearls Publishing LLC.: Treasure Island (FL).
221. Rui, L., *Energy metabolism in the liver*. Compr Physiol, 2014. 4(1): p. 177-97.
222. Piper, T., et al., *Investigations on changes in  $^{13}\text{C}/^{12}\text{C}$  ratios of endogenous urinary steroids after pregnenolone administration*. Drug Test Anal, 2011. 3(5): p. 283-90.
223. Flenker, U., et al. *Influence of changes in diet on the dynamics of  $^{13}\text{C}/^{12}\text{C}$  in selected urinary steroids: diet free from cholesterol*. in *Proceedings of the 23rd Cologne Workshop on Dope Analysis*. Cologne, Germany: Sport und Buch Strauss. 2005.
224. Riedinger, C., et al., *High-glucose toxicity is mediated by AICAR-transformylase/IMP cyclohydrolase and mitigated by AMP-activated protein kinase in Caenorhabditis elegans*. J Biol Chem, 2018. 293(13): p. 4845-4859.
225. Connolly, G.P. and J.A. Duley, *Uridine and its nucleotides: biological actions, therapeutic potentials*. Trends Pharmacol Sci, 1999. 20(5): p. 218-25.
226. Adams, T.S. and R.W. Sterner, *The effect of dietary nitrogen content on trophic level  $^{15}\text{N}$  enrichment*. Limnology and Oceanography, 2000. 45(3): p. 601-607.
227. Mollick, T. and S. Lain, *Modulating pyrimidine ribonucleotide levels for the treatment of cancer*. Cancer Metab, 2020. 8: p. 12.
228. O'Brien, D.M., *Stable Isotope Ratios as Biomarkers of Diet for Health Research*. Annu Rev Nutr, 2015. 35: p. 565-94.
229. Cohen, G.N., *The aspartic acid family of amino acids. Biosynthesis*, in *Microbial Biochemistry*, G.N. Cohen, Editor. 2004, Springer Netherlands: Dordrecht. p. 139-149.
230. Berg, J.M., et al., *Amino Acids Are Made from Intermediates of the Citric Acid Cycle and Other Major Pathways*, in *Biochemistry*. 2002, W.H. Freeman ; NCBI: New York; [Bethesda, MD.
231. Brosnan, M.E. and J.T. Brosnan, *Formate: The Neglected Member of One-Carbon Metabolism*. Annual Review of Nutrition, 2016. 36(1): p. 369-388.
232. Lobanov, K.V., et al., *Reconstruction of Purine Metabolism in Bacillus subtilis to Obtain the Strain Producer of AICAR: A New Drug with a Wide Range of Therapeutic Applications*. Acta Naturae, 2011. 3(2): p. 79-89.
233. Oliviero, G., et al., *Facile Solid-Phase Synthesis of AICAR 5'-Monophosphate (ZMP) and Its 4-N-Alkyl Derivatives*. European Journal of Organic Chemistry, 2010. 2010(8): p. 1517-1524.
234. Oliviero, G., et al., *Synthesis of 4-N-alkyl and ribose-modified AICAR analogues on solid support*. Tetrahedron, 2008. 64(27): p. 6475-6481.

235. Hülsemann, F., et al., *Do we excrete what we eat? Analysis of stable nitrogen isotope ratios of human urinary urea*. Rapid Communications in Mass Spectrometry, 2017. 31(14): p. 1221-1227.

## Appendix 1

### Acetylation experiment

An experiment was designed to evaluate the level of KIE present in the acetylation reaction and to determine if AICAR and uridine each needed a compound-specific correction  $\delta^{13}\text{C}_\text{D}$  factor. Many substances with primary and secondary alcohols were bought along with their acetylated form. All the compounds were analyzed by EA-IRMS, except for the CU/USADA-33-1 mix which came with a certificate of analysis for  $\delta^{13}\text{C}$  analysis. Details are available in Table A1.1.

Table A1.1: EA-IRMS or certified values for the compounds used in this experiment.

Compound	Supplier	External $\delta^{13}\text{C}$ (‰) value	Standard deviation (‰)	Number of replicates EA-IRMS (n)	Laboratory for isotope analysis	
AICAR 1	TRC	-4.44	0.02	5	UC Davis	
AICAR 2	TRC	-4.34	0.04	5	UC Davis	
Uridine	TRC	-13.21	0.02	5	UC Davis	
AICAR-tri-O-acetate	TRC	-15.53	0.05	6	GEOTOP	
Uridine-3-O-acetate	TRC	-25.21	0.05	5	UC Davis	
Glycerol	Sigma-Aldrich	-26.65	0.07	5	GEOTOP	
D-sorbitol	Sigma-Aldrich	-12.40	0.03	5	GEOTOP	
Triacetine 1	Sigma-Aldrich	-37.20	0.18	4	GEOTOP	
Triacetine 2	Fisher Scientific	-38.45	0.10	5	GEOTOP	
D-sorbitol hexaacetate 1	Sigma-Aldrich	-33.29	0.08	3	GEOTOP	
D-sorbitol hexaacetate 2	Fisher Scientific	-33.30	0.11	5	GEOTOP	
Estriol	Steraloids	-26.67	0.03	5	GEOTOP	
Etiocholanolone	Sigma-Aldrich	-18.46	0.26	3	GEOTOP	
Androsterone	Sigma-Aldrich	-30.83	0.28	5	GEOTOP	
CU/USADA-33-1	Brenna Laboratory	5 $\alpha$ -androstan-3 $\beta$ -ol acetate	-30.61	0.14	16*	Brenna Laboratory (Cornell University)
		5 $\alpha$ -androstan-3 $\alpha$ -ol-17-one acetate	-33.04	0.03		
		5 $\beta$ -androstan-3 $\alpha$ -ol-11,17-dione acetate	-16.69	0.07		
		5 $\alpha$ -cholestane	-24.77	0.13		
Acetic anhydride	Fisher Scientific	-21.78	0.11	5	GEOTOP	

\*Based on Zhang et al. (2009) [204].

Unacetylated compounds were all treated with Ac<sub>2</sub>O and Pyr and were then analyzed by GC/C/IRMS, as described in the “Materials and methods” section. The raw  $\delta^{13}\text{C}$  obtained were first corrected using the standards that had been bought acetylated. The correction for AICAR and uridine was done using the 2-point calibration method like for the urine samples. Estriol, etiocholanolone and androsterone raw measurements were corrected with the CU/USADA-33-1 mix for which the four different steroids were used to build a 4-point calibration curve. Glycerol and D-sorbitol measurements were each adjusted with a 1-point correction that corresponded to the average difference obtained between the raw GC/C/IRMS values and the EA-IRMS values of triacetin and D-sorbitol hexaacetate, respectively. The  $\delta^{13}\text{C}_\text{D}$  value (related to the acetate groups added on the molecules) of each standard bought unacetylated were then calculated using the mass balance formula. The results can be seen in Table A1.2.

Table A1.2:  $\delta^{13}\text{C}_\text{D}$  and SD values for the compounds bought unacetylated.

Acetylated compound	Average $\delta^{13}\text{C}_\text{D}$ (‰)	SD (‰)
AICAR	-44.80	0.13
Uridine	-42.26	0.08
Glycerol	-41.96	0.25
D-sorbitol	-40.23	0.42
Estriol	-42.26	0.85
Androsterone	-42.36	1.36
Etiocholanolone	-39.09	0.94

## Appendix 2

### Method validation supplemental data

Table A2.1: Intra-day precision results for samples U1 to U8.

Sample	n	SD before correction for acetylation (‰)	SD after correction for acetylation (‰)	n	SD before correction for acetylation (‰)	SD after correction for acetylation (‰)
U1	4	0.11	0.18	4	0.45	0.74
U2	4	0.49	0.81	3	0.29	0.48
U3	4	0.37	0.62	4	0.55	0.91
U4	4	0.40	0.67	4	0.31	0.51
U5	4	0.29	0.48	4	0.23	0.39
U6	4	0.14	0.23	3	0.24	0.39
U7	4	0.74	1.23	4	0.17	0.29
U8	4	0.15	0.25	4	0.21	0.34

Table A2.2: Inter-day precision results. A: AICAR and U: uridine.

Batch identification	S1-S8	S9-S17	V1	V2	V3	V4	V5	V6	Accuracy	Stability	Acetylation	Average	SD
Mix-Ac-A	-15.99	-15.19	-17.44	-16.02	-16.91	-16.45	-16.48	-15.90	-16.01	-15.76	-16.51	-16.24	0.61
Mix-Ac-U	-25.71	-26.46	-27.09	-27.01	-26.80	-26.71	-27.16	-26.89	-27.06	-26.96	-27.09	-26.81	0.42
Slope	1.00	1.16	1.00	1.13	1.02	1.06	1.10	1.13	1.14	1.16	1.09	1.09	0.06
Intercept	-0.38	2.89	-1.96	1.60	-1.05	0.02	0.66	1.72	1.72	2.22	0.46	0.72	1.48
Mix-AU-A	-19.59	-19.76	-19.72	-20.45	-20.33	-20.08	-19.73	-19.79	-19.89	-19.59	-20.53	-19.95	0.34
Mix-AU-U	-23.83	-24.67	-24.19	-24.93	-25.47	-25.32	-24.86	-24.96	-24.79	-24.69	-24.83	-24.78	0.46
Acetate-A	-42.47	-42.75	-42.65	-44.47	-44.16	-43.54	-42.65	-42.82	-43.07	-42.46	-44.80	-43.26	0.85
Acetate-U	-39.77	-41.86	-40.66	-42.51	-43.86	-43.48	-42.33	-42.59	-42.15	-41.90	-42.26	-42.13	1.14
QCN-A	/	/	-16.08	-14.27	-15.25	-15.93	-15.16	-15.34	/	/	/	-15.34	0.64
QCN-U			-17.82	-16.98	-16.91	-16.84	-17.43	-17.16				-17.19	0.37
QCP-A			-5.50	-5.40	-3.93	-5.27	-4.49	-5.09				-4.95	0.61
QCP-U			-18.78	-17.26	-15.87	-16.07	-18.23	-18.64				-17.48	1.28

Table A2.3: Accuracy results

Compound	Extracted (n = 3) $\delta^{13}\text{C} \pm \text{SD}$ (‰)	Reference (n = 3) $\delta^{13}\text{C} \pm \text{SD}$ (‰)	Difference $\delta^{13}\text{C} \pm \text{SD}$ (‰)
AICAR	$-20.08 \pm 0.02$	$-19.89 \pm 0.13$	-0.19
Uridine	$-25.00 \pm 0.19$	$-24.79 \pm 0.07$	-0.21

Table A2.4: Validation parameters assessed for each batch analyzed.

Batch identification	Sample description	Validation parameters					Reference samples included		
		Intra-day precision	Inter-day precision	Accuracy	Stability in urine	Sample population	Acetylated	Non-acetylated	QCN/QCP reference
S1-S8	U1-U8 (n = 3 or 4 each)	X	X			X	X	X	
S9-S17	U9-U17		X			X	X	X	
V1	U10, U18-U22		X	X		X	X	X	X
V2	U23-U28		X	X		X	X	X	X
V3	U29-U35		X	X		X	X	X	X
V4	U36-U41		X	X		X	X	X	X
V5	U42-U46		X	X		X	X	X	X
V6	U1, U20 and U31		X	X		X	X	X	X
Accuracy	Surrogate urine matrix (also included AICAR bought online)	X	X	X			X	X	
Stability	Volunteer's urine spiked with 5 $\mu\text{g/mL}$ of AICAR and uridine				X		X	X	
Acetylation	Various acetylated compounds (Appendix 1)						X	X	

### Appendix 3

#### Individual $\delta^{13}\text{C}$ measurements for all samples

Out of the 46 urines analyzed (labelled as U1 to U46), 44 individual  $\delta^{13}\text{C}$  values for AICAR and uridine could be obtained. Samples for which values were missing were as follows: U32 had an AICAR concentration too low for analysis, the same was true for uridine in U10 and the values for U11 had to be rejected for insufficient analyte recoveries leading to unreliable data. The volume of urine subsequently left was too small for re-analysis. This means that the AICAR/uridine complete duo could be analyzed in a total of 43 samples. Insufficient volume also explains why steroid analysis was only performed on 35 samples.

Table A3.1: All individual  $\delta^{13}\text{C}$  results for AICAR and uridine in the 46 urines samples analyzed.

Urine number	Analysis number	Bottle A or B	Intensity (nA)	$\delta^{13}\text{C}$ (‰) AICAR without correction	$\delta^{13}\text{C}$ (‰) AICAR with normalization	$\delta^{13}\text{C}$ (‰) AICAR with correction for acetates	Intensity (nA)	$\delta^{13}\text{C}$ (‰) Uridine without correction	$\delta^{13}\text{C}$ (‰) Uridine with normalization	$\delta^{13}\text{C}$ (‰) Uridine with correction for acetates
1	1	A	1.10	-22.80	-22.31	-8.88	1.30	-26.59	-26.09	-16.97
		A	1.10	-22.96	-22.47	-9.14	2.54	-26.45	-25.95	-16.74
		B	0.97	-22.93	-22.44	-9.09	1.86	-26.71	-26.21	-17.17
		B	0.73	-23.78	-23.29	-10.50	2.09	-26.61	-26.11	-17.00
	2	A	3.20	-23.93	-22.60	-9.12	0.23	-29.53	-27.54	-17.51
2	1	A <sup>1</sup>	0.49	-	-	-	6.79	-26.16	-25.66	-16.25
		A	0.71	-28.94	-28.43	-19.06	7.03	-25.38	-24.88	-14.96
		B	0.91	-28.47	-27.96	-18.28	8.11	-26.50	-26.00	-16.82
		B	1.00	-28.42	-27.91	-18.20	6.66	-25.76	-25.26	-15.59
		A	0.95	-28.17	-27.66	-17.79	2.58	-28.98	-28.47	-20.93
3	1	A	0.74	-28.97	-28.46	-19.11	3.95	-28.62	-28.11	-20.34
		B	0.59	-28.08	-27.57	-17.64	1.87	-29.14	-28.63	-21.20
		B	1.85	-27.65	-27.14	-16.92	4.12	-28.31	-27.80	-19.82
		A	2.56	-26.54	-26.04	-15.08	3.78	-27.52	-27.01	-18.51
4	1	A	1.76	-26.86	-26.36	-15.61	4.08	-27.56	-27.05	-18.58
		B <sup>2</sup>	-	-	-	-	3.07	-27.66	-27.15	-18.74
		B	2.17	-27.15	-26.64	-16.09	3.00	-28.38	-27.87	-19.94

Urine number	Analysis number	Bottle A or B	Intensity (nA)	$\delta^{13}\text{C}$ (‰) AICAR without correction	$\delta^{13}\text{C}$ (‰) AICAR with normalization	$\delta^{13}\text{C}$ (‰) AICAR with correction for acetates	Intensity (nA)	$\delta^{13}\text{C}$ (‰) Uridine without correction	$\delta^{13}\text{C}$ (‰) Uridine with normalization	$\delta^{13}\text{C}$ (‰) Uridine with correction for acetates
5	1	A	2.51	-28.22	-27.71	-17.87	8.84	-27.18	-26.67	-17.95
		A	2.54	-28.42	-27.91	-18.20	12.29	-26.65	-26.15	-17.07
		B	2.27	-28.68	-28.17	-18.63	10.71	-26.59	-26.09	-16.97
		B	1.81	-28.72	-28.21	-18.70	13.17	-26.57	-26.07	-16.93
6	1	A	0.94	-28.07	-27.56	-17.62	3.74	-27.20	-26.69	-17.98
		A	1.19	-27.85	-27.34	-17.26	1.64	-27.27	-26.76	-18.10
		B	1.82	-27.61	-27.10	-16.86	3.76	-27.14	-26.63	-17.88
		B	1.57	-27.56	-27.05	-16.77	2.24	-27.46	-26.95	-18.41
7	1	A	2.29	-28.55	-28.04	-18.42	1.81	-26.81	-26.31	-17.33
		A	2.85	-28.53	-28.02	-18.38	1.59	-27.07	-26.57	-17.76
		B	2.66	-28.35	-27.84	-18.09	0.96	-28.01	-27.50	-19.32
		B	2.11	-28.77	-28.26	-18.78	0.75	-28.36	-27.85	-19.90
8	1	A	2.78	-28.08	-27.57	-17.64	6.15	-26.30	-25.80	-16.49
		A	2.60	-28.12	-27.61	-17.70	5.80	-26.33	-25.83	-16.54
		B	2.93	-27.88	-27.37	-17.31	8.13	-26.15	-25.65	-16.24
		B	2.69	-28.38	-27.87	-18.13	5.33	-26.51	-26.01	-16.83
9	1	A	7.39	-28.22	-26.72	-16.03	2.37	-29.60	-27.90	-18.60
10	1	A	0.68	-29.85	-27.98	-18.20	0.20 <sup>3</sup>	(-28.6)	(-26.7)	(-17.4)
	2	A	1.49	-28.85	-27.26	-16.94	0.17 <sup>3</sup>	(-30.5)	(-28.7)	(20.0)
11 <sup>4</sup>	1	A	(1.11)	(-28.0)	-	(-16.7)	(0.70)	(-28.4)	-	(-17.4)
12	1	A	4.93	-28.00	-26.53	-15.71	0.39	-29.63	-27.93	-18.63
13	1	A	6.06	-27.73	-26.30	-15.34	3.48	-31.72	-29.73	-21.64
14	1	A	1.21	-27.68	-26.26	-15.26	2.41	-29.75	-28.03	-18.80
15	1	A	2.31	-27.51	-26.11	-15.02	5.67	-28.66	-27.09	-17.24
16	1	A	2.24	-29.38	-27.71	-17.69	7.51	-30.32	-28.52	-19.62
17	1	A	4.47	-27.30	-25.93	-14.71	5.43	-29.59	-27.89	-18.57
18	1	A	0.93	-30.00	-28.12	-18.44	1.21	-28.94	-27.06	-17.99
19	1	A	1.75	-29.56	-27.68	-17.70	4.01	-29.46	-27.58	-18.86
20	1	A	4.67	-25.72	-23.84	-11.30	5.12	-26.92	-25.03	-14.61
	2	A	3.28	-25.86	-24.30	-11.96	0.94	-27.66	-25.89	-14.76
21	1	A	5.74	-29.17	-27.29	-17.05	2.60	-29.95	-28.07	-19.68
22	1	A	8.09	-28.84	-26.97	-16.51	4.47	-29.03	-27.16	-18.16
23	1	A	7.42	-28.47	-26.50	-14.51	4.31	-29.30	-27.23	-17.03
24	1	A	5.64	-28.44	-26.47	-14.47	5.32	-29.95	-27.80	-17.99
25	1	A	3.37	-28.18	-26.24	-14.08	6.46	-29.37	-27.29	-17.15
26	1	A	2.96	-29.40	-27.32	-15.88	7.87	-30.54	-28.32	-18.86

Urine number	Analysis number	Bottle A or B	Intensity (nA)	$\delta^{13}\text{C}$ (‰) AICAR without correction	$\delta^{13}\text{C}$ (‰) AICAR with normalization	$\delta^{13}\text{C}$ (‰) AICAR with corection for acetates	Intensity (nA)	$\delta^{13}\text{C}$ (‰) Uridine without correction	$\delta^{13}\text{C}$ (‰) Uridine with normalization	$\delta^{13}\text{C}$ (‰) Uridine with correction for acetates
27	1	A	2.00	-29.10	-27.05	-15.44	9.86	-29.56	-27.46	-17.42
28	1	A	2.21	-30.12	-27.95	-16.94	7.71	-30.24	-28.06	-18.42
29	1	A	1.60	-28.36	-26.74	-15.12	14.12	-28.82	-27.19	-16.07
30	1	A	1.36	-28.58	-26.96	-15.49	9.10	-28.52	-26.90	-15.59
31	1	A	2.15	-26.18	-24.60	-11.56	6.86	-29.32	-27.68	-16.90
	2	A	3.83	-26.81	-25.14	-13.36	3.76	-29.73	-27.71	-17.79
32	1	A <sup>3</sup>	-	-	-	-	0.97	-26.97	-25.37	-13.05
33	1	A	1.12	-28.52	-26.90	-15.39	5.99	-30.53	-28.86	-18.86
34	1	A	0.92	-28.23	-26.61	-14.91	12.01	-28.74	-27.11	-15.95
35	1	A	0.83	-27.02	-25.43	-12.94	7.22	-28.01	-26.39	-14.75
36	1	A	0.82	-27.54	-25.99	-14.28	8.47	-28.12	-26.53	-15.23
37	1	A	1.33	-28.08	-26.49	-15.13	11.38	-28.16	-26.58	-15.30
38	1	A	0.39	-28.44	-26.84	-15.70	3.83	-28.39	-26.79	-15.67
39	1	A	1.55	-28.49	-26.89	-15.78	6.43	-29.01	-27.38	-16.64
40	1	A	3.10	-28.45	-26.85	-15.72	9.50	-29.40	-27.74	-17.25
41	1	A	1.35	-29.14	-27.50	-16.81	8.88	-28.86	-27.23	-16.40
42	1	A	4.23	-25.03	-23.28	-10.37	8.17	-28.30	-26.24	-15.51
43	1	A	4.45	-27.38	-25.41	-13.92	13.09	-29.42	-27.26	-17.21
44	1	A	4.62	-30.43	-28.18	-18.53	10.61	-31.61	-29.25	-20.52
45	1	A	2.46	-29.45	-27.28	-17.04	15.17	-30.75	-28.46	-19.21
46	1	A	2.51	-27.99	-25.97	-14.84	4.06	-29.55	-27.37	-17.40

1. Visible contamination co-eluting.
2. No signal due to solvent evaporation.
3. Signal lower than minimum required for analysis. Value not considered for general statistics.
4. Approximative  $\delta^{13}\text{C}$  results. Insufficient volume for re-analysis after first result was rejected for low analyte recoveries in the batch.

Table A3.2: All individual  $\delta^{13}\text{C}$  results for Pd, Et and Andro in the 35 urines samples analyzed for steroids.

Sample	Pd $\delta^{13}\text{C}$ (‰)	Et $\delta^{13}\text{C}$ (‰)	Andro $\delta^{13}\text{C}$ (‰)	Sample	Pd $\delta^{13}\text{C}$ (‰)	Et $\delta^{13}\text{C}$ (‰)	Andro $\delta^{13}\text{C}$ (‰)
1	-19.87	-20.30	-19.55	24	-20.60	-21.09	-20.86
2	-19.55	-21.46	-20.05	25	-19.06	-20.40	-19.07
3	-22.70	-23.96	-22.55	26	-23.45	-24.46	-23.14
4	-19.36	-19.88	-19.01	27	-20.62	-22.03	-20.77
5	-19.54	-21.36	-19.89	28	-20.43	-22.08	-21.10
6	-18.37	-19.54	-18.46	29	-19.59	-20.27	-19.71
7	-19.68	-21.38	-19.89	30	-19.27	-20.32	-18.92
8	-19.50	-21.02	-19.66	31	-20.20	-21.48	-20.08
9	-19.40	-21.28	-19.65	32	n/d	n/d	n/d
10	-19.10	-20.00	-19.37	33			
11	-19.39	-20.69	-19.88	34			
12	-18.36	-20.96	-20.13	35			
13	-21.39	-22.21	-21.41	36			
14	-20.19	-20.38	-20.84	37			
15	-18.78	-19.33	-18.62	38			
16	-21.38	-22.26	-21.11	39			
17	-18.39	-18.57	-17.72	40			
18	-20.75	-21.55	-20.28	41			
19	-19.65	-23.17	-21.74	42	-17.09	-20.01	-18.33
20	-18.90	-19.59	-18.58	43	-19.08	-19.63	-19.13
21	-19.97	-21.23	-19.97	44	n/d	n/d	n/d
22	-19.98	-20.98	-19.65	45	-20.79	-21.77	-20.61
23	-19.29	-20.04	-19.16	46	-20.72	-21.77	-20.45

\*n/d: Not determined due to insufficient urine volume.

## Appendix 4

### AICAR and uridine concentration in urine samples

Table A4.1: Measured concentration values for AICAR and uridine.

Sample	[AICAR] ( $\pm$ SD for replicates) $\mu\text{g/mL}$	[Uridine] $\pm$ SD (for replicates) $\mu\text{g/mL}$
U1	4.0 $\pm$ 0.4 (n = 2)	0.6 $\pm$ 0.03 (n = 4)
U2	2.8 $\pm$ 0.1 (n = 3)	1.5 $\pm$ 0.05 (n = 3)
U3	2.3	0.6
U4	4.6	0.5
U5	5.4	2.1
U6	2.7	0.5
U7	5.6	0.3
U8	11.3	1.8
U9	9.4	0.4
U10	1.7	<LQ (0.01)
U11	10.7	1.2
U12	6.1	0.1
U13	3.5	0.2
U14	2.7	0.3
U15	4.7	1.3
U16	1.5	0.4
U17	5.3	1.0
U18	4.0	N/A
U19	3.5	0.8
U20	8.2	1.2
U21	10.0	0.4
U22	N/A	0.6
U23	3.6	0.7
U24	3.1	0.3
U25	5.9	0.8
U26	1.4	0.3
U27	2.0	0.3
U28	2.1	0.9
U29	1.5	0.9
U30	2.1	0.3
U31	2.8	0.7
U32	< LQ (0.1)	N/A
U33	0.6	0.3
U34	0.8	0.6
U35	0.5	0.7
U36	0.4	0.5
U37	1.1	1.2
U38	0.3	0.2
U39	0.7	0.5
U40	1.0	0.9
U41	0.6	0.4
U42	2.3	0.5
U43	3.2	1.6
U44	2.2	0.6
U45	3.4	0.8
U46	2.4 $\pm$ 0.1 (n = 2)	0.8 $\pm$ 0.09 (n = 3)

N/A: No result available due to an unresolved peak.

Table A4.2: Results for LC-MS/MS QCs.

QC identification	Analyte	[Expected] (µg/mL)	[Measured] (µg/mL)	Relative difference (%)
QCA	AICAR	0.75	0.82	+9.9
	Uridine	25.0	21.4	-14.6
QCB	AICAR	3.50	2.40	-31.5
	Uridine	3.50	3.61	+3.1
QCC	AICAR	25.0	27.1	+8.6
	Uridine	0.75	0.62	-17.0

Table A4.3: Results for LC-MS/MS calibration curves.

Curve identification	$r^2$
AICAR 0.25 to 2.5 µg/mL	0.9998
AICAR 2.5 to 30 µg/mL	0.9994
Uridine 0.25 to 2.5 µg/mL	0.9999
Uridine 2.5 to 30 µg/mL	0.9978